

3D data interpretation petro physical Analysis and reservoir Modeling through Inversion and Rock Physics Modeling



BY

Muhammad Mubeen Ahmed

M.Phil. Geophysics

DEPARTMENT OF EARTH SCIENCES

QUAID-I-AZAM UNIVERSITY

ISLAMABAD

Certificate

It is certified that Mr. Mubeen Ahmed (Registration No.0211 2011014) carried out the work contained in this dissertation under my supervision and accepted in its present form by Department of Earth Sciences as satisfying the requirements for the award of M.Phil. Degree in Geophysics.

RECOMMENDED BY

Dr. Anees Ahmed Bangash

Assistant Professor/Supervisor

External Examiner

Dr. Aamir Ali

Chairperson

DEPARTMENT OF EARTH SCIENCES

QUAID-I-AZAM UNIVERSITY

ISLAMABAD

Acknowledgement

All praises to ALLAH Almighty, the most bountiful, merciful and the great creator of this universe, who blessed the knowledge to me and created a potential in me to complete this research work. All respect for the Holy Prophet Hazrat Muhammad (P.B.U.H) who portrayed the best model of the world for humanity. Surely! I haven't such a potential to complete this work and reach at this spot but Allah showered his mercy.

This research reached in this current form with the assistance and mentorship of several people. I am especially indebted to my research supervisor **Dr. Anees Ahmed Bangash** for giving me an opportunity as well as an initiative to this study. His calm nature, vast knowledge and positive criticism motivated me to complete this thesis work. Thanks for absorbing my mistakes and whenever I could not meet the deadlines. I am also thankful to my all teachers, faculty of Earth Science Department Quaid-e-Azam University, for their kind contributions directly or indirectly.

I specially want to mention the help, the encouragement, endless love and prayers of my family specially my sister **TALLHA** for being my big supporter of all the times, my father and my other siblings, whose valuable prayers, salutary advices and emboldening attitude kept me motivated spiritually to achieve this milestone.

I am indebted to my seniors as well specially **TAIMOOR HASSAN** who is not only a friend but also a mentor to me for proper guidance at every spot of this journey. I am glad to express my gratitude to my most senior brother **ZAHID ULLAH WAZIR** as a great mentor to me who spared his valuable time for me. I am also most thankful and very glad to have **ZURIYAT BATOOL** in this crucial time truly I didn't have words to explain her personality towards me as she always used to be available for me at any cost no matter what are the circumstances but I saw her always stand stood with me. She is always a great motivation for me as a mentor and guider. I also admire the recommendations and help from **YAWAR KHAN, JAWAD AHMED**.

I always used to be circled with a lot of friends generally but to choose a friend specifically for me that will be everything to me is always a dilemma. I am always extremely choosy in this context. It is not possible that I ever forgot to mention my brother like friend **NASIR MAHMOOD** for guiding me spiritually, professionally as well as personally. I always learnt a lot from his company. I must say that my words are not sufficient to explain the value of his presence in my life. Only I can say thanks to him for being there whenever I was in any difficulty.

Muhammad Mubeen Ahmed

MPhil Geophysics

Abstract

There are many special techniques in geophysics that are implied to delineate the under surface natural resources of any area. To untapped the hydrocarbon reserves seismic reflection method is widely used technique. To map potential of reservoir in a comprehensive way 3D data is more feasible because it gives high resolution of subsurface. To measure and evaluate the hydrocarbon strength and sand channels of area this study has gone through on Sawan field. Here 3D seismic interpretation, Rock physics, and Seismic Inversion techniques with Petrophysical analysis for the interpretation purpose of study area. 3D data is given as in-lines from 720-860 and cross-lines are given as 880-1000 with three wells as Sawan-01, Sawan-07 and Sawan-08 as gas producing.

The work is gone through proper sequence as with generation of synthetic seismogram with (0.718) correlation and then three horizons of interest are picked as Lower Goru, D-Interval and finally C-Interval as reservoir. To overview the depth variations of these horizons time contour maps are created and it is clear that sand interval (2190ms to 2260ms) of Lower Goru formation of age cretaceous age are proven as strong reservoir that is present in middle and lower indus basin but specially in Sawan area these are much deep and heterogeneous.

Petrophysical analysis is also taken into account for calculation of reservoir properties that are as volume of shale ($V_{sh}=20\%$), Porosity ($\Phi=17.3\%$), Average effective Porosity ($\Phi=11.4\%$) Resistivity of water formation ($R_w=66\%$), Saturation of water ($S_w=66\%$), Saturation of hydrocarbon ($S_h=34\%$) that definitely incorporated help in identification of potential zones by evaluation of reservoir properties by well logs. Reservoir sand is clearly dominating by facies trend and porosity variations are defined by cross plots.

Seismic Inversion is initiated by acoustic impedance that undoubtedly played an important role. Model based inversion of 3D data is performed for the recognition of dimensional dispersion of acoustic impedance in potential zone. Actually, Acoustic impedance gives a reflection between layer property and suitable interface property. It is a vast level translator so from well position a zero phase wavelet is calculated by the help synthetic trace and seismic trace contrasting filter. Then, by the translated horizon and well log data a low impedance model is built. Using acoustic impedance to predict porosity far from the well position by the help of seismic inversion. Core objective of Seismic backward modeling is to get high determination from low determination seismic info. Furthermore, Inversion technique combines rock physics and model based inversion. Undoubtedly seismic inversion is a non-unique problem and always ambiguities are associated with this method. Keeping in mind an equation is obtained which found that clean C-sand is shown by acoustic impedance and porosity. Successfully results are demonstrating the porosity, density bulk and shear moduli as well as P and S velocity in the prospect zone.

Table of Content

Chapter 1.....	1
INTRODUCTION.....	1
1.1 Introduction of Sawan Area	2
1.2 Previous Exploration Work	2
1.3 Data Sources	3
1.4 Seismic Data Details.....	3
1.5 Well Data Details.....	4
1.6 Objective of Study.....	4
1.7 Data Sets for Study.....	5
1. 8 Methodology.....	5
Chapter 2.....	7
GENERAL GEOLOGY.....	7
2.1 Introduction to General Geology	7
2.2 Play Summary.....	7
2.3 Tectonic Setting	7
2.4 Stratigraphic aspects of zone of study	8
2.5 Hydrocarbon Play of Area	9
2.5.1 Source rock	9
2.5.2 Reservoir	9
2.5.3 Trap and Seal.....	11
Chapter 3.....	12
3D Seismic data Interpretation	12
3.1 Types of Seismic data interpretation	12
3.1.1 Structural interpretation.....	12
3.1.2 Stratigraphic interpretation.....	12
3.2 Seismic Interpretation Workflow.....	13
3.3 Synthetic Seismogram.....	13
3.4 Marking of Seismic Horizons.....	14
3.5 Contour Plots	16

3.5.1 Time Contour Map of D-Sand	17
3.5.2 Depth Contour Map of D-Sand	18
3.5.3 Time Contour Map of C-Sand.....	19
3.5.4 Depth Contour Map of C-Sand:.....	20
3.5.5 Time Contour Map of B-Sand.....	21
3.5.6 Depth Contour Map of B-Sand.....	22
Chapter 4.....	24
Interpretation of Well Data	24
4.1: Introduction	24
4.2 Methodology.....	24
4.3 Objectives of petrophysical analysis	25
4.4 Volume of Shale	25
4.5 Porosity	26
4.6 Density Porosity	27
4.7 Sonic Porosity.....	27
4.8 Total Porosity	27
4.9 Effective Porosity	28
4.10 Neutron Porosity.....	28
4.11 Water Saturation (Sw)	28
4.11.1 Resistivity of Water (Rw).....	29
4.12 Hydrocarbon Saturation	30
4.13 Well Log Interpretation of Sawan-01.....	30
4.14 Well Log Interpretation of Sawan-07.....	32
4.14.1 Reservoir zone using Well Log Interpretation of Sawan-07	32
Chapter 5.....	35
Detailed Inversion Analysis of Sawan Area	35
5.1 Introduction	35
5.2 Model Based Inversion.....	36
5.2.1 Extracted Wavelet.....	37
5.2.2 Seismic to well correlation.....	37
5.2.3 Initial Model/Low frequency Model	38
5.3 Inversion Analysis.....	39

5.3.1 Model Based Inversion.....	39
5.3.1.1 Slice of Model Based Inversion	41
5.3.2 Band Limited Inversion	43
5.3.2.1 Slice of Model Based Inversion	45
5.3.3 Maximum Likelihood Sparse Spike Inversion.....	47
5.3.3.1 Slice of Maximum Likelihood Sparse Spike Inversion	49
5.4 Comparison between these deterministic Inversion techniques	51
Chapter 6.....	52
Rock-Physics Analysis with Cross-Plots	52
6.1 Introduction	52
6.2 Bulk Modulus	52
6.3 Shear Modulus	52
6.4 Poisson's ratio	52
6.5 Gassmann Theory	52
6.6 Cross-Plots of different parameters with porosity and density.....	54
DISCUSSIONS & CONCLUSIONS.....	63
REFERENCES.....	65

List of Figures:

Figure 1.1: Location map of study area.	3
Figure 2.1: Structural map of Lower Indus Basin with area of interest marked on the map.	8
Figure 2.2: Straightigraphic map of Sawan area. The C-Interval which is the member of Lower Goru Formation and a potential reservoir has been highlighted with red color.....	10
Figure: 3.1: Workflow for interpretation carried out in this case study.....	13
Figure 3.2: Synthetic Seismogram developed for Sawan-01 well correlated with the nearby traces. The wavelet indicates a correlation coefficient of 0.718 between the synthetic seismogram and the seismic traces.....	14
Figure 3.3: Seismic Section depicting the marked horizons after seismic to well tie with Sawan-01 well. The horizons of interest are D-sand, C-sand and B-sand of the Lower Goru Formation.....	15
Figure 3.4: Seismic Section with marked horizons based on the generated synthetic seismogram for Sawan-07 well.	16
Figure 3.5: Time Contour map of D Interval in Study area depicting greater time values towards south-east.....	18
Figure 3.6: Depth Contour map of D Interval in Study area depicting that the depth of formation is more towards the south-east.....	18
Figure 3.7: Time Contour Map of C-Sand of Study area depicting greater travel time values towards south-east.	20
Figure 3.8: Depth Contour Map of C-Sand of Study area indicating that the formation is deeper towards south-east.	21
Figure 3.9: Time Contour Map of B-Sand of Study area indicating more travel time towards south-east.....	22
Figure 3.10: Depth Contour Map of B-Sand of study area indicating that the formation is deeper towards south-east.	23
Figure 4.1: The workflow followed in this study to carryout petro-physical analysis.	25
Figure 4.2: Petro-physical results of well Sawan-01 representing reservoir zone.	31
4.3: Petro-physical results of well Sawan-07 representing reservoir zone.	33
Figure 5.1: Workflow for the carried out inversion.	35
Figure 5.2: Zero phase wavelet extracted from the seismic data near the well.	37
Figure 5.3: Synthetic Seismogram generated for Inversion analysis.....	38
Figure 5.4: Initial Modal generated for inversion.	39
Figure 5.5: Correlation wavelet for Model based inversion with error plot.....	40
Figure 5.6: Results for model based inversion.....	41
Figure 5.7: Slice showing the vertical view of Model based inversion for D sand.....	42
Figure 5.8: Slice showing the vertical view of Model based inversion for C sand.	43
Figure 5.9: Correlation wavelet for Band Limited inversion with error plot.	44
Figure 5.10: Band Limited inversion results indicating low impedance values in the zone of interest.....	45
Figure 5.11: Slice view of Band Limited inversion of D sand indicating Sawan-07 and 08 wells lies in the low impedance zone.	46
Figure 5.12: Slice view of Band Limited inversion of C sand indicating low impedance zone surrounding the wells.....	47

Figure 5.13: Correlation of Maximum Likelihood Sparse spike inversion.	48
Figure 5.14: Inversion results of Maximum Likelihood Sparse Spike.	49
Figure 5.15: Slice view of Maximum Likelihood Sparse Spike Inversion of D sand.	50
Figure 5.16: Slice view of Maximum Likelihood Sparse Spike Inversion of C sand.....	51
Figure 6.1: Lambda-Rho log crossplotted against Mu-Rho log from Sawan-01 well indicating gas zone with low lambda-Rho and moderate Mu-Rho values.....	55
Figure 6.2: Mu-Rho crossplotted against Lambda- Rho with effective porosity on z-axis indicating zone of interest.....	56
Figure 6.3: VpVs Ratio crossplotted with Lambda-Rho colored coded with shale volume indicating the zone of interest.	57
Figure 6.4: VPVs Ratio crossplotted against Lambda-Rho color coded with effective porosity indicating the zone of interest.....	58
Figure 6.5: VpVs Ratio crossplotted with P-Impedance with effective porosity on z-axis indicating zone of interest.....	59
Figure 6.6: VpVs Ratio crossplotted with P-Impedance colored coded with shale volume indicating zone of interest.....	60
Figure 6.7: Crossplot between Mu-Rho and Lambda-Rho colored coded with shale volume indicating zone of interest.	61
Figure 6.8: Crossplot between Mu-Rho and Lambda-Rho colored coded with shale volume indicating zone of interest.....	62

List of Tables:

Table 1: The wells used in this case study.	4
Table 2: Seismic Data used in this data set.....	5
Table 3: Wells Tops in MD (m) information.....	5
Table 4: Petro physical analysis results of zone-A Sawan-01	32
Table 5: Petro physical analysis results of zone Sawan-07	34

Chapter 1

INTRODUCTION

Pakistan is one of those blessed countries who have three major sedimentary basins (2:3 of total area). Indus basin is lying in east while as Baluchistan basin lies in the west and in north east is Pishin basin. Indus basin and Baluchistan are isolated with an Ornach-Nal transform fault zone. Pishin is isolated between Chaman and Indus transform faults. A different type of folds, bowl type structures and monoclines of different styles are available and recognized in Indus and Baluchistan basins due to various geological and geodynamical conditions. Punjab platform is arranged in the central part of Indus basin with a westbound of plunging monocline. Sargodha high are in north of Punjab limited by Sukkur fracture zone in south and in west it penetrated in Suleiman depression.

The hydrocarbons and mineral deposits are explored by using different important geophysical techniques for subsurface exploration. While taking measurements from subsurface to infer subsurface information is similar to remote sensing. Seismic reflection method simply works by sending a wave down the earth and a chain of receivers is laid down for data collection. Due to different densities of rock layers having different lithologies generates acoustic wave to reflect or refract back to surface which will be recorded. In now a days to explore hydrocarbons in petroleum industries 3D seismic method is widely in use because it gives a detailed picture of subsurface information not in vertical direction only but of entire volume of study area. The seismic signal used to alter by interacting with hydrocarbon bearing zones and other potential traps and reflect back to surface created a ground for geoscientists to interpret and extract useful information related to identification of anomalous zones as well as for mapping reservoir quality (Bacon, 2007).

To differentiate between reservoir and non-reservoir zones we always used to incorporate Petrophysical studies. It gives a brief understating about the interactions among rocks and fluids in it or hydrocarbons and related reservoir. Petrophysical properties like porosity, fluid saturation and volume of shale tells about the depositional setting of reservoir. The transmission and storage of hydrocarbons is totally dependent upon the interconnected pores (Donaldson and Tiab, 2004). Permeability of a reservoir is the main source of efficiency of reservoir. Hydrocarbon leads can be easily identified by the effective use of these techniques (Shamim et al, 2014). The well log cross plots are helpful for identifying lithologies with different variations on bigger scales.

Rock physics utilizes to display rock properties to see the concept of seismic wave passage mechanism from them. To thought this we simply have to understand that how the composition of a stone reflects the pressure strain effects in a complete elastic limit and then seismic reaction. Because of the materialness in hydrocarbon industries the pore liquid is specifically compelling its impact. According to standard elucidation process of seismic science of shake material is used

to explain relationship of versatile parameters and impedance picked from seismic information for explicit rock properties. This gives the idea about seismic that for what it will be physically fit and easy to settle and also obtain the non-uniqueness for a particular translation.

1.1 Introduction of Sawan Area

The area under study is Sawan gas field (approximately 2 Tcf) is situated in Khairpur district in Sindh. Further, it is in southern part of Lower Indus basin locked by Jacobabad high in north, in the east by Indian Shield Suleiman thrust fold belt in west and from south is bounded by Karachi Embayment zone. Sawan area is discovered in 1998 by OMV Pakistan and started production in 2003. This field is also considered as the large gas producing field which was a collective project of OMV Pakistan, ENI Pakistan, PPL and Government Holding Private Limited (GHPL). Sawan field is currently in producing phase and 14 wells out of 15 are producing that are supplying a major part of gas to SNGPL and SSGPL. Regionally Sawan field is located in extensional regime which is mostly containing normal faults. Trapping system is distally up-dip stratigraphic traps having structural features as well. The exploratory well Sawan-01 mostly targeting the amplitude anomaly and four way dip closure of small size (Afzal et al., 2005). In study area the major reservoir is C Interval sand which is deposited in shallow marine environment and restricted to northeast-southwest trending fairway. Major source rock found is Sembar formation deposited in shelf marine environment and in whole region it is proven as organic rich rock most suitable source rock along with Lower Goru member (Ahmed et al., 2004).

1.2 Previous Exploration Work

In Pakistan Early-Late Cretaceous Lower Goru sands are main source of production from previous two decades. Miano, Sawan, Badin and Kadanwari areas are the main producers in whole basin. Mostly companies like OGDCL and OMV etc. investigated Lower Goru sediments as a whole over the wider region. According to the several study models created by the OMV for the Sawan C sand, a proper and comprehensive model of the reservoir was established in 2003 by Oolithica Geoscience Ltd that was based on core sedimentology and well logs from 7 wells and 12 inlines and crosslines passing through the wells. The major outcome of this study was the identification of a depositional model in which 3 prograding major clinoforms were recognized in whole Sawan field (Afzal et al, 2005).

Sawan block have three divisions in general by two strike slip faults south, center and north compartment (Rehman and Ibrahim, 2009). My seismic 3D cube (10×10 km) is present in southern part. Central part of Sawan field is consisting with maximum drilled wells in whole Sawan block that is why it known as main tank of gas.

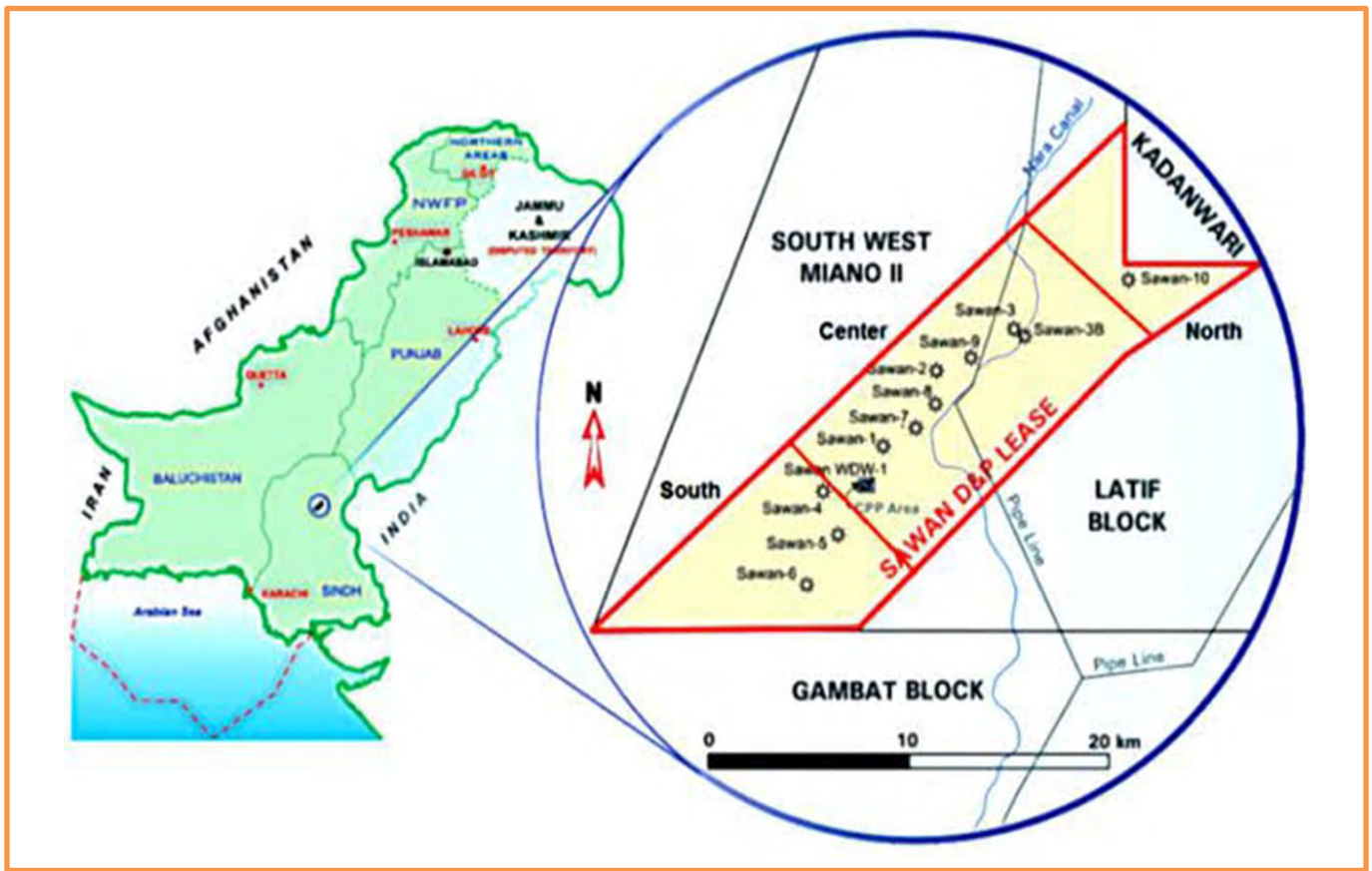


Figure 1.1: Location map of study area (Nadeem et al, 2004).

Study area in Lower Indus basin having following geographical coordinates ranging from:

Latitude of area is from $27^{\circ} 0' 9.666''$ N to $27^{\circ} 1' 21.5688''$ N

Longitude of area is from $68^{\circ} 53' 51.5832''$ E to $68^{\circ} 56' 47.76''$ E

1.3 Data Sources

To continue my study in Sawan block with the permission of Directorate General of Petroleum Concessions (DGPC) data is acquired from Land Mark Resources (LMKR). Details of data used for the study are as under:

- ❖ Formation tops
- ❖ Seismic Header files
- ❖ 3D Seismic Cube
- ❖ Navigation files
- ❖ Well Logs (Las Files)

1.4 Seismic Data Details

To study the area I have used 3D seismic cube of (10×10 km), horizons are marked in a proper way and because in Lower Indus basin especially in Sawan area due to normal faulting that is extended over the region with minor faults no proper explicit structure is found and marked.

Seismic data is provided by LMKR by the kind permission of DGPC. My cube of 3D data is consisting of In-lines and cross-lines. In-lines are from 718-864 in range and cross-lines are from 874-1005 in range.

1.5 Well Data Details

In my study data total three wells are used to for the proper guidance of seismic data, accurate horizon positions as well as other in-situ conditions, from well logs. Sawan-01, Sawan-07 and Sawan-08 helped me a lot in my research objectives. Sawan-07 well was most suitable for my research goals because it was in the middle of my 3D cube as well as other two wells.

To generate synthetic seismogram for the proper identification of horizons by well and seismic tie here I used Sawan-07 well and Upper Goru and C-Interval are successfully identified. All three wells Sawan-01, 07 and 08 are used for Petro-Physical analysis of the reservoir rock. All the details of coordinates, depth of wells and Upper Goru tops of every well is given below in Table.1.1

Table 1: The wells used in this case study.

Well Name	Latitude_N	Longitude_E	Well depth (m)	Formations (m) TLG
Sawan_1	26.991830	68.906994	3583	2692
Sawan_7	26.999291	68.923403	3398	2688
Sawan_8	27.009162	68.933396	3429	2695

1.6 Objective of Study

The main objective of this thesis work is proper demarcation of reservoir of Lower Goru Formation by integrated study of Seismic data and Petrophysical assessment.

- ❖ Identification of prominent structures by using seismic data for the most probable hydrocarbon zones for better accumulation of oil and gas as well as for the true information of subsurface configuration of prominent structures.
- ❖ Well logging analysis is also gone through for sake of proper calculation of reservoir properties like Resistivity of Formation water (R_w), Saturation of hydrocarbons (S_h), Saturation of water (S_w), Porosity (Φ), Volume of shale (V_{sh}) than after evaluating the well log data this will help us in identification of probable hydrocarbon zones.
- ❖ A simple rock physics analysis is also included for the calculation of basic rock physics properties like V_p , V_s and Density etc.
- ❖ A proper seismic inversion analysis is conducted by using Petrophysical analysis for reverse modeling of seismic data to resolve low frequency problems.

1.7 Data Sets for Study

There are two type of data sets are used for this dissertation;

Table 2: Seismic Data used in this data set.

Survey	Operator	Process Level	Area (Approximately)
SAWAN-3D-1998	OMV	FINAL FILTERED MIGRATION	10 Sq. Km

Table 3: Wells Tops in MD (m) information

Formation	Sawan-01	Sawan-07	Sawan-08
Habib Rahi	274	284	283
Ghazij	301	303	304
Sui Main limestone	1118	1117	1120
Ranikot	1262	1260	1259
Upper Goru	2449	2443	2433
Lower Goru	2697	2690	2715
D Interval	3181	-	3195
C Interval	3247	3242	3240
B Interval	3459	-	-

Base Map:

In following figure the base map of the study area is given in which Well location and the orientation of Inline and Crosslines of 3D seismic survey are shown that are used for the research purpose of Sawan area.

1. 8 Methodology

In study area to attain the objectives of interest study is gone through the following steps:

- ❖ The horizons of interest are marked on inlines according to previous knowledge and continuity of patterns of reflection on seismic sections by using different possibilities and literature review.
- ❖ Synthetic Seismogram is created using density and sonic logs of Sawan-01 well.
- ❖ Horizons of interest are tied properly with well to seismic tie on all seismic sections.
- ❖ To identify the sweet zone in study area amplitude maps (D, C and B horizons) are generated.
- ❖ Depth maps of these horizons are also prepared by using velocity models, simple velocity model creation technique, of zone of interest in study area.
- ❖ To identify the original depth of reservoir zone and also to check accuracy of velocity model depth contour maps are created.

- ❖ To proceed for inversion analysis after data input seismic traces are converted into reflectivity by deconvolving this inverse series (RC).
- ❖ By following the previous procedure here also synthetic seismogram is generated for correlation of seismic to well data.
- ❖ In deterministic inversion three types (MBI, BL and MLSS) are used to characterize the Zones of interest in study area.
- ❖ Separate models of all three inversion types are created through well to seismic correlation.
- ❖ Slices of these models are also generated to identify the extent of zone of interest in study area.
- ❖ Petrophysical and rock physics analysis are also gone through in study area for the calculation of different parameters of interest in reservoir zone.

Chapter 2

GENERAL GEOLOGY

2.1 Introduction to General Geology

Geological information of any area is very important in a sense that it gives maximum information about that area regarding geological features in which depositional sequences, structure types, modes of deformation and types of rocks etc. can be identified. According to the location of study zone it is in Khairpur district in Lower Indus Basin of Pakistan. Khairpur zone is a basement high which is covered by deserts of sands from eastern side and some carbonates of Eocene near Sukkur and Khairpur areas (Afzal et al., 2005). In general view study area is bounded by Jacobabad high in north, India Shield in east, Suleiman thrust and fold belt in west and Karachi embayment in south of Sawan area (Kadri, 1995).

2.2 Play Summary

In Lower Goru C interval is producing reservoir which contains sands and in fairway it is trending in northeast-southwest (Afzal et al., 2005). Sembar formation is source rock which is Lower Cretaceous shale with shelf marine deposits. Almost from 0.5-1.7% total organic content is available in source rock that is type-III kerogen which is present in gas generation window in late Cretaceous to early Tertiary times (Wandrey et al., 2004). In Eocene times the latest inversion process is took place and mechanism of trapping is exactly relative to generation, migration and then prevention (Ahmed et al., 2004).

2.3 Tectonic Setting

In Lower and Central Indus basins mostly reservoir zones are situated on different structural highs like Mari and Jacobabad high etc. These structures are much more important for a substantial accumulation of hydrocarbons during migration (Kazmi and Jan, 1997). First Tertiary unconformity was built in Cretaceous Tertiary (K-T) uplift and recognized as base unconformity and almost all faults terminate at this boundary. Mostly in whole Cretaceous strata fault is NW-SE oriented and from single Chiltan to many faults in Lower and Upper Goru level. All these features are due to first unconformity generation when Eurasian and Indian plates were transtensionally interacted with each other and counter clockwise movement of Indian plate. Second uplift occurred in Late Eocene Oligocene in Central and Lower Indus basins. The structural highs possibly experienced frequent periods of disturbance in response to the succeeding phases of thrust loading in the west and northwest. This is probably the time in which shapes of the traps finally improved and possibly the secondary migration and reservoir charge took place (Ahmad et al., 2004).

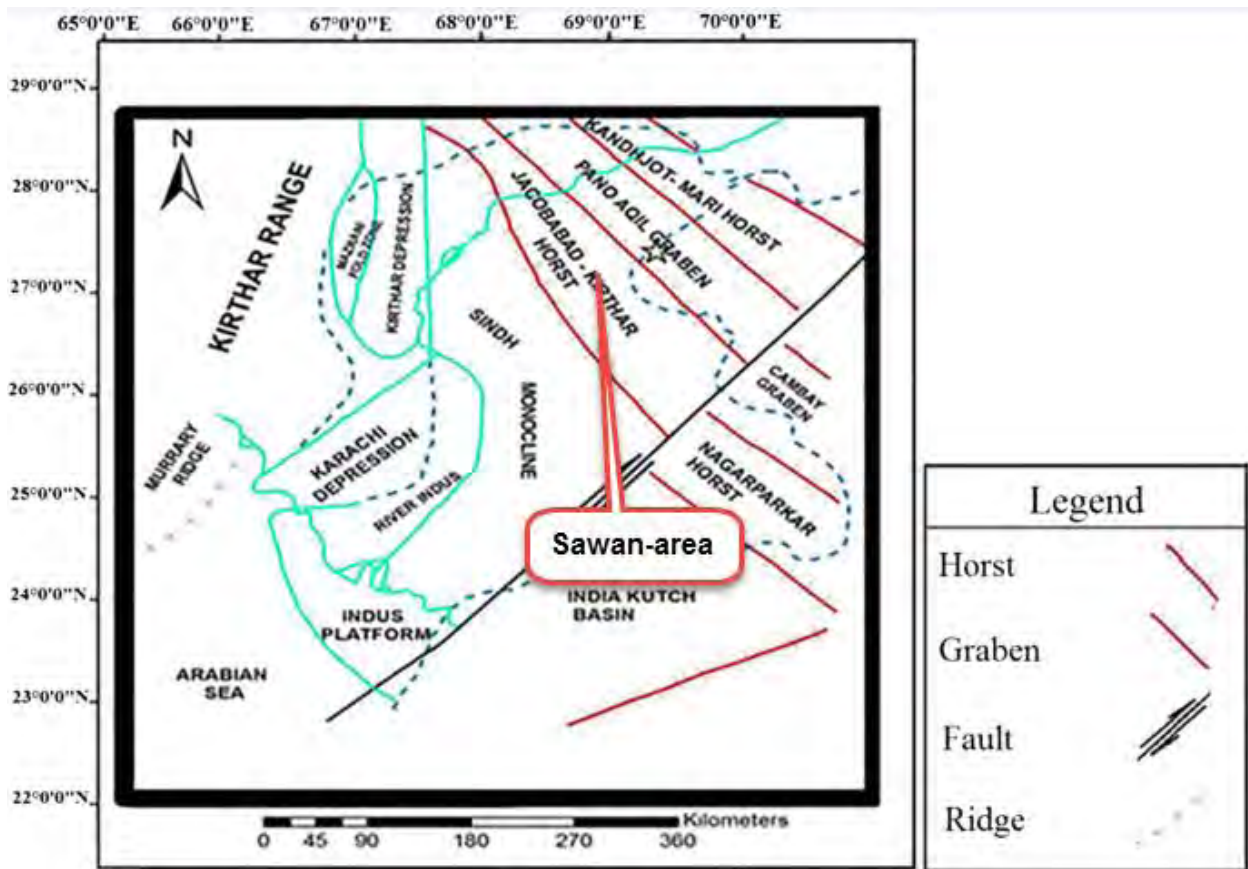


Figure 2.1: Structural map of Lower Indus Basin with area of interest marked on the map (Razza et al, 1990).

Cretaceous times because of extensional regime development of tilted fault is evident at large scale in eastern parts of Lower Indus sub-basin. Analysis of seismic reflectors of interested area reveal that these tilted fault systems having normal dip broke down strata of Cretaceous and older times, whereas these faults of Cretaceous times have strike from N 30° W to N 50° W.

The system of tilted fault traps existed at the time of generation of hydrocarbons. Additionally traps formed due to faults in sandstones of Lower Goru are controlling the trapping mechanism of hydrocarbons in vicinity of Miano block (Kemal, 1991). The regional framework of active tectonic of Pakistan is observable and by utilizing coordinates study zone is marked.

2.4 Stratigraphic aspects of zone of study

In figure 2.2 the stratigraphic chart of zone of interest shows the generalized regional stratigraphy of Lower Indus basin and illustrates that the rocks age ranges between Jurassic and Tertiary. The Triassic rock sequence is overlain by the Jurassic limestone of Chiltan in Sawan area, whereas the Chiltan limestone is overlain by heavy strata of Sember formation shales

having approximate thickness of 610m. Lower Goru formation is present just above the Sembar formation that acts as main source strata in the region. Further classification of Lower Goru includes five divisions, in which Sembar formation is overlain by Basal sands, Basal sands are overlain by Lower shales, whereas Lower shales are overlain by Middle sand, and fifth unit of Lower Goru is present between Upper and Middle sand, which is displayed in Fig 2.2. The environment of deposition was shallow to deltaic marine conditions in case of Upper sands hence in Lower part of Indus basin it is considered as an excellent reservoir (Alam et al. 2002).

Stratigraphically, early Cretaceous inter-bedded shales of Lower Goru as well as shales of Sembar formation are the major documented source strata of petroleum present in southern part of the Indus basin. Whereas the secondary source strata in west of southern Indus basin are the transgressive marine shales of Upper Paleocene age, which are buried (Zaigham and Mallick, 2000).

Target formation in zone of study is basal sands, which is sub-unit of Lower Goru Formation. Huge Sands having multiple thicknesses in the area also acts as a remarkable reservoir, which is producing state. It may be possible that sub-unit of lower Goru i.e. Basal sands are overlain by the reservoir rock, though it is not proven till today (Kadri I.B, 1995).

Generally, in southern part of Lower Indus basin seal rocks are Cretaceous Sembar formation composed of transgressive shales and Kirthar, Laki-Gazij and Bara-lakhira of Tertiary age (Zaigham and Mallick, 2000). Effective horizontal and vertical seal is provided by Lower Goru shales, which are Inter-bedded. These shales successfully offer effective seal across the fault; however it is obvious that faults sometimes also provide an operative seal. Talhar shales, shales of Upper and Lower Goru perform as principal seal rocks for reservoir sands of Lower Goru (Kadri et al, 1995).

2.5 Hydrocarbon Play of Area

Total petroleum play includes three important Formations as follow:

- ❖ **Sembar Formation**
- ❖ **Goru Formation**
- ❖ **Chiltan Formation**

2.5.1 Source rock

The Sembar Formation of Cretaceous age is the vital hydrocarbon generating source rock which is organic rich shales deposited in shelf marine environment in this region and other parts of the Indus Basin.

2.5.2 Reservoir

The Upper Cretaceous Lower Goru C sands are reservoir in Sawan Gas Field. The Sawan structure is seismically interpreted to represent a low stand wedge, the product of a fall in

relative sea level or forced regression (Ahmad et al., 2004). The identified low stand wedge is a well-defined seismic feature. It is more difficult to define where the reservoir sands merge with the more typical shelf facies of the C interval. The reservoir strata in Sawan area is Basal Sand, which is sub-unit of Lower Goru formation and produces hydrocarbons from its several sands layers having varying thicknesses. The overlain reservoir probability on Basal sands in Lower Goru is difficult to ignore however the existence of this reservoir is still a subject to be proven (Kadri, 1995).

The Lower Goru sandstones are the primary targets for hydrocarbon producing reservoir rocks. These sandstones were formed due to rifting episodes during end times of early Cretaceous as a result of erosion occurred on Indian shield and re-deposition of the sediments because of sequences of barrier bars and deltaic sands in various parts of middle and lower Indus Basin, down dip to West (Hussain et al, 1991).

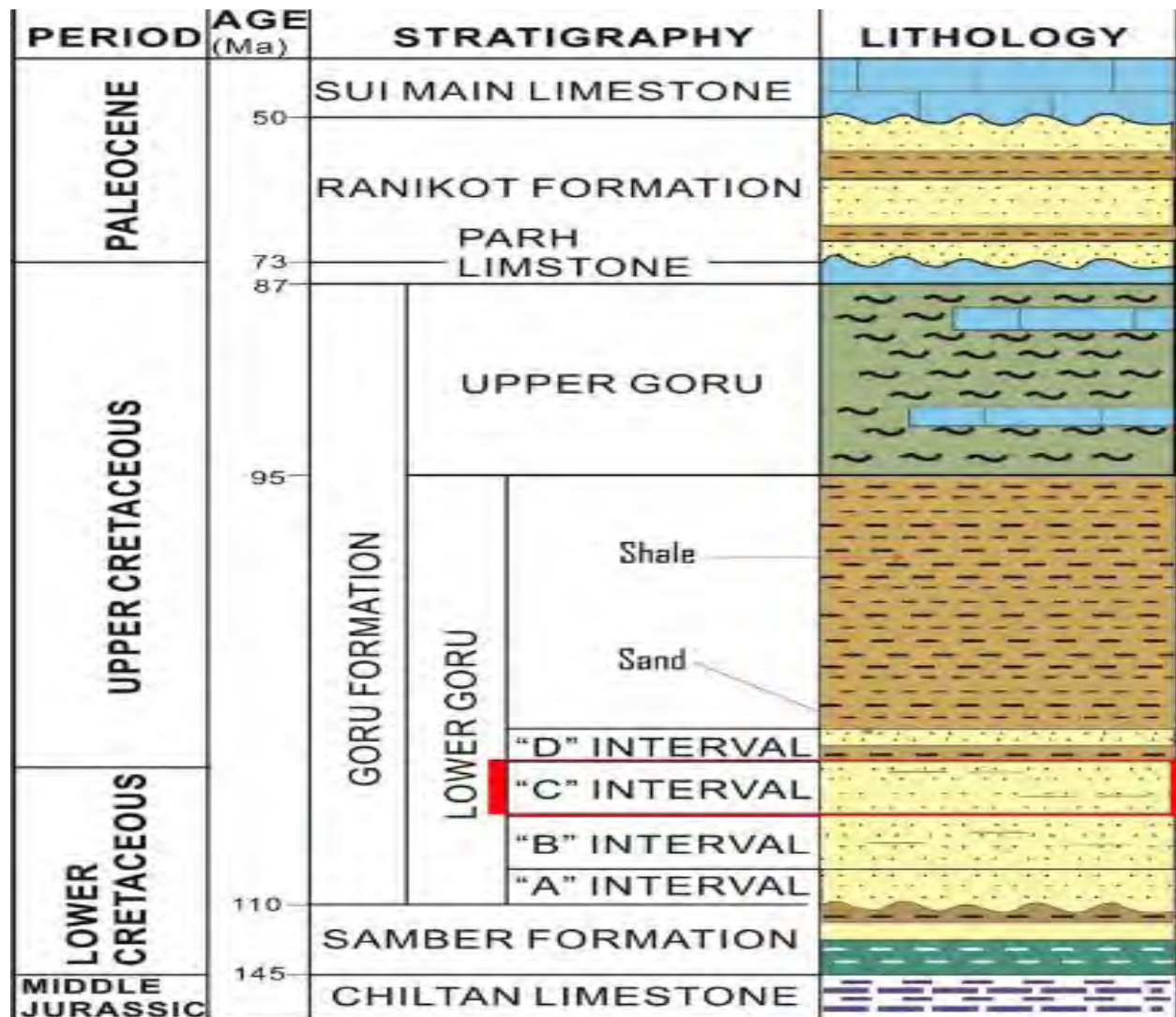


Figure 2.2: Straightigraphic map of Sawan area.

The C-Interval which is the member of Lower Goru Formation and a potential reservoir has been highlighted with red color.

2.5.3 Trap and Seal

The Sawan gas accumulation is a combined structural/stratigraphic trap identified at top C interval and has a small northeast-southwest trending four-way dip closure with a seismic pinchout towards the north, northwest and southeast. The feature is 17Km in length and cut by small fault in the southwest. The mapped areal size is approximately 63km². Forced regressive deltaic distributary channel and mouth bars and upper shore face belts form the stacked sand bodies of Sawan C sand reservoir. In the vicinity of the fresh water entry points early diagenetic Fe-Chlorite coatings around the coarse and medium sand grains preserve the porosity and permeability during late burial. Due to Paleotopography and accommodation space, thicker sedimentary pile was deposited in the Sawan north area whereas thinner sand sheets were deposited in the south. In the Sawan north area a significant thickness of these stacked survived erosion during regression and subsequent transgression. However, in the south only a part is present is preserved which is why the prediction of the reservoir sand presence is highly uncertain in the Sawan south region. There is very thick sequence of shales and marl overlying the Sawan reservoir sands which act as regional top seal. Shales within the Lower Goru C interval also act as bottom and lateral seal (Munir et al., 2011).

Structural traps are the major source of hydrocarbon's production in zone of study. Traps formed by tilted faults are result of extension regime because of rifting events as well as of horst and grabens geometry. The chronological associations between generations of hydrocarbon, formation of traps, exclusion, migration, as well as trapping of hydrocarbons is not consistent all over the Indus Basin, providing appropriate trapping mechanism alongside negative structures and slanted fault blocks.

The seal rocks in south of Indus basin are Kirthar, Laki-Ghazij and Bara-Lakhra formations (Zaigham & Mallick, 2000). Effective primary vertical as well as horizontal seal in Lower and Upper part of Indus basin is provided by Lower inter-bedded Goru Shales. The top flat seal for topmost sands division of Lower Goru are offered by Upper Goru formation (Kadri, 1995).

Chapter 3

3D Seismic data Interpretation

The transformation of seismic reflection data into a structural image of the subsurface or the extraction of useful facts and figures using processed data obtained after collection and processing of data from seismic surveying, this process of conversion is termed as Interpretation of Seismic data. Seismic data interpretation is considered as an essential component during exploration of Hydrocarbon's (Avseth et al., 2005). The basic idea is to get the subsurface information. The subsurface information obtained from the seismic data shows horizon boundaries and sub-surface fault locations (Hilterman, 2001).

Based on the interpreted Seismic data useful Models are generated to get the better understanding of subsurface by Identifying and marking consistent Horizons for mapping any Geological structures, Stratigraphy, which help to get the understanding of Reservoir's build up style, hydrocarbon accumulations, extent and volume of the reserve (Stewart, 1984). Delineation of faults and demarcation of Horizons is the most significant job that is performed during interpretation of seismic data. Traditionally all reflectors are marked by utilizing shot points alongside the upright seismic section. Time for these picked points decided through observing various reflection times. After determining times, a map of these times is prepared along with a contour map, which represents local features having more elevations or structures such as local anticlinal features, which may have vast potential hydrocarbons (Sheriff, 1973).

3.1 Types of Seismic data interpretation

Interpretation of processed seismic data extracted from the extensive processing of the acquired seismic data is carried out by two different methods:

3.1.1 Structural interpretation

The Structural interpretation aims to map structural traps on the seismic section in the search for the structures containing hydrocarbons, discontinue reflections clearly shows faults and undulating shows folded beds. These sub-surface structures are traps in which hydrocarbons may be trapped, featuring a potential reservoir (Coffeen 1986).

3.1.2 Stratigraphic interpretation

Seismic sequences are identified and mapped during Stratigraphic interpretation of the seismic data. This approach develops the understanding the depositional environment of various lithological units through detailed study of multiple characteristics of seismic facies, which are most probably an accurate indicator of depositional environment. Whereas the examination of variations in reflection physiognomies is used to determine changes both in depositional as well as stratigraphic environment keeping in view the prospect for hydrocarbons. Seismic reflection amplitudes and velocities are the helpful tools for detail study. Drainage patterns are incredibly

significant in identifying unconformities, after recognizing these unconformities depositional environment of some specific area can be easily developed. An unconformity is a prominent stratigraphic trap (Telford et al., 1990).

3.2 Seismic Interpretation Workflow

Procedure adapted for seismic data interpretation. First, it is necessary to install Kingdom software (2017) on the computer. Preparation of base map involves steps such as loading of SEG-Y files and navigation data in software. Differentiations of prominent reflectors in which researchers are interested are marked manually with the help of synthetic seismogram. Additionally, faults are recognized and marked during this course Horizon marking. Contours are computed for reflectors along with generation of polygons for faults to determine structural anticlines as well as synclines or depressions.

Schematic interpretation of three-dimensional seismic data comprises of various following stages:

- ❖ Loading Navigation and SEG-Y data
- ❖ Base map formulation
- ❖ Tying of well data with seismic data
- ❖ Identifying marking of prominent reflectors
- ❖ Time and Depth contour maps generated

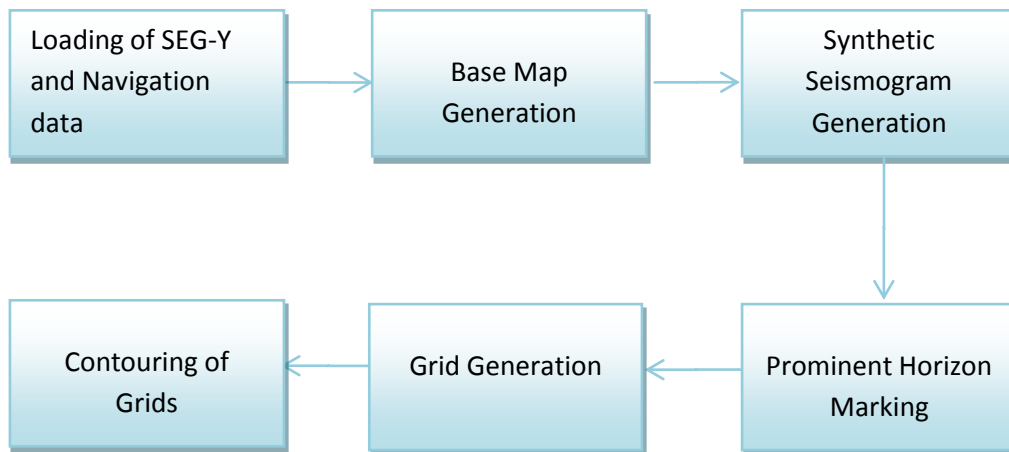


Figure: 3.1: Workflow for interpretation carried out in this case study.

3.3 Synthetic Seismogram

Modeled traces in seismic interpretation that are obtained from synthetic seismograms and are significantly crucial while correlating seismic reflections with encountered subsurface stratigraphy. Seismic data is provided in time scale, and well tops are given in depth so we cannot mark horizons in time form. So, the purpose of generation of synthetic is to find two way travel time against each depth for marking of horizons. A sonic log is usually incorporated to generate a synthetic seismogram. However, the involvement of density log is also suggested

ideally, but their availability is a major concern. By using DT and RHOB logs reflectivity series is obtained which is further convolved with the source wavelet to get synthetic seismogram. In procedure of relating seismic section to borehole geology synthetic seismograms appears as a beneficial tool due to their ability to develop direct relationships among patterns of seismic reflections and investigated subsurface lithology's (Handwerger et al., 2004)

For the identification of the exact position of the concerned horizons in the subsurface of Sawan area, a synthetic seismogram is produced by utilizing Sawan-01 that is situated at Inline-721, and cross-line 960 is prepared which is shown in Figure 3.2. The primary area of interest consists of those horizons, which were identified on a seismic section. In figure 3.2 the designated horizon at the lowermost part of the figure represents a portion of Lower Goru that locates the position of D interval, C Interval and B Interval respectively. C Interval is main reservoir in these horizons.

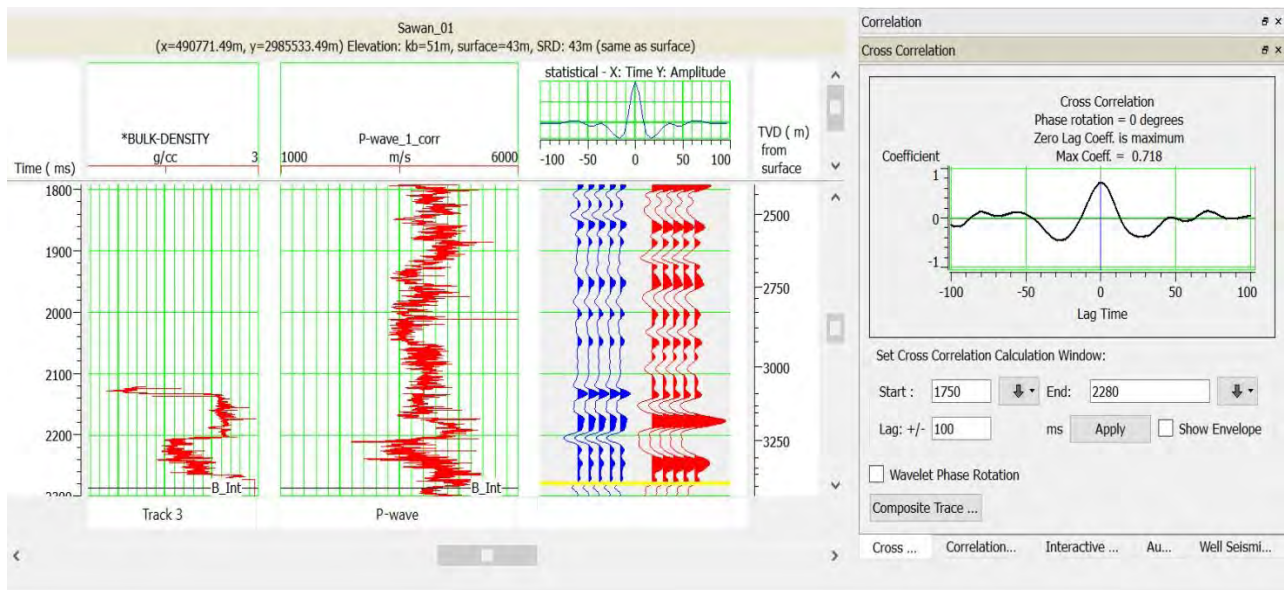


Figure 3.2: Synthetic Seismogram developed for Sawan-01 well correlated with the nearby traces. The wavelet indicates a correlation coefficient of 0.718 between the synthetic seismogram and the seismic traces.

3.4 Marking of Seismic Horizons

The primary task of interpretation is the identification of various horizons as an interface between geological formations. Change in lithology causes the acoustic impedance contrast, due to which primary reflection originates. These reflections are marked on the seismic sections to understand the relationship between geology and seismic sections (Badly, 1985). The reflectors D Interval, C-Interval and B Interval are marked on the seismic data after generating synthetic (Figure 3.3, 3.4).

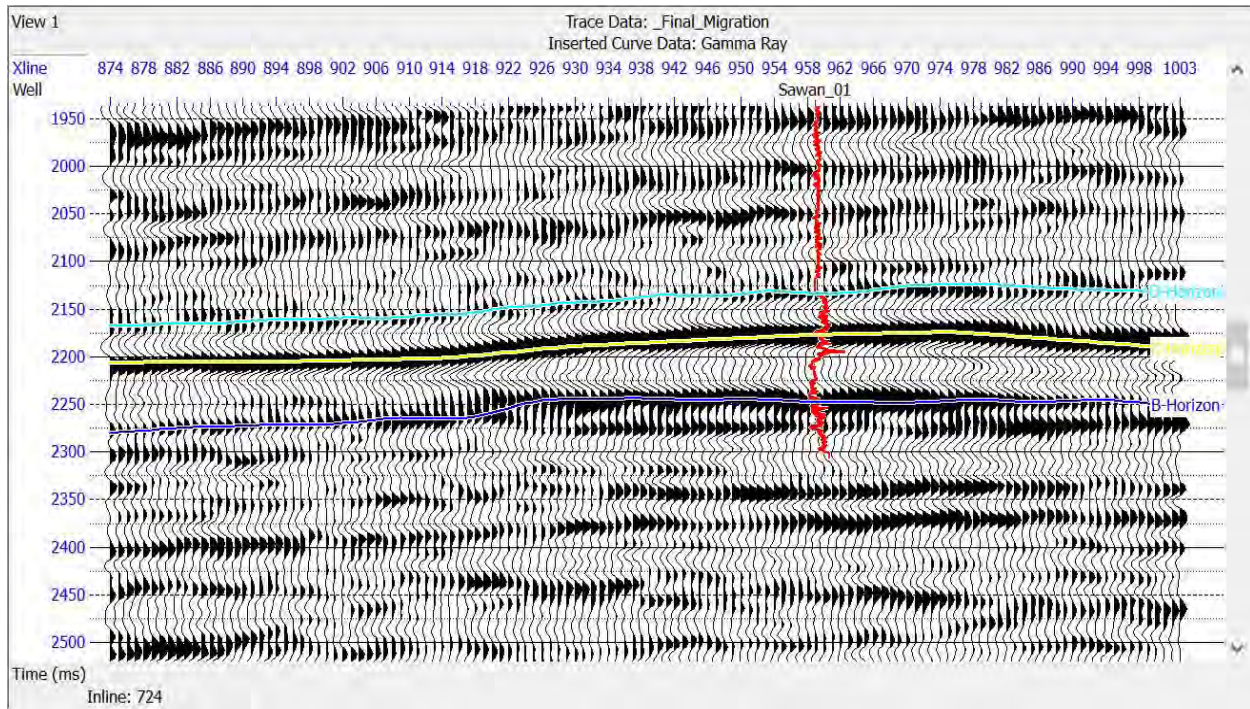


Figure 3.3: Seismic Section depicting the marked horizons after seismic to well tie with Sawan-01 well. The horizons of interest are D-sand, C-sand and B-sand of the Lower Goru Formation.

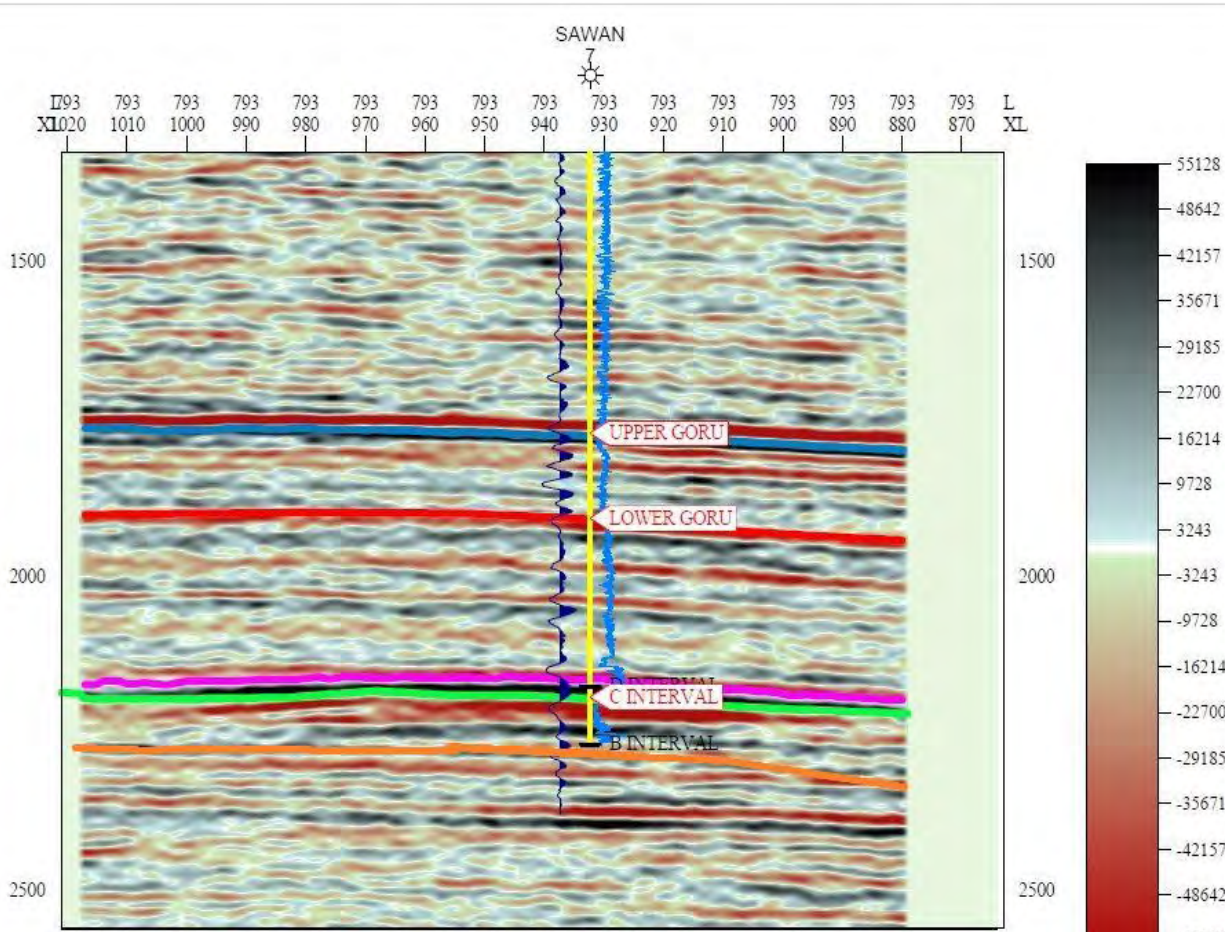


Figure 3.4: Seismic Section with marked horizons based on the generated synthetic seismogram for Sawan-07 well.

3.5 Contour Plots

The most significant and primary constituent during interpretation of seismic data is contouring. Contours are the lines of equal values, whereas these values may be of depth or time scattered throughout the map (Coffeen, 1986). The contours present on a map of a given formation show its topography style as it would appear if the rocks above that particular formation are removed. With the help of Base Map as well as incorporating time sections that were interpreted, contour maps of time for D Interval, C-interval and B Interval are developed.

Essential information such as information about formation dip, nature of folding and faulting, nature of formation structural relief and trusted information of formation slope could be extracted from these contours maps. Whereas data used to generate contour maps is acquired from picked times of concerned reflectors having prospects for hydrocarbons on the seismic section.

The 3D seismic cube (10 sq. km) issued by DGPC has no prominent faults or other structure. The upper part of Lower Goru formation encompasses abundant shales that act as a seal for the

whole region. The lowermost stratum of formation of Lower Goru contains sands with shales that are inter-bedded. The sands of Lower Goru are further classified into different categories like A, B, C, D sands. Sembar formation act as source rock and lies below Lower Goru formation while above Lower Goru lies Upper Goru Formation.

3.5.1 Time Contour Map of D-Sand

Lower Goru contains in Sawan area, which fulfills the requirements of reservoir rock in that region, thus prove its ability to be a good quality reservoir sands. Moreover, source rock for these sands is the underlying Sembar Formation.

D Interval present in the Lower Goru formation acts as reservoir stratum in the interested area of study. In time map the Contour interval is 1.2ms (i.e. 0.0012s). The Lower Goru time Contour range is from 2.190s (i.e., 2190ms) to 2.226s (i.e., 2226ms) (Figure 3.5). The time Contour map of D-Sand is shown. The yellow colour in the colour bar represents shallower part while the blue colour represents the deeper part (Figure 3.5). The North to NW corner and the center of the map shows the shallowest part while the deeper part lies in the NE and Southern corner. Close lines in the NE and Southern part of the Contour map shows steepness which indicates a sharp change in the depth of D-Sand (Figure 3.5).

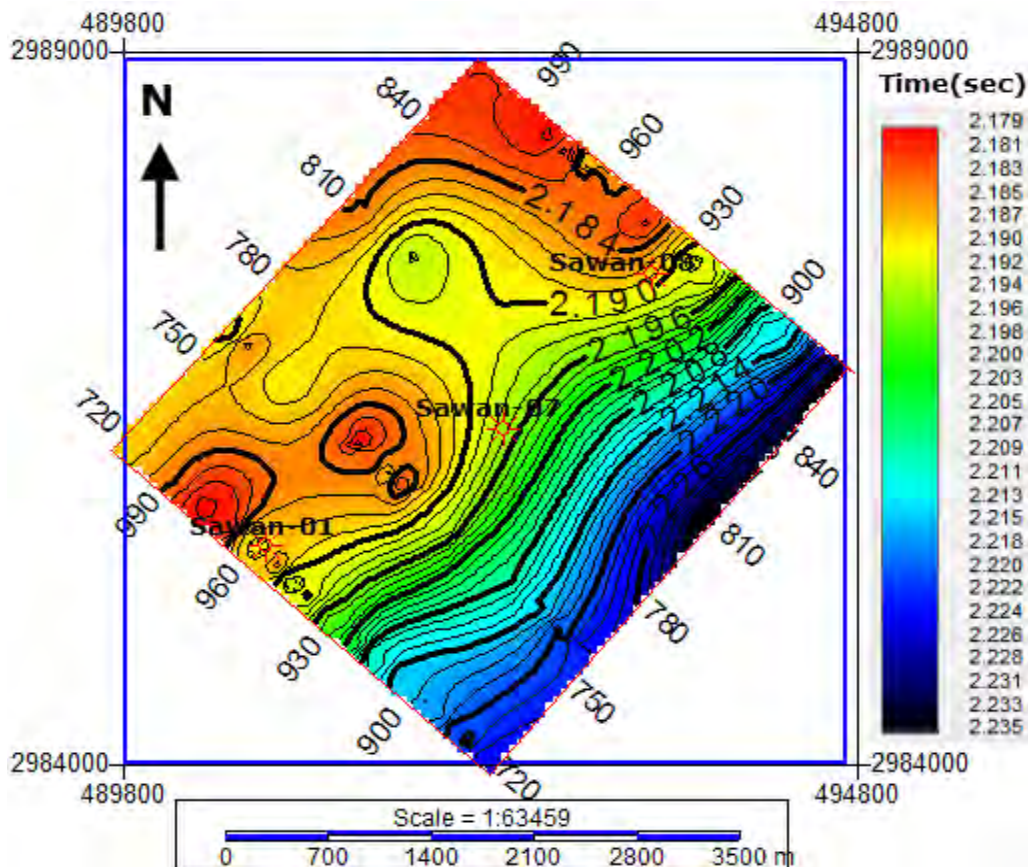


Figure 3.5: Time Contour map of D Interval in Study area depicting greater time values towards south-east.

3.5.2 Depth Contour Map of D-Sand

Lower Goru contains in Sawan area, which fulfills the requirements of reservoir rock in that region, thus prove its ability to be a good quality reservoir sands. Moreover, source rock for these sands is the underlying Sembar Formation.

D Interval present in the Lower Goru formation acts as reservoir stratum in the interested area of study. In depth map the Contour interval is 2.6m. The D Interval depth Contour range is from 3185m to 3250m. The depth Contour map of D-Sand is shown in Figure 3.6. The yellow colour in the colour bar represents shallower part while the blue colour represents the deeper part (Figure 3.6). The North to NW corner and the center of the map shows the shallowest part while the deeper part lies in the NE and Southern corner (Figure 3.6). Close lines in the NE and Southern part of the Contour map shows steepness which indicates a sharp change in the depth of D-Sand (Figure 3.6).

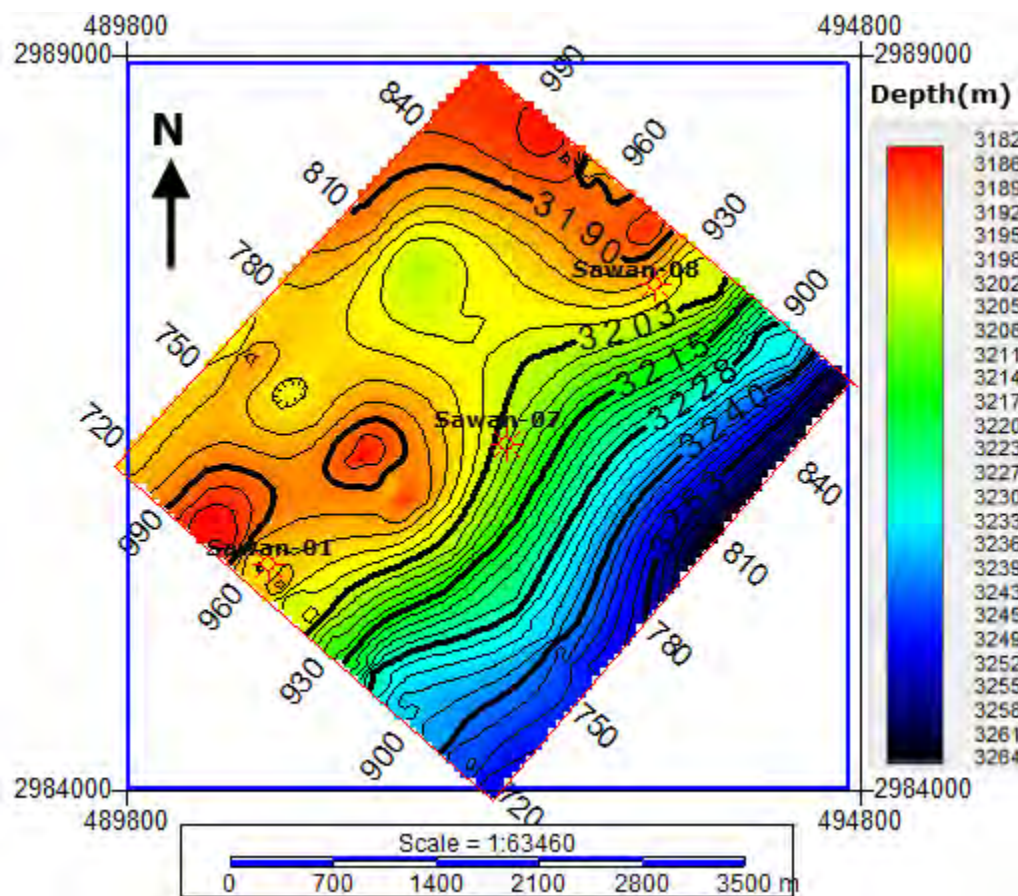


Figure 3.6: Depth Contour map of D Interval in Study area depicting that the depth of formation is more towards the south-east.

3.5.3 Time Contour Map of C-Sand

Lower Goru contains in Sawan area, which fulfills the requirements of reservoir rock in that region, thus prove its ability to be a good quality reservoir sands. Moreover, source rock for these sands is the underlying Sembar Formation.

C Interval present in the Lower Goru formation acts as reservoir stratum in the interested area of study. In time map the Contour interval is 1.2ms (i.e. 0.0012s). The C Interval time Contour range is from 2.225s (i.e., 2225ms) to 2.280s (i.e., 2280ms). The time Contour map of C-Sand is shown in Figure 3.7. The yellow colour in the colour bar represents shallower part while the blue colour represents the deeper part (Figure 3.7). The North to NW corner and the center of the map shows the shallowest part while the deeper part lies in the NE and Southern corner. Close lines in the NE and Southern part of the Contour map shows steepness which indicates a sharp change in the depth of C-Sand (Figure 3.7).

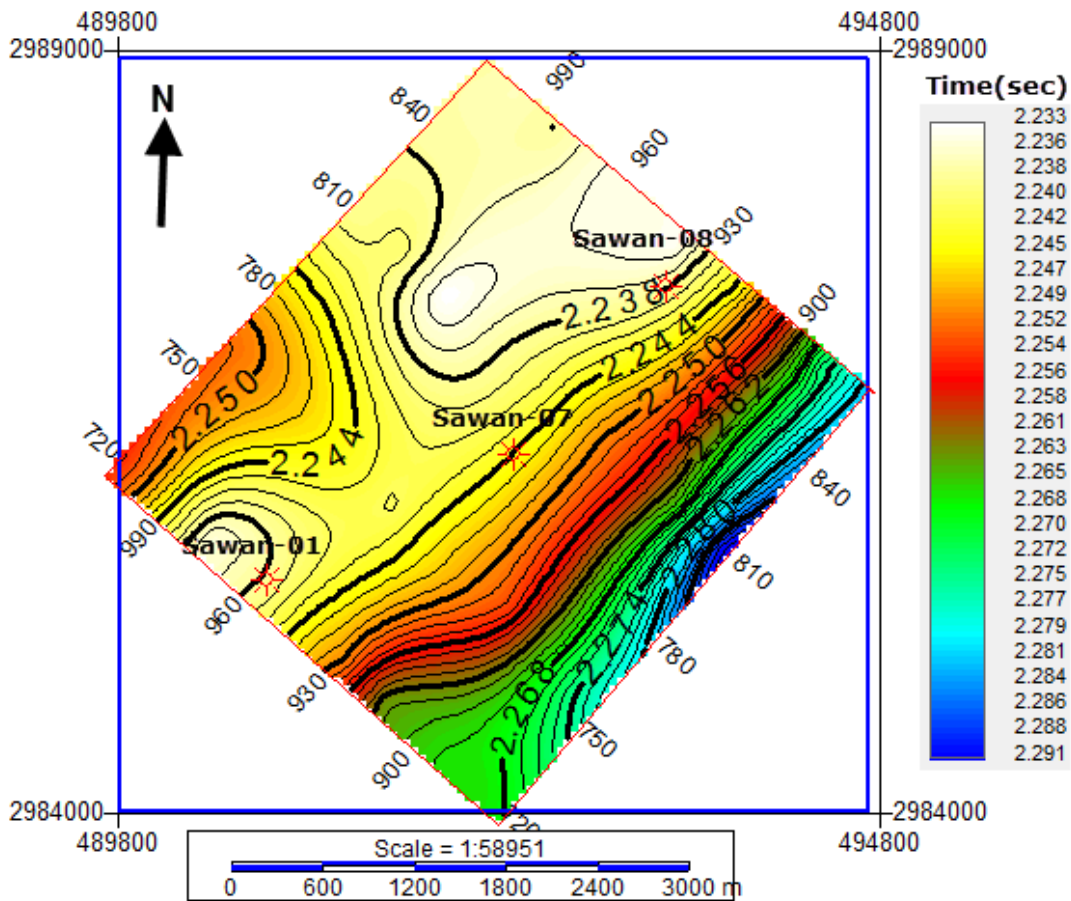


Figure 3.7: Time Contour Map of C-Sand of Study area depicting greater travel time values towards south-east.

3.5.4 Depth Contour Map of C-Sand:

Lower Goru contains in Sawan area, which fulfills the requirements of reservoir rock in that region, thus prove its ability to be a good quality reservoir sands. Moreover, source rock for these sands is the underlying Sembar Formation.

C Interval present in the Lower Goru formation acts as reservoir stratum in the interested area of study. In depth map the Contour interval is 2m. The C Interval depth Contour range is from 3220m to 3310m. The depth Contour map of C-Sand is shown. The yellow colour in the colour bar represents shallower part while the blue colour represents the deeper part (Figure 3.8). The North to NW corner and the center of the map shows the shallowest part while the deeper part lies in the NE and Southern corner (Figure 3.8). Close lines in the NE and Southern part of the

Contour map shows steepness which indicates a sharp change in the depth of C-Sand (Figure 3.8).

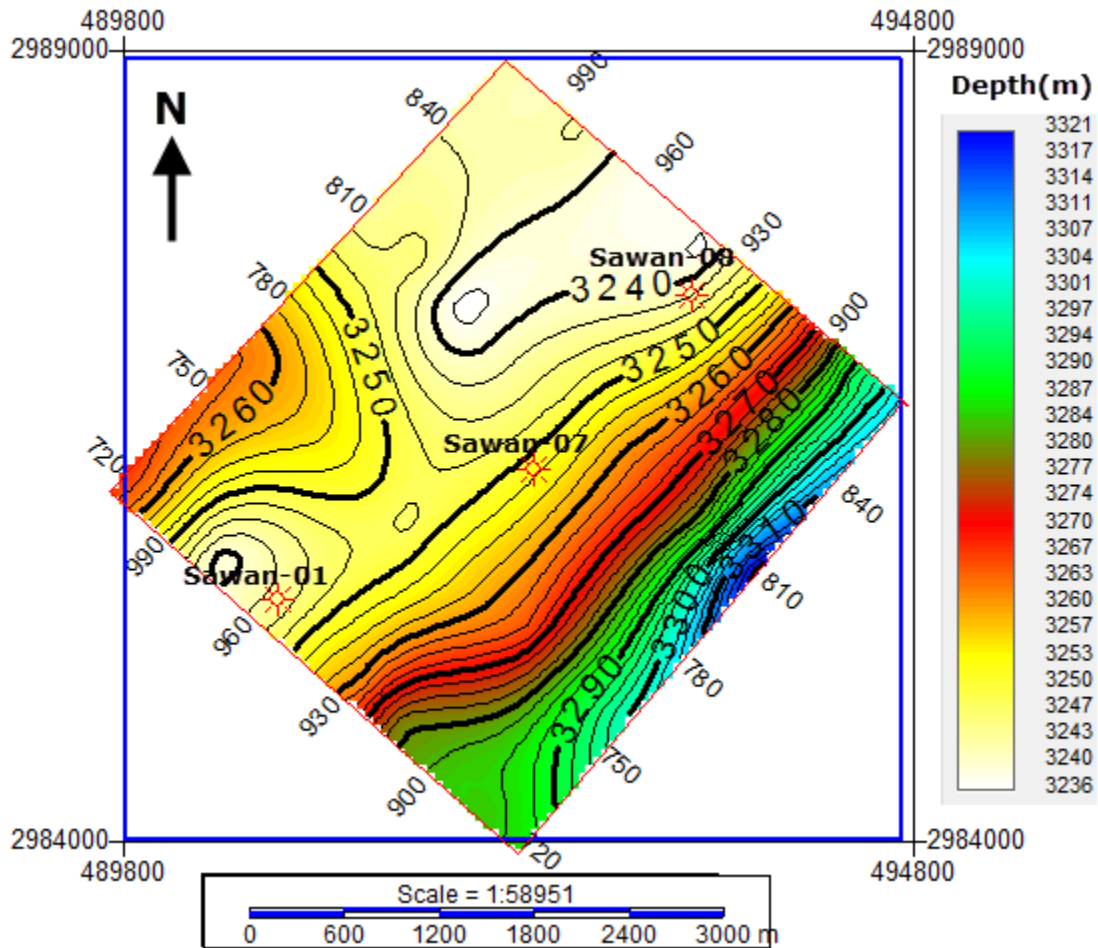


Figure 3.8: Depth Contour Map of C-Sand of Study area indicating that the formation is deeper towards south-east.

3.5.5 Time Contour Map of B-Sand

Lower Goru contains in Sawan area, which fulfills the requirements of reservoir rock in that region, thus prove its ability to be a good quality reservoir sands. Moreover, source rock for these sands is the underlying Sembar Formation.

B Interval present in the Lower Goru formation acts as reservoir stratum in the interested area of study. In time map the Contour interval is 1ms (i.e. 0.001s). The B Interval time Contour range is from 2.330s (i.e., 2330ms) to 2.360s (i.e., 2360ms). The time Contour map of B-Sand is shown. The yellow colour in the colour bar represents shallower part while the blue colour represents the

deeper part (Figure 3.9). The North to NW corner and the center of the map shows the shallowest part while the deeper part lies in the NE and Southern corner (Figure 3.9). Close lines in the NE and Southern part of the Contour map shows steepness which indicates a sharp change in the depth of B-Sand (Figure 3.9).

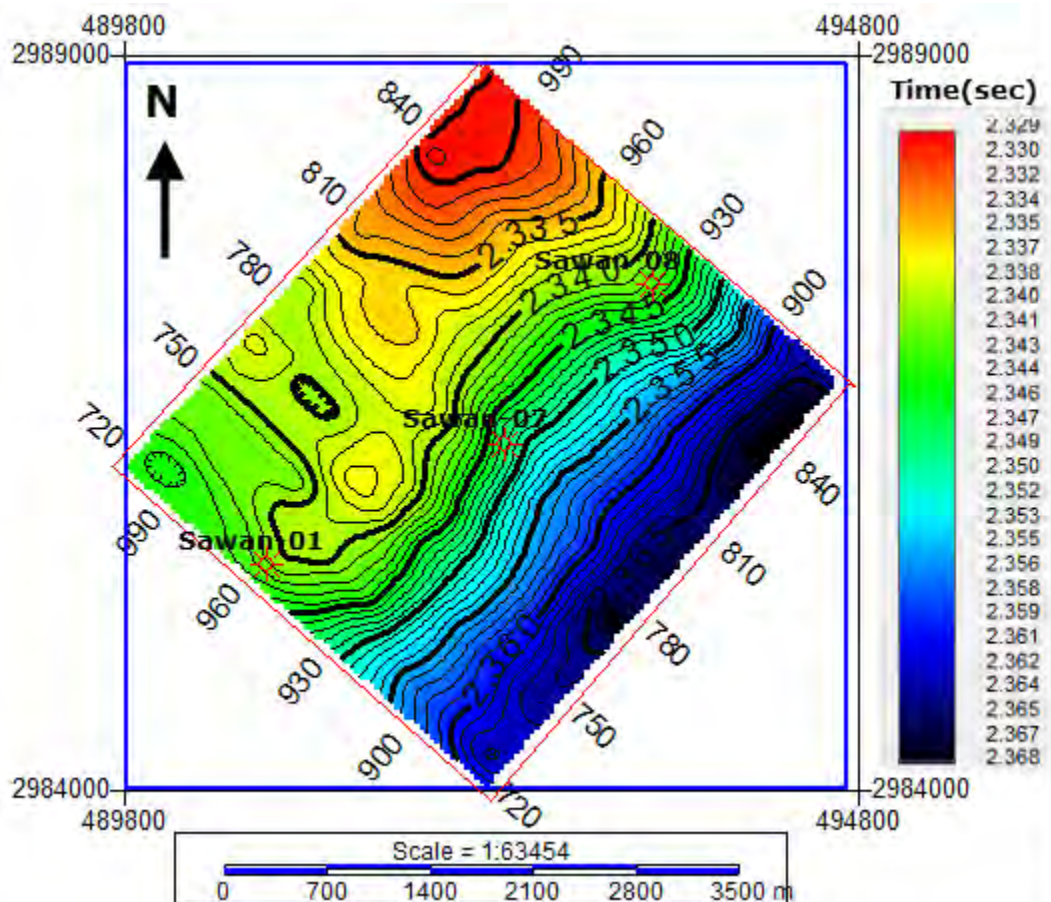


Figure 3.9: Time Contour Map of B-Sand of Study area indicating more travel time towards south-east.

3.5.6 Depth Contour Map of B-Sand

Lower Goru contains in Sawan area, which fulfills the requirements of reservoir rock in that region, thus prove its ability to be a good quality reservoir sands. Moreover, source rock for these sands is the underlying Sembar Formation.

B Interval present in the Lower Goru formation acts as reservoir stratum in the interested area of study. In depth map the Contour interval is 1.2m. The B Interval depth Contour range is from 3450m to 3498m. The depth Contour map of B-Sand is shown. The yellow colour in the colour bar represents shallower part while the blue colour represents the deeper part (Figure 3.10). The North to NW corner and the center of the map shows the shallowest part while the deeper part lies in the NE and Southern corner (Figure 3.10). Close lines in the NE and Southern part of the

Contour map shows steepness which indicates a sharp change in the depth of B-Sand (Figure 3.10).

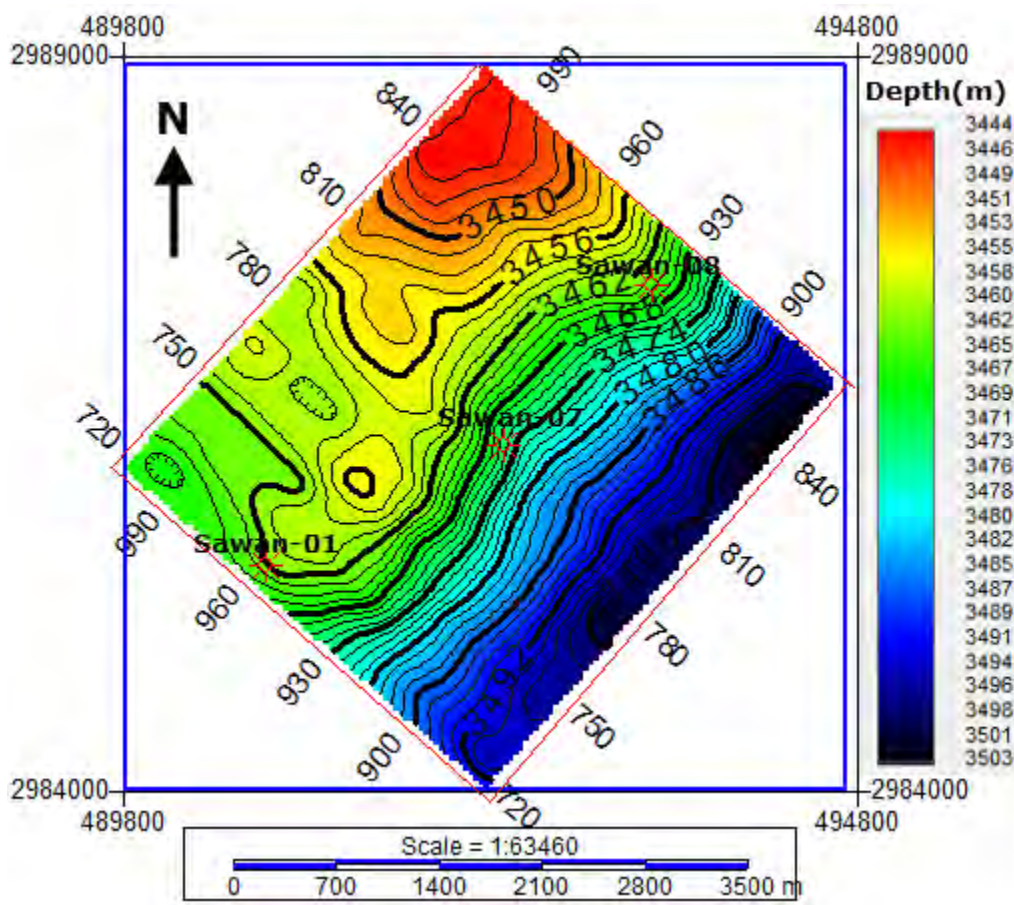


Figure 3.10: Depth Contour Map of B-Sand of study area indicating that the formation is deeper towards south-east.

Chapter 4

Interpretation of Well Data

4.1: Introduction

Petrophysical analysis gives a deep insight of fluid, its identification and quantification in reservoir rocks (Ali et al., 2015). Petrophysical analysis centered on the well log which is continuous record of any geophysical parameter against the depth in the well bore (Rider, 1906). Basically well logs are used to confirm the lithologies and fluid presence in rock. The purpose of Petrophysical analysis is to measure the different rock properties and also their connections to the fluids (Donaldson and Tiab, 2004). The potential prospect and non-prospect zones are identified by integrating Petrophysical results with rock physics which authorizes geoscientists to extract essential results. The description of reservoir is done on the basis of Petrophysical results.

There are lot of newly established geophysical well logs be present. Geophysical logs made up of highly focused tools are most well-known among others because of their structure. These logs can be run before casing of well without delay after drilling which is called as Measurement While Drilling (MWD) and also at the time of formation drilling called as Logging While Drilling (LWD). Usually, the deviation of directional well are determined by MWD logs and log type measurements such as resistivity, density and others are done by LWD (Rider, 1996).

4.2 Methodology

Treasured extracted information through log data help to identification of reservoir, separation of payable reservoir zone by applying a constraint on rock properties and volumetric reserve estimation. Petrophysical studies have been accomplished for the classification of reservoir properties of Sawan area. Well logs data of Sawan-07 has been utilized to assess the different formations. Following parameters are projected using logs data are shale volume, density porosity, effective porosity, total porosity, water saturation and hydrocarbon saturation. Wireline log data comprises Gamma ray log (GR), Caliper log, Spontaneous log (SP), Laterolog deep (LLD), Laterolog Shallow (LLS), Micro spherically focused log (MFSL). Neutron log (NPHI), Density log (RHOB) and Sonic log (DT), Wireline logs placed into three different tracks on the basis of reservoir properties approximation and working principle shown in Figure 4.1. First

track is known as lithology track, second track is known as resistivity track and third track is known as porosity track.

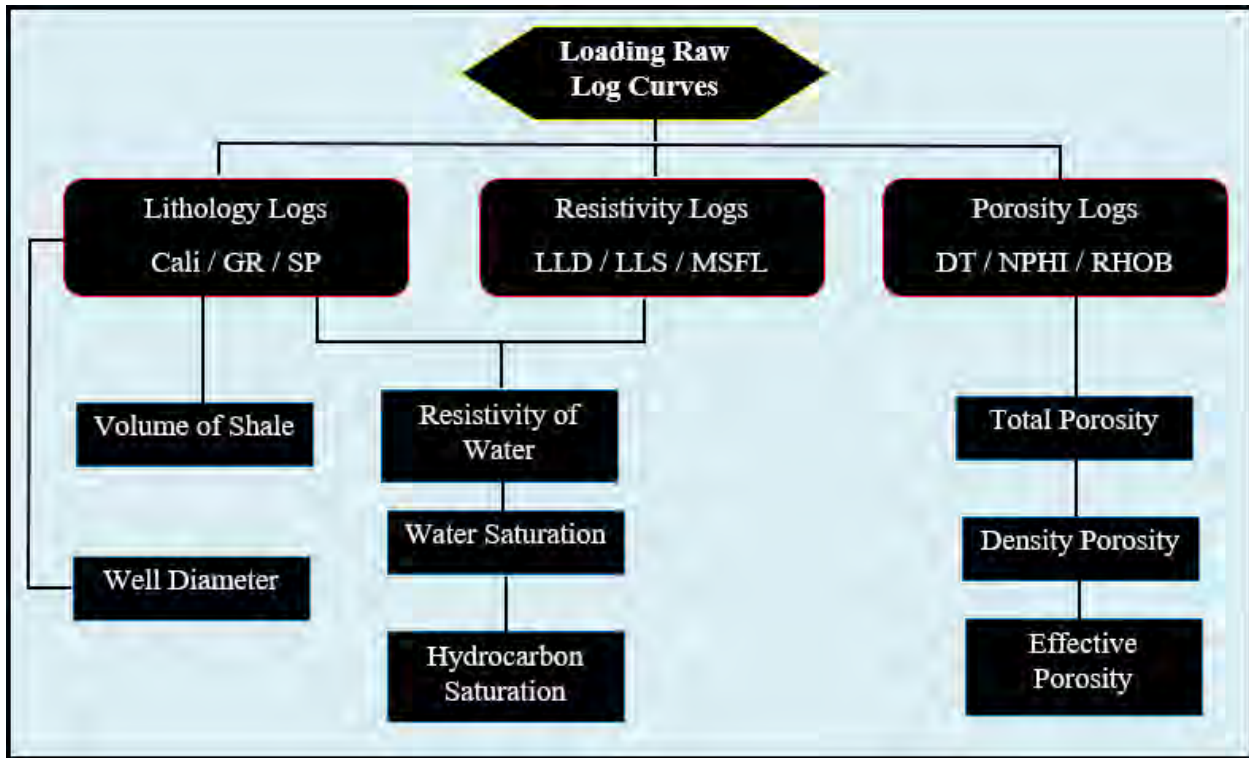


Figure 4.1: The workflow followed in this study to carryout petro-physical analysis.

4.3 Objectives of petrophysical analysis

The Petrophysical analysis has been carried out in order to measure the reservoir description of the Sawan area using the borehole data of Sawan-01 and Sawan-07 well. The logs defined above will be used in order to calculate the reservoir parameter such as:

- ❖ Volume of shale (Vsh)
- ❖ Porosities (PHID, PHIT, PHIE)
- ❖ Water Saturation (Sw)
- ❖ Hydrocarbon Saturation (H.C)
- ❖ Net Pay or Net Reservoir

4.4 Volume of Shale

We have two methods:

❖ Linear method

In linear method we compute Index Gamma Ray by following formula:

$$IGR = \frac{GR_{log} - GR_{min}}{GR_{max} - GR_{min}} \quad (4.1)$$

❖ Non-Linear Method:

In non-linear method we have various formulas like Stabier, Larinov and Clavier to compute minimum volume of shale. We apply the one which give us minimum volume of shale. And mostly Stabier give us minimum volume of shale.

➤ **Stabier:** (Most preferable)

$$Vsh = \frac{IGR}{3 - 2 IGR} \quad (4.2)$$

Where, IGR=Index Gamma Ray, Vsh is Volume of Shale

➤ **Larinov:** (Used for Older rocks)

$$Vsh. = 0.33(2^{2 * IGR} - 1). \quad (4.3)$$

➤ **Clavier:**

$$Vsh. = 1.7 - (3.38 - (IGR + 0.7)^2)^{0.5} \quad (4.4)$$

4.5 Porosity

In the next step, we have to calculate porosity parameters, like:

- ❖ Density Porosity
- ❖ Sonic Porosity
- ❖ Total Porosity
- ❖ Effective Porosity
- ❖ Neutron Porosity (Given)

4.6 Density Porosity

Density log is the porosity log that measure electron density of the formation (Asquith et al., 2004). Formation electron density is related to bulks density of formation. It is the sum of fluid density multiplies its relative volume plus matrix density time relative volume.

Density log can be used to find out the correct porosity of the formation, if the matrix densities in the formation or rock type are known (Asquith et al., 2004).

$$RHOB \phi = \frac{RHOB \text{ mat} - RHOB \text{ log}}{RHOB \text{ mat} - RHOB \text{ fluid}} \quad (4.5)$$

Where $RHOB \phi$ is the density porosity, $RHOB \text{ log}$ is density log, $RHOB \text{ mat}$ is value of matrix density, $RHOB \text{ fluid}$ is density of fluid. The value of $RHOB \text{ mat}$ given in the exercise is 2.65 g/cm^3 , which is for sandstone and $RHOB \text{ fluid}$ is 1 g/cm^3 .

4.7 Sonic Porosity

Sonic logs measure the interval transit time (Δt) of the compressional sound wave through the formation. The interval transit time is related to the porosity of the formation. The unit of measure is the microseconds per foot or microseconds per meter (Asquith et al., 2004). Porosity of the formation can be calculated by using the following formula:

$$\phi_s = \frac{\Delta T_{\text{log}} - \Delta T_{\text{matrix}}}{\Delta T_{\text{fluid}} - \Delta T_{\text{matrix}}} \quad (4.6)$$

Where ϕ_s represents the sonic porosity, ΔT_{matrix} is the interval transient time of the matrix, ΔT_{log} interval transient time of formation, represents the transient time of the fluid (salt mud=185 and fresh mud=189).the interval transient time of the formation depends upon the matrix material, its shape and cementation (Wyllie et al , 1956).If fluid (hydrocarbon or water) is present in the formation, transient interval time is increases and this behavior shows increase in porosity which can be calculated by using sonic log (Asquith et al , 2004).

4.8 Total Porosity

Sum of the porosities that are obtained from the different logs divided by number of logs from which porosity is calculated. Here C-Interval is reservoir for which the average porosity is

calculated, to zone of interest reservoir, all the logs are interpreted. The relation is given below through which average porosity is calculated:

$$\phi_{avg} = \frac{\phi_n + \phi_d + \phi_s}{3}, \quad (4.7)$$

Where, ϕ_{avg} is the average porosity calculated from the available porosities, ϕ_n is the neutron porosity, ϕ_d is the density porosity and ϕ_s is the sonic porosity.

4.9 Effective Porosity

This will define as “the ratio of the volume of interconnected pore spaces in a rock unit to the total volume of the rock by removing shale effect that rock unit”. The zone rich in the shale, effective porosity will be zero there. Effective porosity is used to mark the saturated zone. The effective porosity can be calculated by the following formula (Asquith et al, 2004).

$$\phi_e = \phi_{avg} \times (1 - V_{sh}) \quad (4.8)$$

Where ϕ_e is effective porosity which is to be calculated, ϕ_{avg} represent the average porosity and V_{sh} represent volume of the shale.

4.10 Neutron Porosity

Neutron log is sensitive to the hydrogen atoms present in a formation and determination of the porosity of a formation. Count rate will be low in high porosity rocks and vice versa. Neutron porosity is given in the data and calculated by well log with respect to depth.

4.11 Water Saturation (Sw)

Water saturation in the formation can be defined as “The percentage of the pore volume filled by water in the formation”. Different models are used for water saturation such as Archie's equation, Indonesian and Dual water based on the lithology. For a clean sand Archie's equation (4.12) gives an accurate result. Indonesian equation is used for dirty formation. Thin interbedded shale sequences degrade the quality of C-Interval sand. So, water saturation is estimated through Indonesian equation (4.9).

$$SW_{Indonesia} = \left\{ \frac{\sqrt{\frac{1}{Rt}}}{\left(\frac{V_{sh}^{(1-0.5V_{sh})}}{\sqrt{Rsh}} \right) + \sqrt{\frac{\phi_e^m}{a.Rw}}} \right\}^{(2/n)} \quad (4.9)$$

Where, Sw is water saturation. Rt is a true resistivity of formation, V_{sh} is shale volume, Rsh is a resistivity of shale, ϕ_e is effective porosity, Rw is water resistivity value, m is a cementation factor and 'a' is tortuosity factor.

4.11.1 Resistivity of Water (Rw)

Calculation of resistivity of water (Rw) is key for water saturation. Numerous parameters like bottom hole temperature (BHT), surface temperature, water salinity in ppm and SP (Static) are important for valuation of water resistivity (Rw) (Amigun et al., 2012).

Two methods have been applied for resistivity of water:

- ❖ SP Method
- ❖ Pickett cross plot Method

SP Method

In this method, we must have borehole temperature and resistivity of mud filtrate.

$$Ssp = -K * \log \left(\frac{Rmf}{Rw} \right), \quad (4.10)$$

For K:

$$K = 65 + 0.24 * T^{\circ}C \quad (4.11)$$

We can find value of SSP from $Sp \log$ curve as SSP is the maximum deflection towards negative side, and Rmf is given resistivity of mud filtrate.

So then saturation of water in the formation can be calculated by the following Archie equation:

$$S_w = \sqrt[n]{\frac{F \times R_w}{R_t}}, \quad (4.12)$$

Where, F is formation factor which is

$$F = \frac{a}{\phi^m}, \quad (4.13)$$

Here, R_w is the resistivity of water calculated from above equation, R_t is the true formation resistivity, n is the saturation exponent, a is the constant, in case of sand represents effective porosity, m is the cementation factor and its value is taken 2.15 for the sandstone.

4.12 Hydrocarbon Saturation

Hydrocarbon saturation can be defined as “the pore in formation is filled with hydrocarbon”. It can be calculated by using the following mathematical relation:

$$S_H = 1 - S_w \quad (4.14)$$

Where S_H represents hydrocarbon saturation and S_w represents Water saturation.

4.13 Well Log Interpretation of Sawan-01

Lower Goru formation encountered in sawan-01 well assessed as most prolific sands for hydrocarbon exploration. A zone of interest has been marked on the basis of separation between LLD and LLS, large cross over between neutron porosity and density and low volume of shale as shown in Figure 4.2. The calculated Petrophysical results of the zone of interest listed in Tables 4.1 suggested that Lower Goru Formation dominated by clean sand with high effective porosity value 10-16% and low water saturation 35-45%. The depth of zone-A ranges from 3250-3270 m (Figure 4.2).

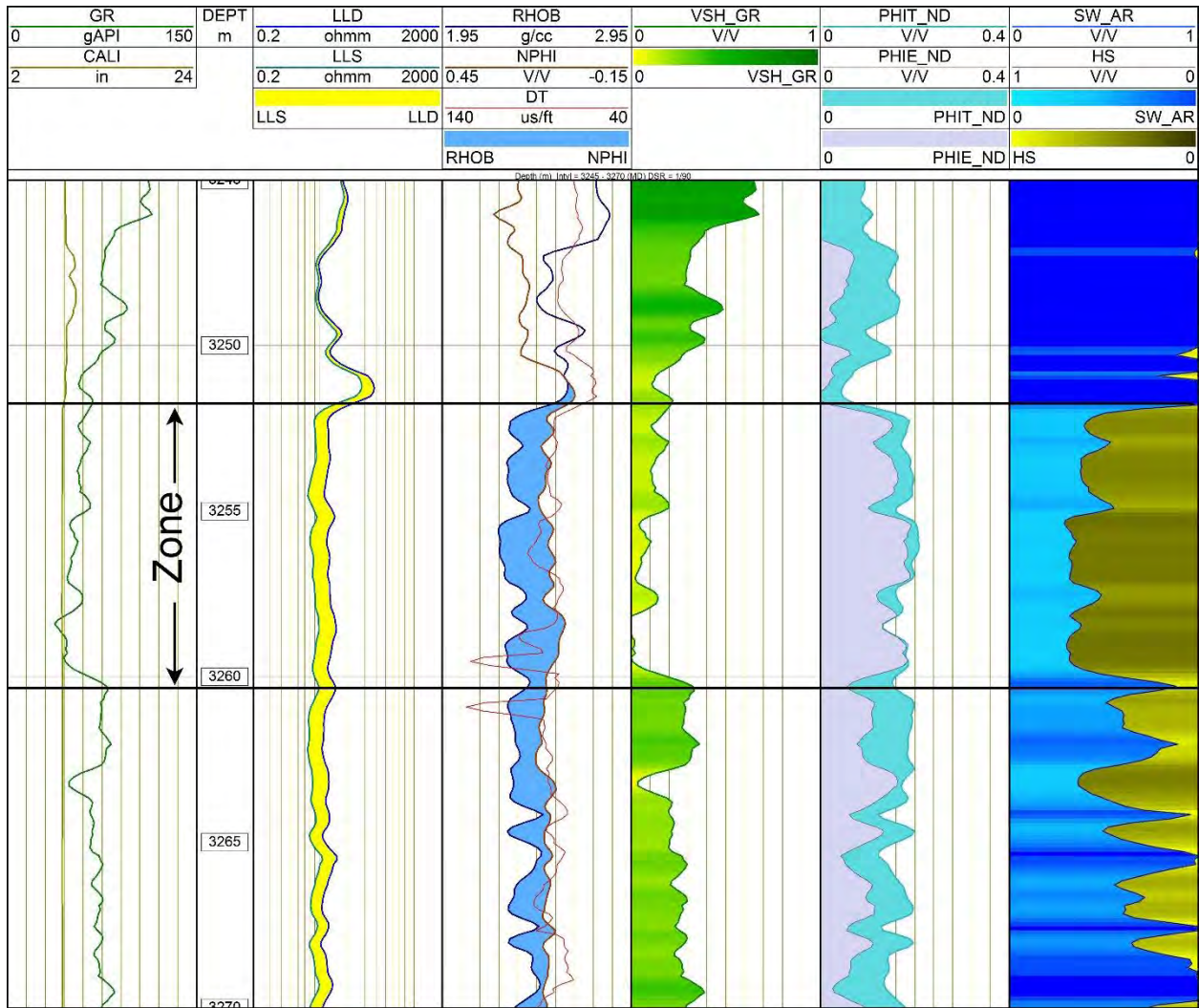


Figure 4.2: Petro-physical results of well Sawan-01 representing reservoir zone.

Table 4: Petro physical analysis results of zone-A Sawan-01

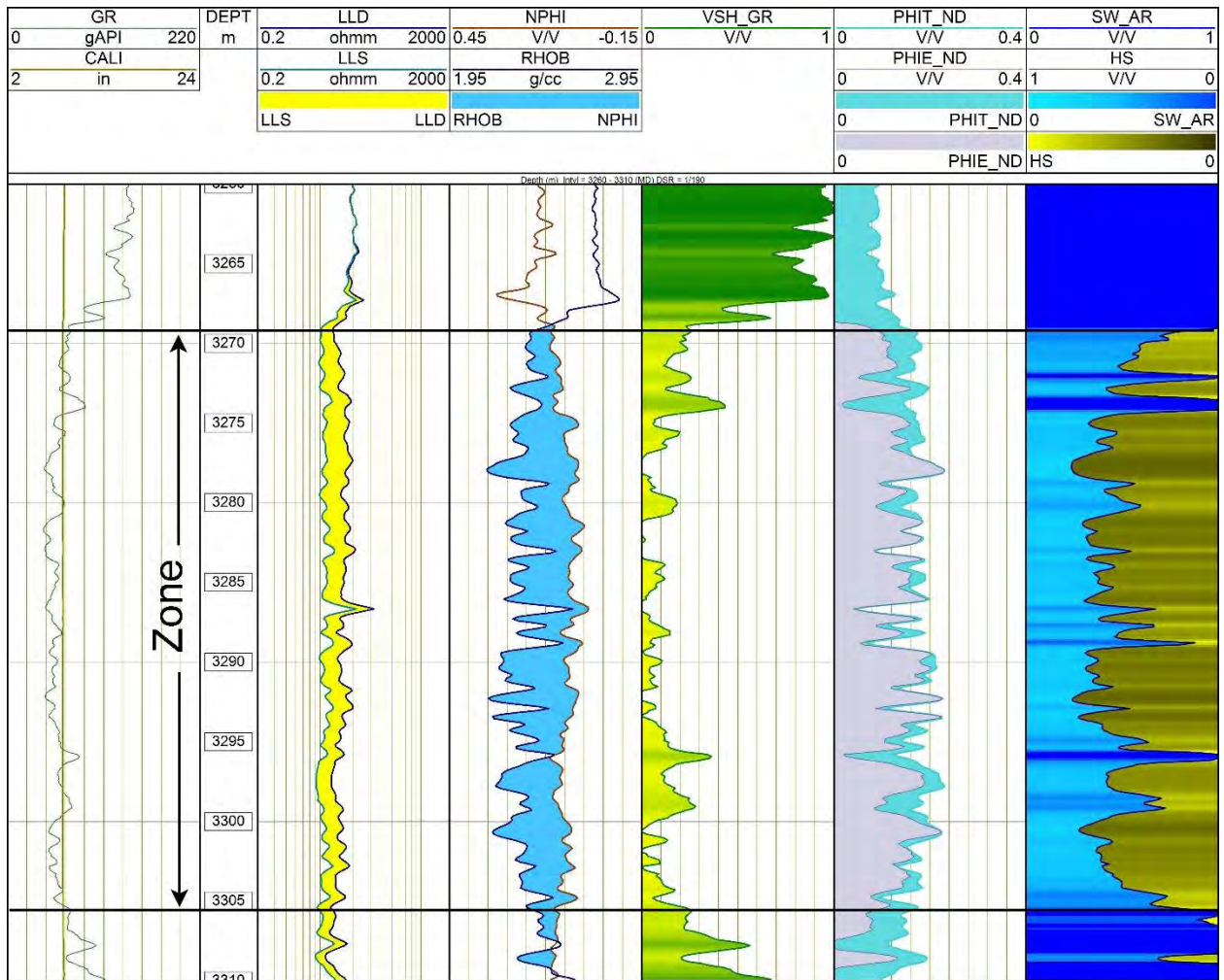
Serial Number	Calculation Parameter	Percentage
1	Average Volume of Shale = V_{sh}	20%
2	Average Porosity in(PHIT) Percentage = ϕ_{avg}	17.3 %
3	Average Effective Porosity in Percentage = ϕ_{eavg}	11.4%
4	Average water Saturation in Percentage = S_{Wavg}	66%
5	Average Hydrocarbon in Percentage = S_{Havg}	34%

4.14 Well Log Interpretation of Sawan-07

On the basis of log response thickest zone in Lower Goru formation of Sawan-07 marked from depth 3269 to 3306, thickness of 66 meter. As clearly shown in Figure 4.5, there is GR log response is low caliper log is quite stable that there is no wash-outs, separation between LLS and LLD and cross over between NPHI and RHOB which indicates the presence of hydrocarbon in greater amount. Total and effective porosities are good enough and water saturation is decreases in marked zone of Lower Goru. Zone of interest Petro physically analyzed which is shown in Figure 4.2.

4.14.1 Reservoir zone using Well Log Interpretation of Sawan-07

Reservoir zone is marked which is about 66 m thick having clean sand. Water saturation is 52% and Reservoir zone is shown in Figure 4.3.



4.3: Petro-physical results of well Sawan-07 representing reservoir zone.

Table 5: Petro physical analysis results of zone Sawan-07

Serial Number	Calculation Parameter	Percentage
1	Average Volume of Shale = Vsh	14.5%
2	Average Porosity in (PHIT) Percentage = ϕ_{avg}	16.6%
3	Average Effective Porosity in Percentage = ϕ_{eavg}	12.5%
4	Average water Saturation in Percentage = S_{wavg}	52%
5	Average Hydrocarbon in Percentage = S_{Havg}	48%

Chapter 5

Detailed Inversion Analysis of Sawan Area

5.1 Introduction

Seismic inversion is the estimation of subsurface physical properties by using the seismic data as input. Seismic inversion can be applied "AFTER STACK" and "BEFORE STACK".

Different suppositions are used for BEFORE & AFTER STACK inversions. The After stack Inversion based on Zero offset assumption and before stack multi-offset assumption. For Inversion understanding of Forward modeling is important because inversion inverse of forward modeling. Work flow of Inversion is given below.

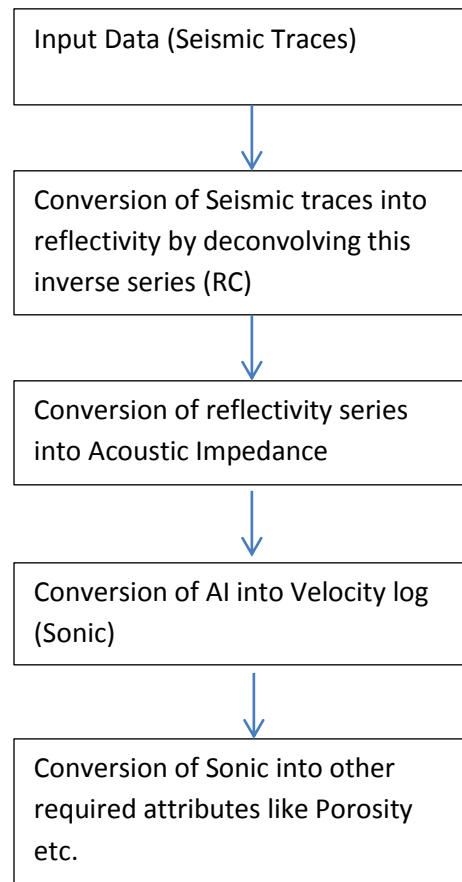


Figure 5.1: Workflow for the carried out inversion.

5.2 Model Based Inversion

There are different types of inversions here we will use the Model Based, Band Limited and Maximum Likelihood Sparse Spike Inversion techniques. Model Base Inversion is commonly used in industries. In Seismic inversion a single parameter called acoustic impedance play very important roll which is immediately recognizable. A model based inversion of 3D seismic data was performed to calculate dimensional distribution of impedance in study area. Amplitude & layer property are the interface property, defined by acoustic impedance. For significant interpretation acoustic impedance used Zero phase statistical wavelet was extracted at well position from data via a comparing filter between synthetic trace and seismic trace. By combining interpreted horizons and well log information a priory model (low impedance) is then constructed. Porosity and Acoustic impedance are usually inversely proportional to each other. Now porosity can be predicted in seismic reservoir characterization by using acoustic impedance from seismic inversion away from well position. The main objective is getting impedance of high resolution from low resolution seismic data through seismic inversion (Kneller et al., 2013).

For Model Based Inversion a widely linear inversion problem-solving procedure is used. For This problem-solving procedure wavelet (W) and seismic trace (S) were assumes and modifying initial model up to synthetic trace matching with real trace until acceptable level is not obtain (Gavotti et al., 2014). OR modifying geological model until seismic trace and synthetic trace error is not reduced. Substantial knowledge of geology is required for making this method efficient for obtaining logical model (Kneller et al., 2013). The essential approach utilized as a part of the calculation is to limit the accompanying capacity given in equation, as the fundamental suspicion of inversion is to quantify nonconformist amongst genuine and manufactured information (Gavotti et al., 2014).

$$J = \text{weight} \times (S - W * R) + \text{weight} \times (M - HR) \quad (5.1)$$

Where,

S-Real seismic trace,

W-Extracted wavelet,

R-Final reflectivity series,

M- Initial predicted model

H- Integration operator developing final impedance by convolution with reflectivity series (RC).

Now above logical models initial segment is the seismic trace and for the second portion of models is the underlying conjecture impedance. The product equip a "Constrained Model Inversion", is zero, and the last impedance esteems are balanced amongst upper and lower

esteems (Gavotti et al., 2014). The difficult obliged (well information) controls the little measure of commotion or error's in modeling. Extra data, for example, introductory figure model can likewise be fused by utilizing delicate obliged (variorum demonstrate) yet for the most part hard compelled are proposed for reversal system (Gavotti. 2014).

5.2.1 Extracted Wavelet

For correlation of extracted and inverted reflectivity from seismic at well site a constant phase wavelet was estimated shown in figure below. The 0.718% correlation found between real and synthetic trace. The length 1750-2280ms is set for window for the extraction of wavelet having wavelength of 530ms. The procedure utilizing for wavelet use seismic data close to the well logs.

Seismic inversion depends on the convolution model i.e. synthetic trace is then got by convolving extracted wavelet and reflectivity series (Cooke and Cant., 2010). Required results for inversion and seismic interpretation the wavelet must be minimum or zero phases. Phase shift amount for input wavelet influences the inversion results greatly. If the phase shift is greater the error will be higher in resultant impedance (Jain 2013).

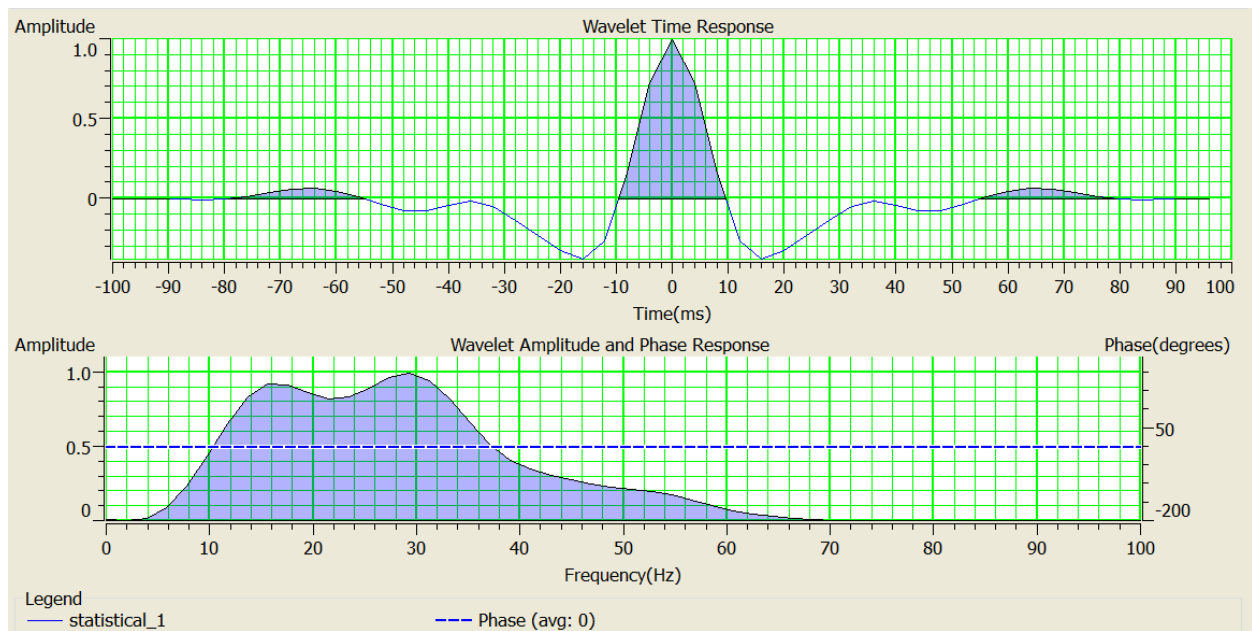


Figure 5.2: Zero phase wavelet extracted from the seismic data near the well.

5.2.2 Seismic to well correlation

Seismogram is correlated with the line Inline-724 where Sawan-01 well is located identification of exact location. Sonic and density log is used to generate reflectivity series.

Estimation of seismic wavelet is difficult due to its variation with frequency, time and with space. There are two basic methodologies used for extraction of wavelet which are the statistical and deterministic techniques. If already well tie exist then deterministic approach is used and for

statistical approach an average wavelet is calculated from a particular window of 3D seismic information (Ziolkowski et al., 1998). Statistical wavelet is extricated from seismic data having zero phases. Synthetic trace generated by convolution of computed reflectivity and source wavelet. The phase of extracted wavelet is zero because it has maximum amplitude at $t=0$ ms. The range of frequency is from 5 to 50 Hz and average amplitude of source wavelet is 0.50Hz.

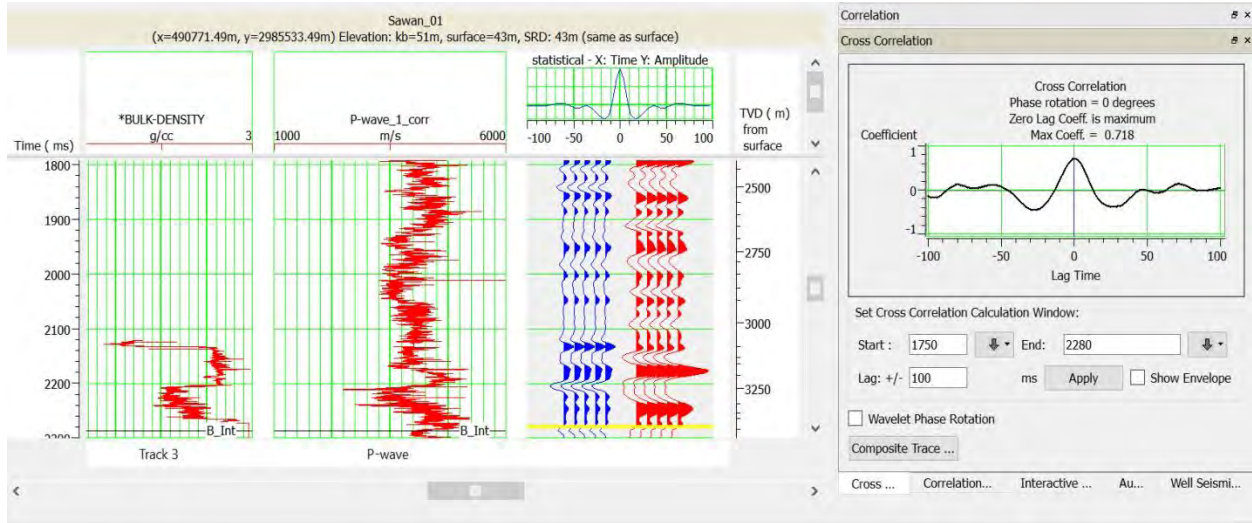


Figure 5.3: Synthetic Seismogram generated for Inversion analysis

For confirmation of seismic and synthetic matching, Seismic section and synthetic trace are compared at well Sawan-01. There is 0.718 correlations between them.

5.2.3 Initial Model/Low frequency Model

For acoustic impedance there are two terms utilized that is absolute and relative. In low frequency model generation relative acoustic impedance does not incorporated, it is used for quantitative interpretation due to its relative layer property .Through low frequency range from 0 to 15Hz absolute impedance is generated by inverting given amplitude data given to inversion calculation.

Low frequencies are added in model base inversion instead of forming different low frequency model for quantitative and qualitative interpretation absolute acoustic impedance is used (Cooke and Cant., 2010). A low impedance demonstrate created for display based reversal is appeared in To get absolute acoustic impedance from reversal comes about a low frequency model must be included from hard limitations, for we generate low impedance model after well to seismic tie which example, sonic and density logs. For model base inversion absolute acoustic impedance initial model is obtained shown below

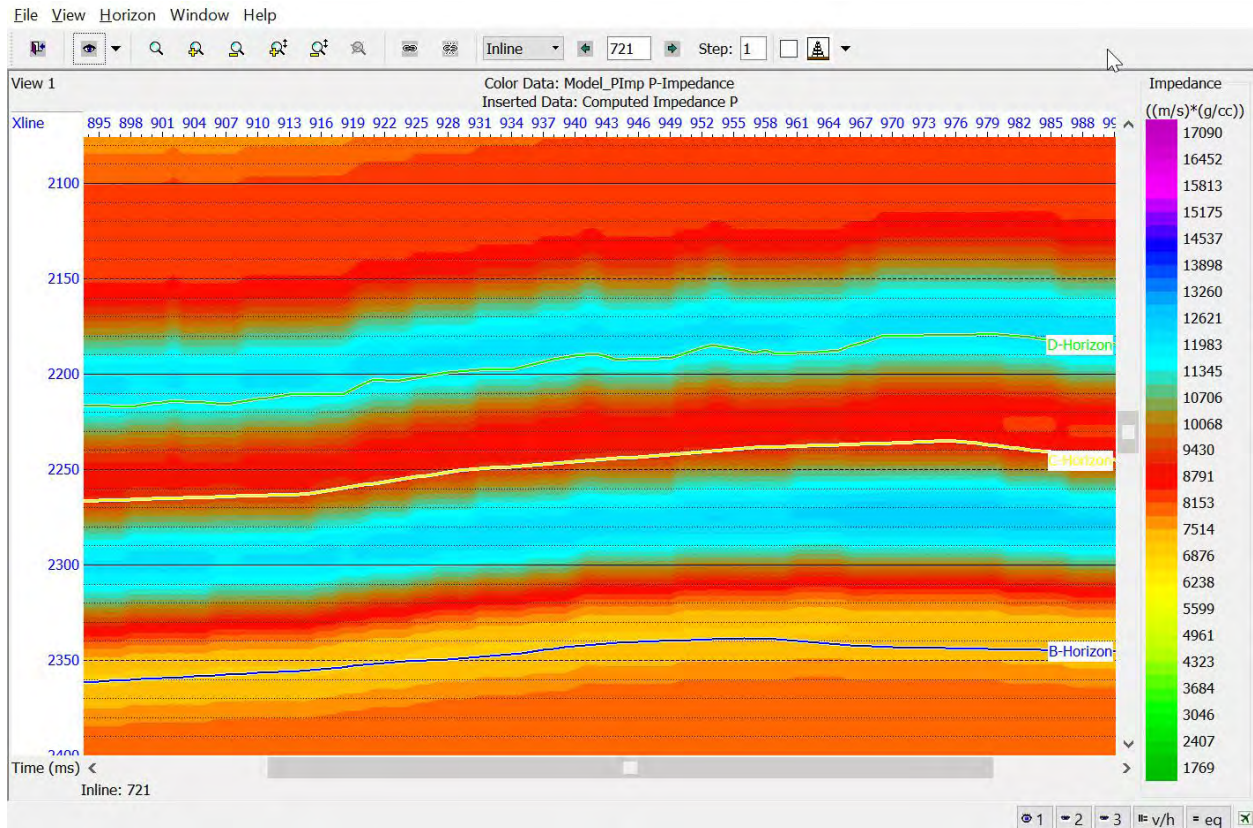


Figure 5.4: Initial Modal generated for inversion.

5.3 Inversion Analysis

5.3.1 Model Based Inversion

Ensuing the examination at the well area the **Modal Based Inversion** was performed with respect to the given 3D seismic data. A statistical wavelet was extricated in time window from 1750-2280ms. Frequency range of extricated wavelet was balanced by inverted trace at well area and the synthetic trace. The relationship between synthetic (red) and seismic trace (blue) is great with high correlation coefficient (0.99) is appeared in Figure below. The assessed RMS error between the synthetic and seismic trace is 0.10. The evaluated RMS error between the inverted trace and the impedance log was 1128.93 (m/s)*(g/cc).

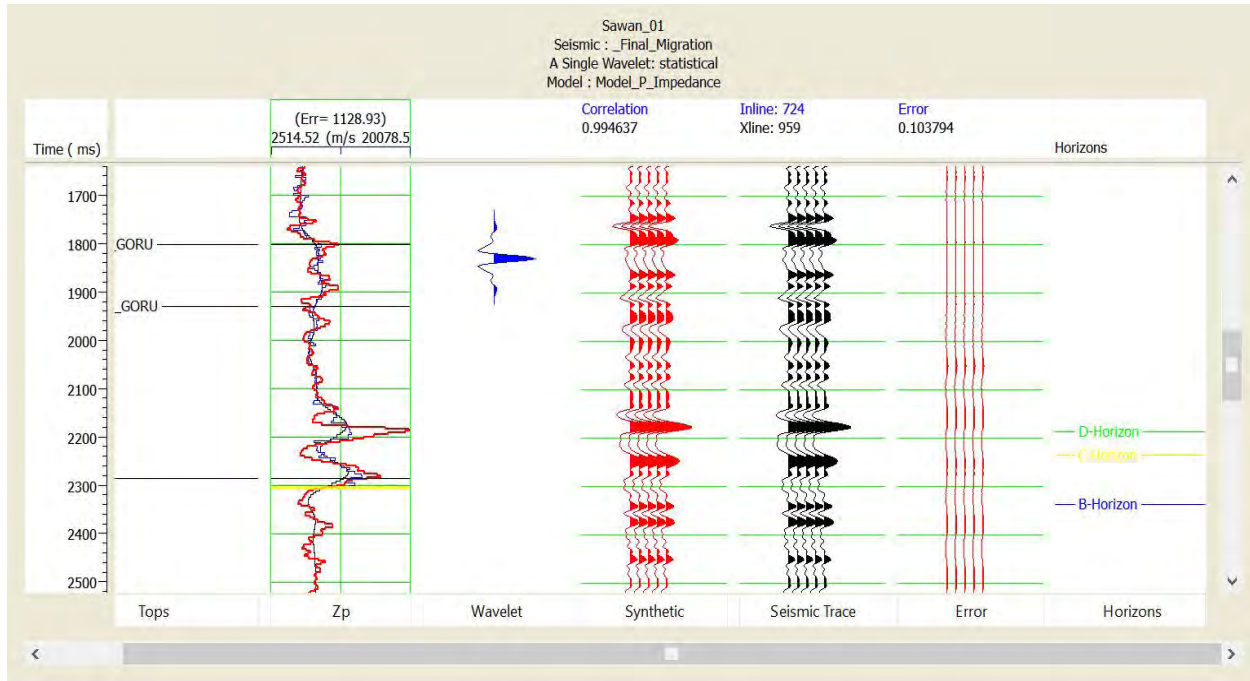


Figure 5.5: Correlation wavelet for Model based inversion with error plot.

The consequences of Model Based reversal seismic cube (10*10) the inversion was performed just on the chosen time window 1750-2280ms in which the all three main horizons are distinguished as separate producing zones. The inversion comes about show colored layers showing diverse estimations of acoustic impedance for each layer over zone of intrigue which is D sand, C sand and B sand from Lower Goru lies in this picked window profundity known from check shot information. Petro- physics comes about talked about in past section likewise feature a good zone at a similar profundity. The light blue shading layer over the low impedance layer demonstrates higher impedance esteem. Higher impedance compares the shale units (Gavotti, 2014). This high impedance layer can be going about as a seal for C-sands. The low impedance layers demonstrate a sidelong squeeze out towards SE. This demonstrates thickness of Sand-intervals is diminishing towards SE compartment and making a stratigraphic trap. Sawam-01 lies According to data given by Co-chief at OMV; Sawan-01 is at development stage. An alternate pattern of low and high impedance layers is observed in the selected time window which is due to the alternate sand shale layering present in the Lower Goru. The model based inversion results show a good lateral variations in low acoustic impedance within the zone of interest i.e. C-sand (Figure 5.6).

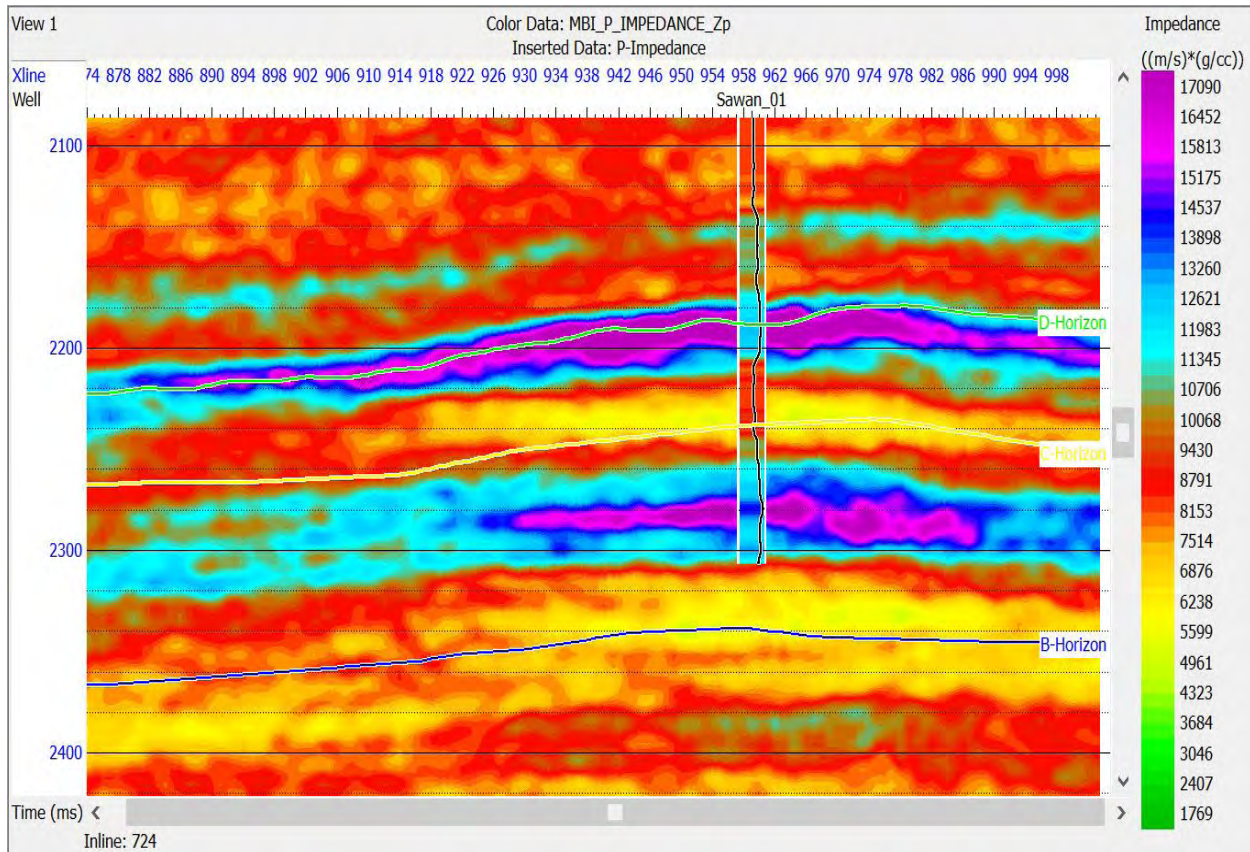


Figure 5.6: Results for model based inversion.

5.3.1.1 Slice of Model Based Inversion

As all the parameters are picked for seismic window 1750-2280 and results are discussed above. Now, for the vertical overview of reservoir zones two reservoirs D-sand and C-sand are cut down at their intervals and found the results exactly according to petroleum play as all three wells are in low impedance area between 7000-11000 indicating that area is gas producing as exactly it is already producing. In further detail slice is just to view the overall spread of impedance effects or we can say it is the view of seismic data from another angle and in 3D view we always used to see both horizontal and vertical view of results. Detailed view of both prominent sand zones is given in Figures 5.7,5.8.

The results indicate that the impedance values are favorable (low) in the region surrounding the wells Sawan-07 and 08 for the zone of interest in D-sand (Figure 5.7). There is low impedance values indicating a potential zone of interest south-east of the Sawan-01 well (Figure 5.7).

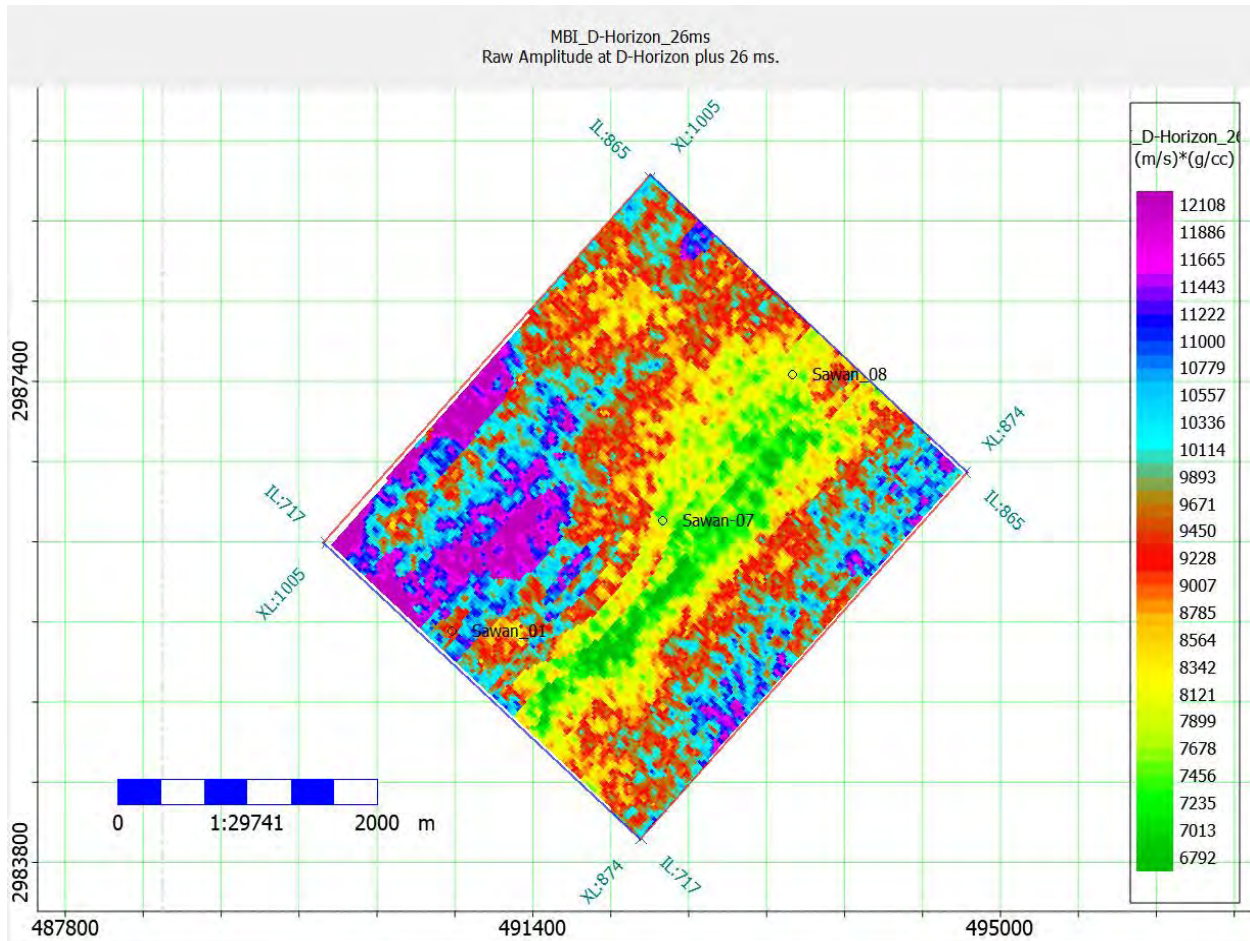


Figure 5.7: Slice showing the vertical view of Model based inversion for D sand.

In case of C-sand, the impedance values are relatively low for all the three wells i.e. below 10500 (m/s)*(g/cc) (Figure 5.8). A potential zone can be seen towards the north-west of the Sawan-01 well in case of C-sand (Figure 5.8).

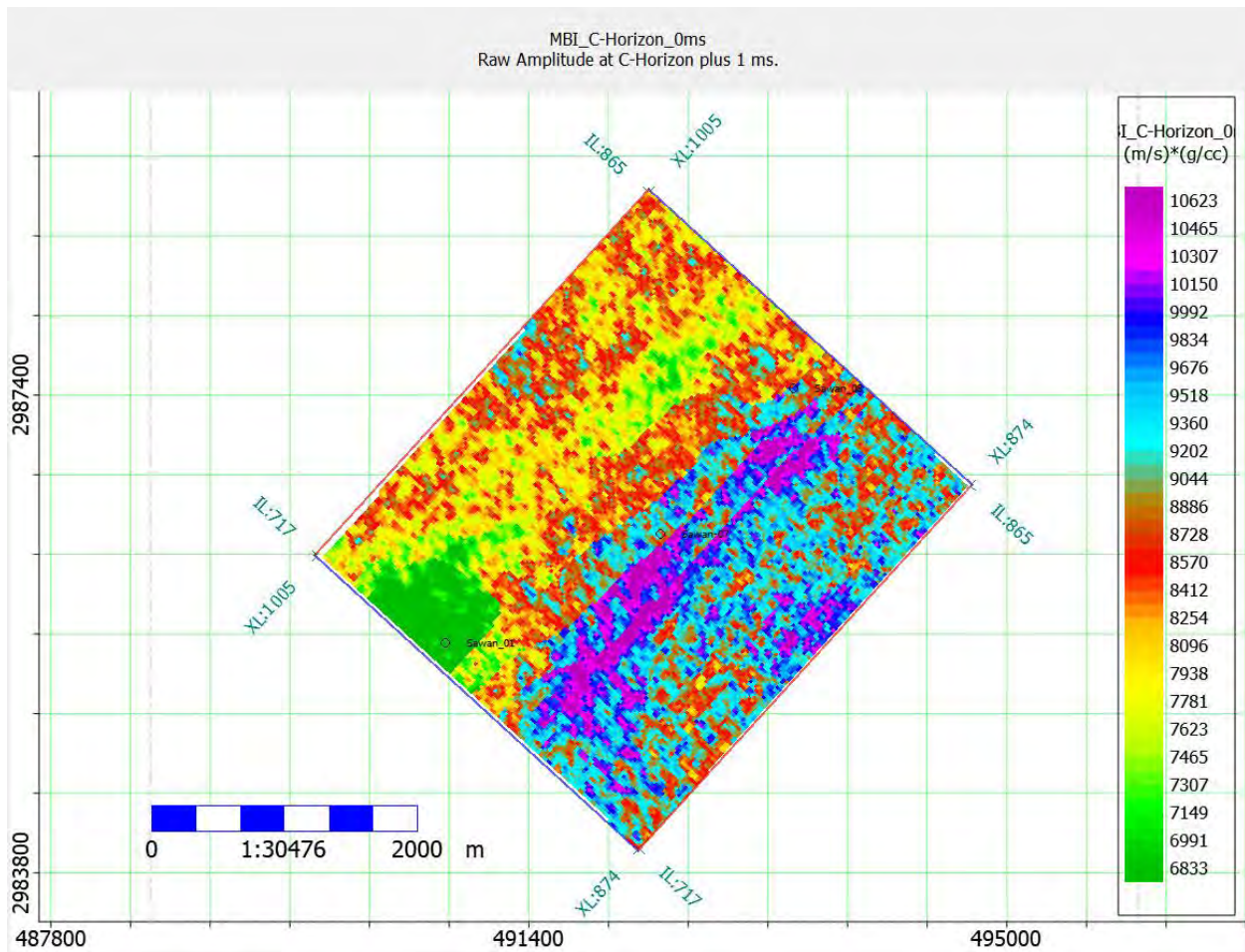


Figure 5.8: Slice showing the vertical view of Model based inversion for C sand.

5.3.2 Band Limited Inversion

Following the examination at the well area the **Band Limited inversion** was performed with respect to the given 3D seismic data. A statistical wavelet was extricated in time window from 1920-2420ms. Frequency range of extricated wavelet was balanced by inverted trace at well area and the synthetic trace. The relationship between synthetic (red) and seismic trace (blue) is great with high correlation coefficient (0.96) is appeared in Figure below. The evaluated RMS error between the inverted trace and the impedance log was 783.28 $(m/s) \cdot (g/cc)$.

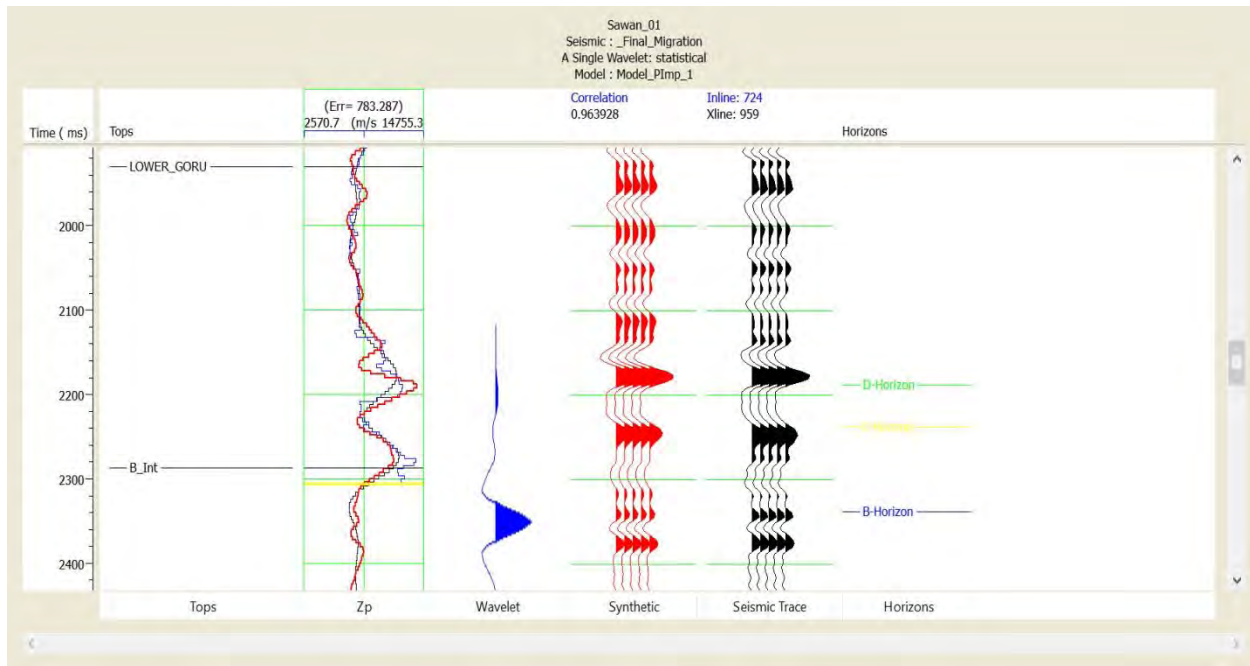


Figure 5.9: Correlation wavelet for Band Limited inversion with error plot.

The consequences of Band Limited reversal seismic cube (10*10) the inversion was performed just on the chosen time window 1920-2420ms in which the all three main horizons are distinguished as separate producing zones but the main producing reservoir is C-sand that's why the whole area is showing the powerful reservoir zone is C-sand. The inversion comes about show colored layers showing diverse estimations of acoustic impedance for each layer over zone of intrigue which is D sand, C sand and B sand from Lower Goru lies in this picked window profundity known from check shot information. Petro- physics comes to talked about in past section likewise feature a good zone at a similar profundity. The light blue shading layer over the low impedance layer demonstrates higher impedance esteem. Higher impedance compares the shale units (Gavotti, 2014). This high impedance layer can be going about as a seal for C-sands. The low impedance layers demonstrate a sidelong squeeze out towards SE. This demonstrates thickness of Sand-intervals is diminishing towards SE compartment and making a stratigraphic trap. Sawam-01 lies According to data given by Co-chief at OMV; Sawan-01 is at development stage. An alternate pattern of low and high impedance layers is observed in the selected time window which is due to the alternate sand shale layering present in the Lower Goru. The Band Limited inversion results show a good lateral extent of variations in acoustic impedance which can be used for depicting shaling out sequence in study area but it is not as much valid as Modal Based Inversion is efficient. BL-Inversion results are given in Figure 5.10. The section indicates low impedance zone in D-sand and C-sand with lateral continuity indicating the zone of interest (Figure 5.10).

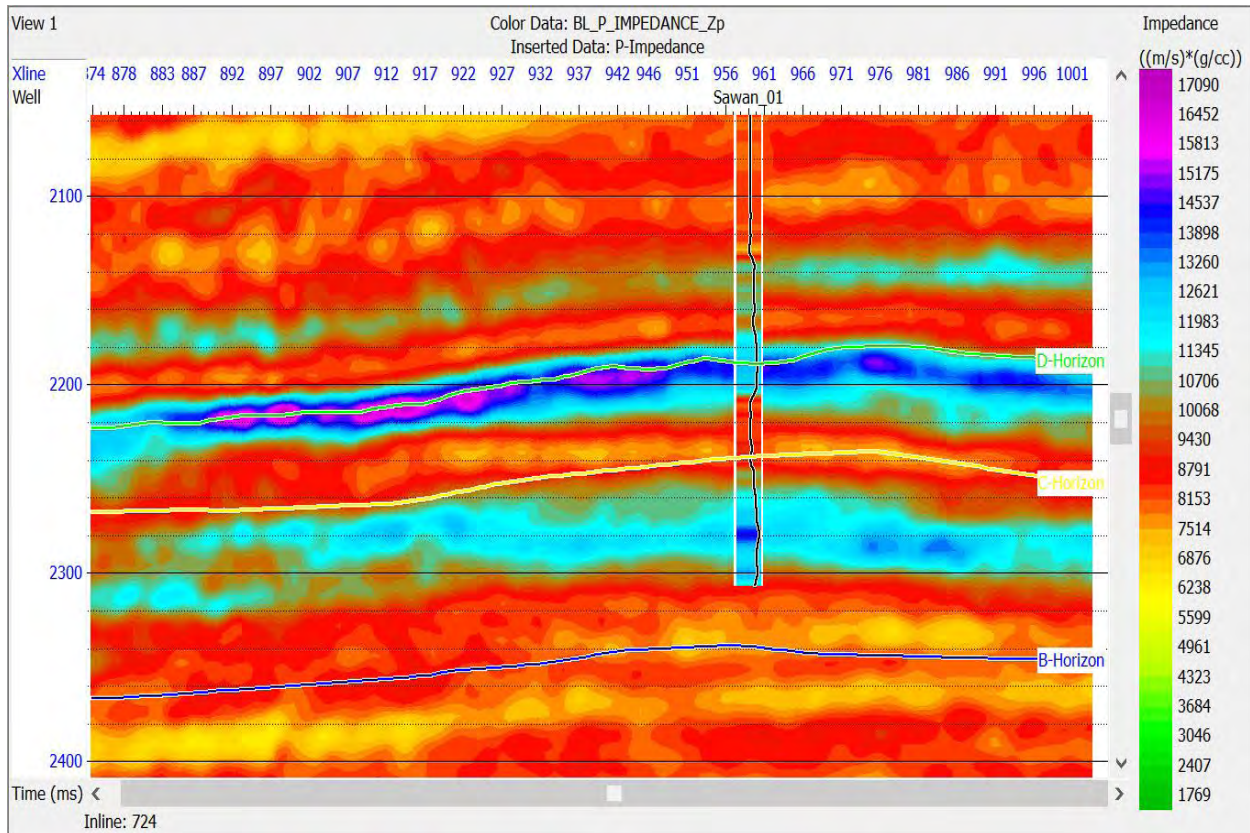


Figure 5.10: Band Limited inversion results indicating low impedance values in the zone of interest.

5.3.2.1 Slice of Model Based Inversion

As all the parameters are picked for seismic window 1920-2420 and results are discussed above. Now, for the vertical overview of reservoir zones only two reservoirs D-sand and C-sand are cut down at their intervals and found the results exactly according to petroleum play as all three wells are in low impedance area between 7000-11000 indicating that area is gas producing as exactly it is already producing. In further detail slice is just to view the overall spread of impedance effects or we can say it is the view of seismic data from another angle/direction and in 3D view we always used to see both horizontal and vertical view of results although this type of inversion technique is not same as Modal Based but even then results are so impressive. Detailed view of both prominent sand zones is given Figures 5.11, 5.12.

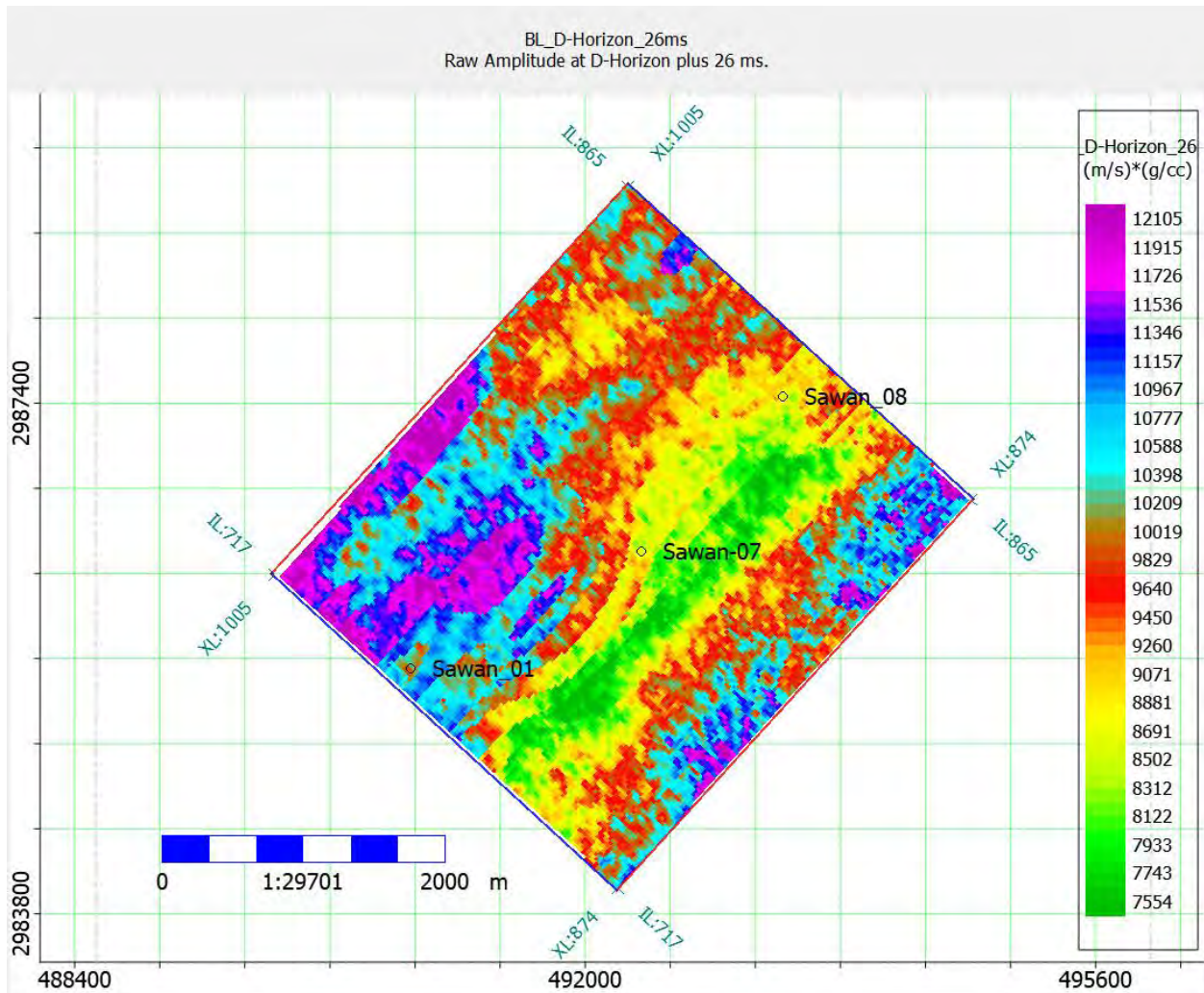


Figure 5.11: Slice view of Band Limited inversion of D sand indicating Sawan-07 and 08 wells lies in the low impedance zone.

The Figure 5.11 indicates that the results from Band Limited inversion follows the results of Model based inversion with the wells located at low impedance values in case of D-sand. The similar trend can also be seen between the results of the two inversion methods in C-sand (Figure 5.12).

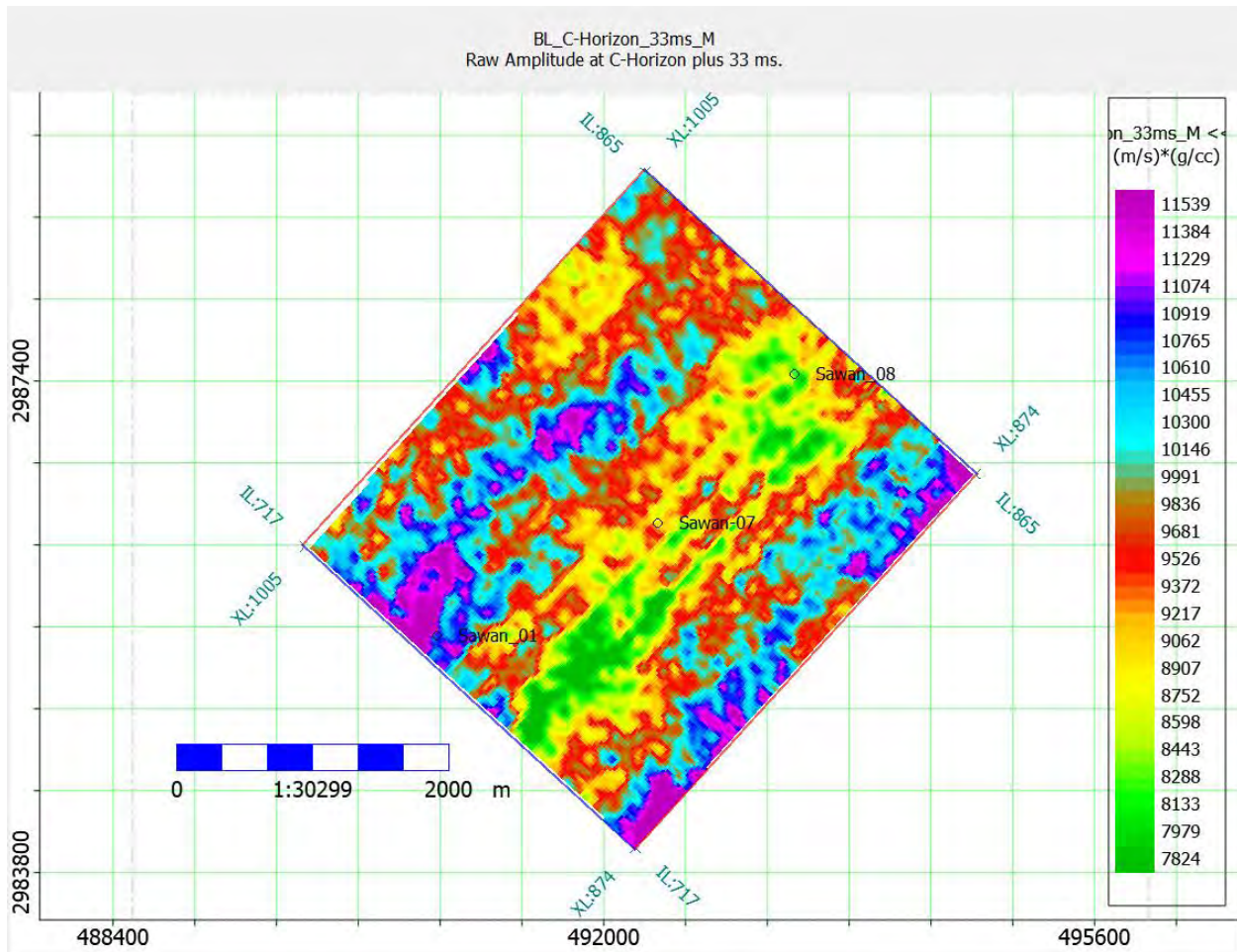


Figure 5.12: Slice view of Band Limited inversion of C sand indicating low impedance zone surrounding the wells.

5.3.3 Maximum Likelihood Sparse Spike Inversion

Continuing the examination at the well area the **Maximum Likelihood Sparse Spike Inversion** was performed with respect to the given 3D seismic data. A statistical wavelet was extricated in time window from 1920-2420ms. Frequency range of extricated wavelet was balanced by inverted trace at well area and the synthetic trace. The relationship between synthetic (red) and seismic trace (blue) is great with high correlation coefficient (0.96) is appeared in Figure below. The assessed RMS error between the synthetic and seismic trace is 0.24. The evaluated RMS error between the inverted trace and the impedance log was 850.79 $(m/s) \cdot (g/cc)$.

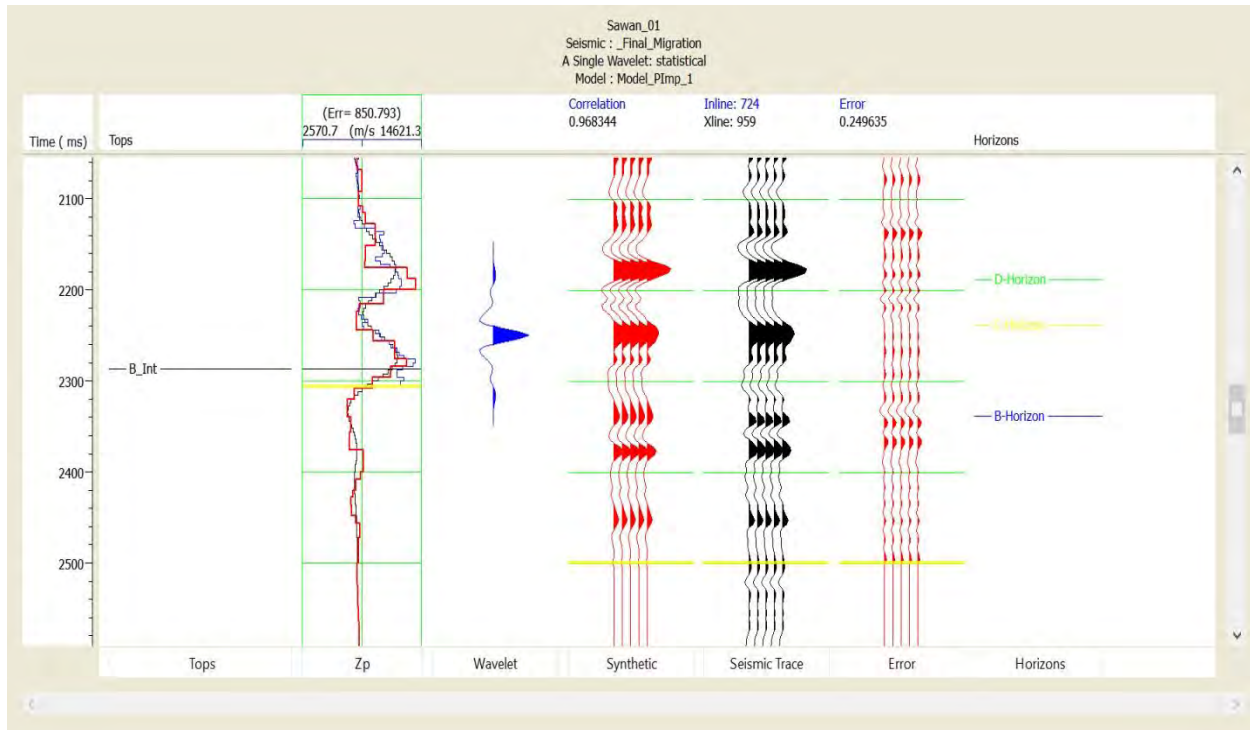


Figure 5.13: Correlation of Maximum Likelihood Sparse spike inversion.

The consequences of Maximum Likelihood Sparse Spike reversal seismic cube (10*10) the inversion was performed just on the chosen time window 1920-2420ms in which the all three main horizons are distinguished as separate producing zones but the main producing reservoir is C-sand that's why the whole area is showing the powerful reservoir zone is C-sand. The inversion comes about show colored layers showing diverse estimations of acoustic impedance for each layer over zone of intrigue which is D sand, C sand and B sand from Lower Goru lies in this picked window profundity known from check shot information. Petro- physics comes to talked about in past section likewise feature a good zone at a similar profundity. The light blue shading layer over the low impedance layer demonstrates higher impedance esteem. Higher impedance compares the shale units (Gavotti, 2014). This high impedance layer can be going about as a seal for C-sands. The low impedance layers demonstrate a sidelong squeeze out towards SE. This demonstrates thickness of Sand-intervals is diminishing towards SE compartment and making a stratigraphic trap. Sawan-01 lies According to data given by Co-chief at OMV; Sawan-01 is at development stage. An alternate pattern of low and high impedance layers is observed in the selected time window which is due to the alternate sand shale layering present in the Lower Goru. The Band Limited inversion results show a good lateral extent of variations in acoustic impedance which can be used for depicting shaling out sequence in study area but it is not as much valid as Modal Based Inversion is efficient.

MLSS-Inversion results are given in Figure 5.14 which shows relatively low impedance values in the zones of interest of D and C-sands.

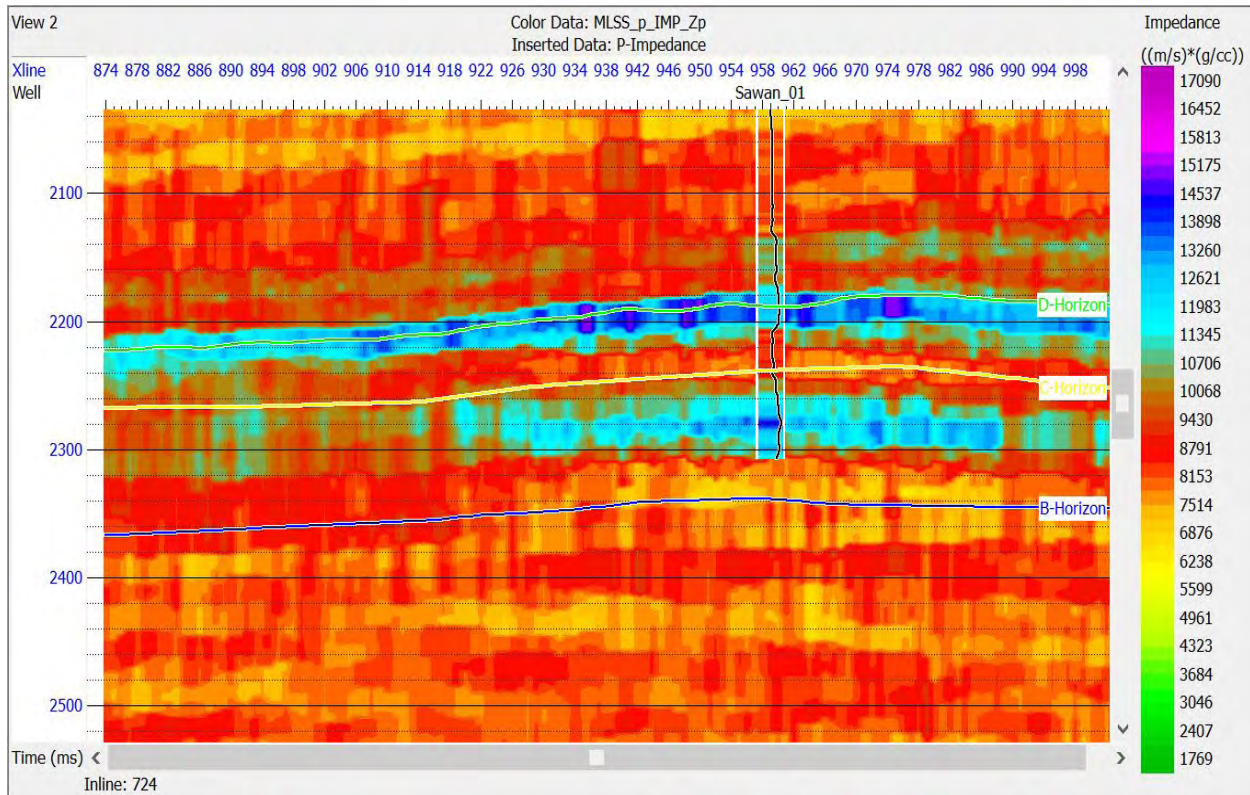


Figure 5.14: Inversion results of Maximum Likelihood Sparse Spike.

5.3.3.1 Slice of Maximum Likelihood Sparse Spike Inversion

As all the parameters are picked for seismic window 1920-2420 and results are discussed above. Now, for the vertical overview of reservoir zones only two reservoirs D-sand and C-sand are cut down at their intervals and found the results exactly according to petroleum play as all three wells are in low impedance area between 8000-11000 indicating that area is gas producing as exactly it is already producing. In further detail slice is just to view the overall spread of impedance effects or we can say it is the view of seismic data from another angle/direction and in 3D view we always used to see both horizontal and vertical view of results although this type of inversion technique is not same as Modal Based or Band Limited but even then results are so impressive. Detailed view of both prominent sand zones is given in Figure 5.15, 5.16.

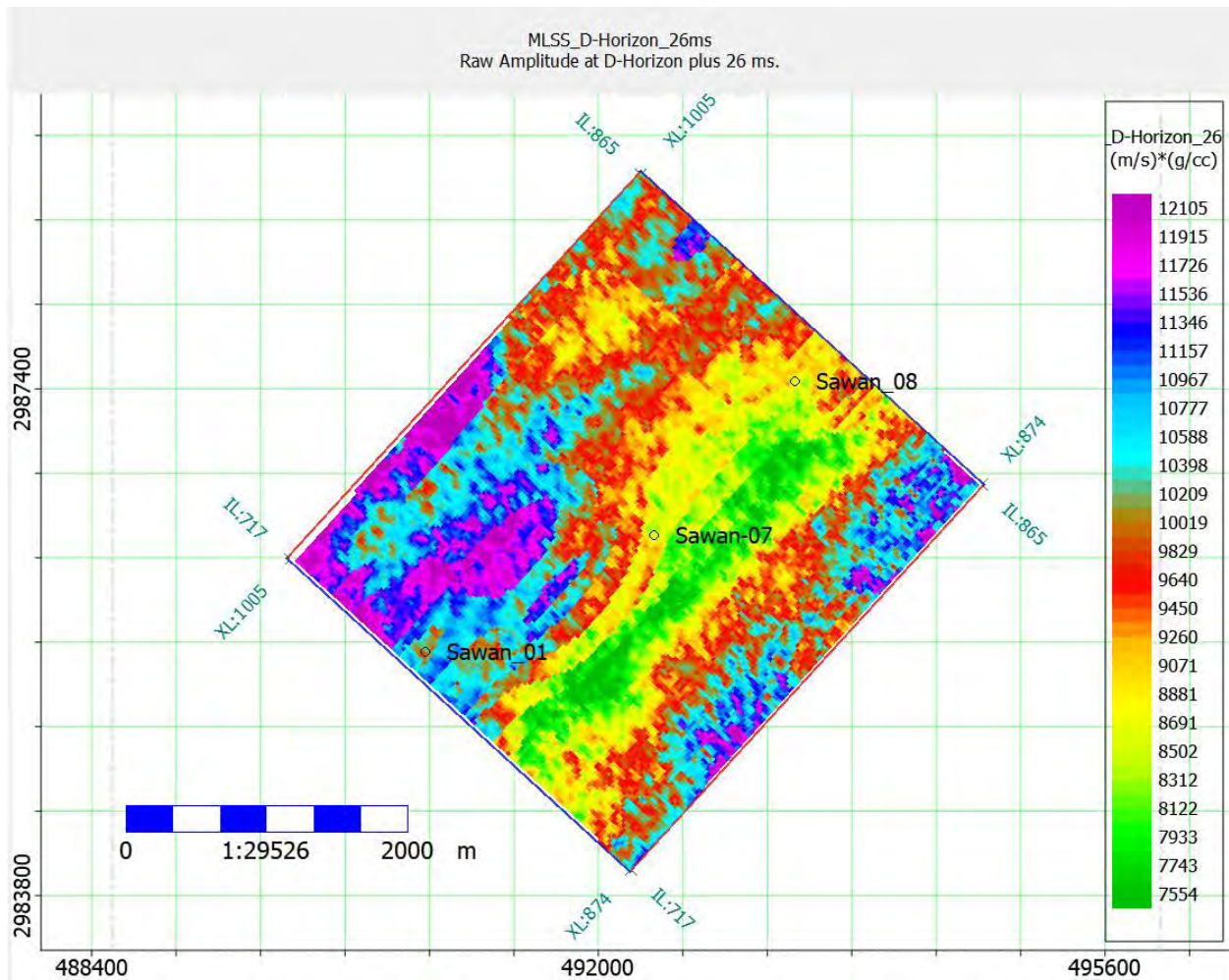


Figure 5.15: Slice view of Maximum Likelihood Sparse Spike Inversion of D sand.

The results of slice generated for the zone of interest in D-sand from Sparse Spiker inversion follows the results obtained from the previous two methods. The values are relatively low around the wells indicating potential gas region (Figure 5.15). This technique does not work efficiently for the C-sand zone of interest as can be seen in Figure 5.16 due to the limitation of the technique. However the values of impedance are low around the wells confirming the presence of gas filled sands (Figure 5.16).

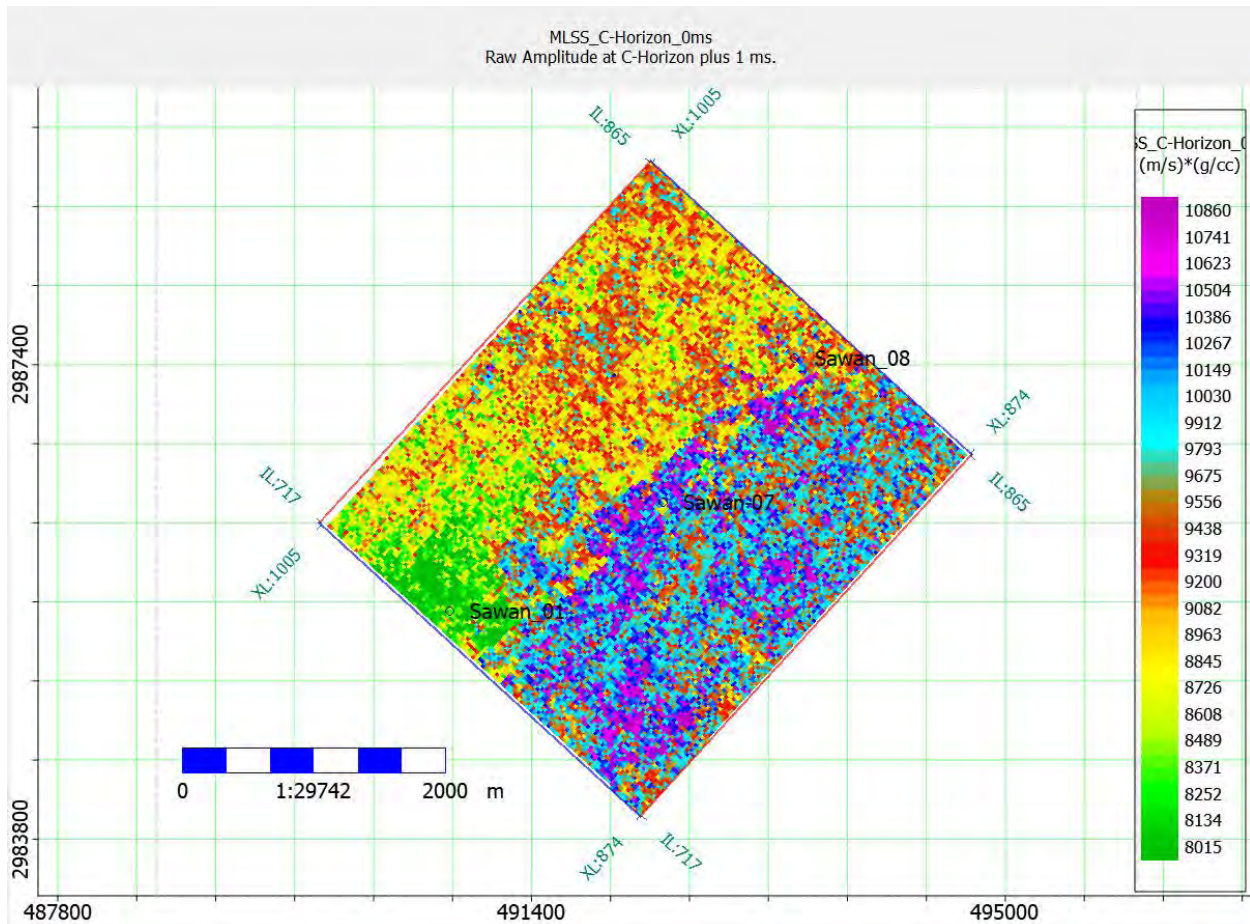


Figure 5.16: Slice view of Maximum Likelihood Sparse Spike Inversion of C sand.

5.4 Comparison between these deterministic Inversion techniques

According to the literature given we thoroughly know that in deterministic inversion techniques the best reliable method is Model Based Inversion due to its high resolution and accuracy but here in my work at some intervals like from 1700ms to 2700ms Modal Based Inversion is not depicting reliable results but at the same time Band Limited is producing more accuracy with high resolution. One of the main reasons is may be at some areas Modal based technique is not as much reliable as the other techniques performing. It is one of the reasons from other solid reasons

In all above inversion sections and slices it is clearly understood and easy to recognize that producing areas are well drilled areas so the impedance value is low for Gas and Oil reservoir areas. Impedance values are not same on every section but on average values are in sequential changing of limit. Like, lower value is almost between 7500-8000 and the upper limit is from 9500-11000 so answer is yes I mean area is strongly depicting the producing zone as per results producing.

Chapter 6

Rock-Physics Analysis with Cross-Plots

6.1 Introduction

Rock physics intends to portray rock properties in view of the conduct of seismic wave's propagation through them. This requires thought of how the composition of a stone directs its pressure strain relationship and hence seismic reaction. The impact of pore liquids is specifically compelling because of its materialness to the hydrocarbon industries. In a standard seismic elucidation work process shake material science is utilized to relate impedance and versatile parameters got from seismic information to particular rock properties. This obliges what seismic information is physically fit for settling and the non-uniqueness related with a particular translation. Distinctive rock physics parameters which are computed in this research work are given underneath.

6.2 Bulk Modulus

The bulk modulus (K) of a substance measures the substance's resistance from uniform pressure. It is the proportion of volume stress to volume strain. It is characterized as the pressure increment expected to influence a given relative decline in volume. It depicts the material's reaction to uniform pressure. Only bulk modulus is important for a liquid.

6.3 Shear Modulus

Shear modulus Is also known as modulus of rigidity (μ), is characterized as the proportion of shear stress to the shear strain (angle of deform). It is related with the deformation of a solid when it encounters a force parallel to one of its surfaces while its contrary face encounters a contradicting force, (for example, friction). It depicts the material's reaction to shearing strains.

6.4 Poisson's ratio

The proportion of transverse strain to longitudinal strain is called Poisson's ratio (ν). At the point when an example of material is extended one way, it tends to contract (or once in a while, grow) in the other two directions. On the other hand, when an example of material is packed one way, it has a tendency to grow (or infrequently, contract) in the other two directions. Measure of this tendency is Poisson's proportion.

6.5 Gassmann Theory

Fluid substitution is a vital piece of the rock physic investigation (e.g., AVO, 4D examination), which gives a device to liquid distinguishing proof and evaluation in reservoir. This is normally performed utilizing Gasman's condition (Gassmann, 1951). The goal of fluid substitution is to show the seismic properties (seismic speeds) and density of reservoir at a given reservoir condition (e.g., weight, temperature, porosity, mineral compose, and water saltiness) and pore

liquid saturation, for example, 100% water Saturation or hydrocarbon with just oil or just gas saturation Isotropic material having Seismic velocity can be estimated using known rock moduli and density. P- and S-wave velocities in isotropic media are calculated by,

$$V_P = \sqrt{\frac{K + \frac{4}{3}\mu}{\rho}} \quad (6.1)$$

$$V_S = \sqrt{\frac{\mu}{\rho}} \quad (6.2)$$

Individually, where V_p and V_s defined the primary and secondary wave velocities, bulk modulus is represented by K , and μ represent the shear moduli, and ρ represents the density. Density of reservoir rock can be basically processed μ with the volume averaging condition (mass adjust). For estimation of velocities in the body after fluid substitution different parameters are required for this purpose we utilized the Gassmann conditions Properties of fluid, frame and bulk modulus from rock to pore is related by equation. The Saturated rock bulk modulus is given by the low frequency Gassmann

Where K_{mat} , K_{frame} , K_{matrix} and K_n these are the bulk modulus of the reservoir rock. Porosity of material is represented by p permeable rock frame, mineral grid, and pore liquid, separatel. In the Gassmann detailing shear modulus is free of the pore liquid and held steady amid the liquid substitutions. Mass modulus (K_{sat}) and shear modulus (μ) at in-situ

$$K = p (V_1^2 - 4v^2) \rho \quad (6.3)$$

$$\mu = p v^2 \rho \quad (6.4)$$

$$P = 0.31 * V.25 P \quad (6.5)$$

$$\sigma = 0.5(V, 2 - 2V, 2) / (V2 - v^2) \quad (6.6)$$

6.6 Cross-Plots of different parameters with porosity and density

Bulk modulus after the fluid substitution plotted along the porosity is shown. Bulk modulus is calculated with three different types of fluids namely water, oil, and gas. Bulk modulus has a high value in case of water-bearing reservoir, then that of oil and gas-bearing reservoir, and the gas-bearing reservoir has the lowest value. The difference between water, oil, and gas-saturated bulk modulus becomes more as porosity increases and is less where porosity is low, as shown. The bulk modulus after the fluid substitution and in-situ conditions are also plotted along the porosity.

The Figure 6.1 indicates a crossplot between Λ - ρ and μ - ρ with shale volume taken as z-axis. The zone of interest has been indicated by a red circle where the Λ - ρ values are low, μ - ρ values are moderate, and shale volume is also low, indicating a gas zone (Figure 6.1). The same two logs crossplotted with effective porosity as a color code confirm that the effective porosity is high in the marked zone, which is a good indicator for potential hydrocarbon presence (Figure 6.2).

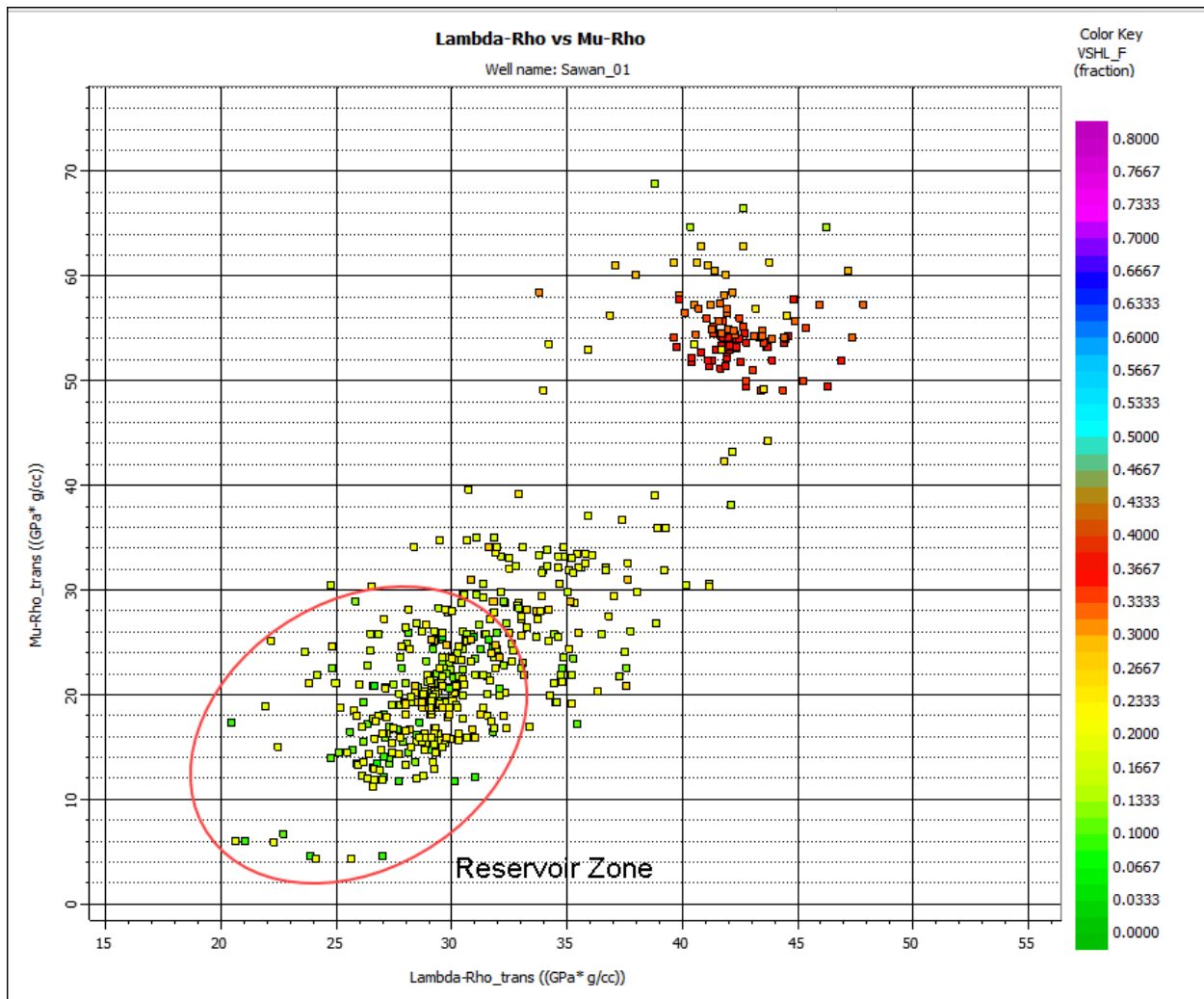


Figure 6.1: Lambda-Rho log cross plotted against Mu-Rho log from Sawan-01 well indicating gas zone with low lambda-Rho and moderate Mu-Rho values.

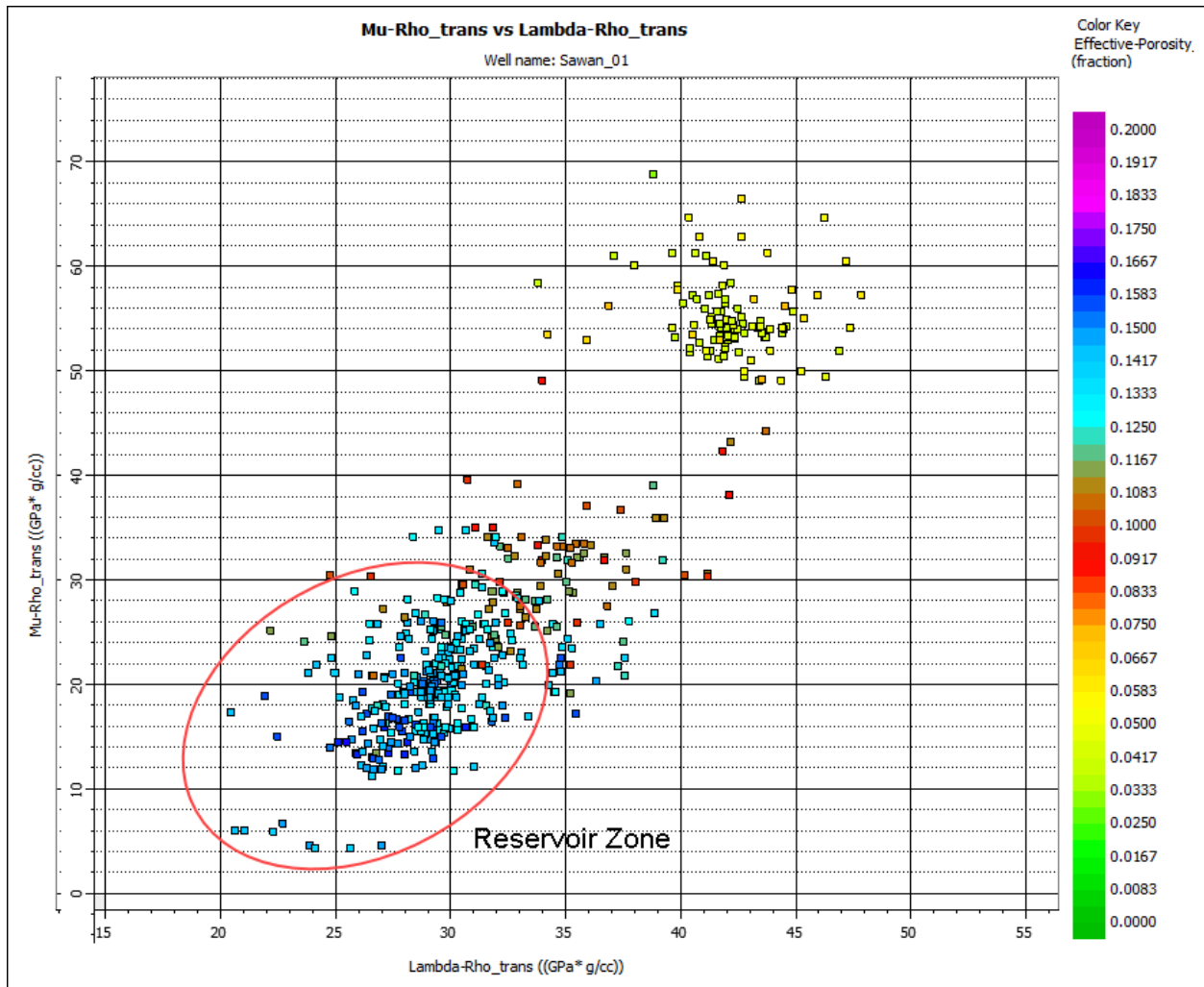


Figure 6.2: Mu-Rho cross plotted against Lambda- Rho with effective porosity on z-axis indicating zone of interest.

Similarly, the cross plot developed between VPVS ratio and Lambda-Rho with shale volume as color code indicates the same zone of interest with low Lambda-Rho values indicating presence of fluid, low shale volume indicating sand lithology, and high VPVS ratio indicating presence of gas (Figure 6.3). The same crossplot with effective porosity taken on z-axis confirms that the marked zone has relatively high effective porosity (Figure 6.4).

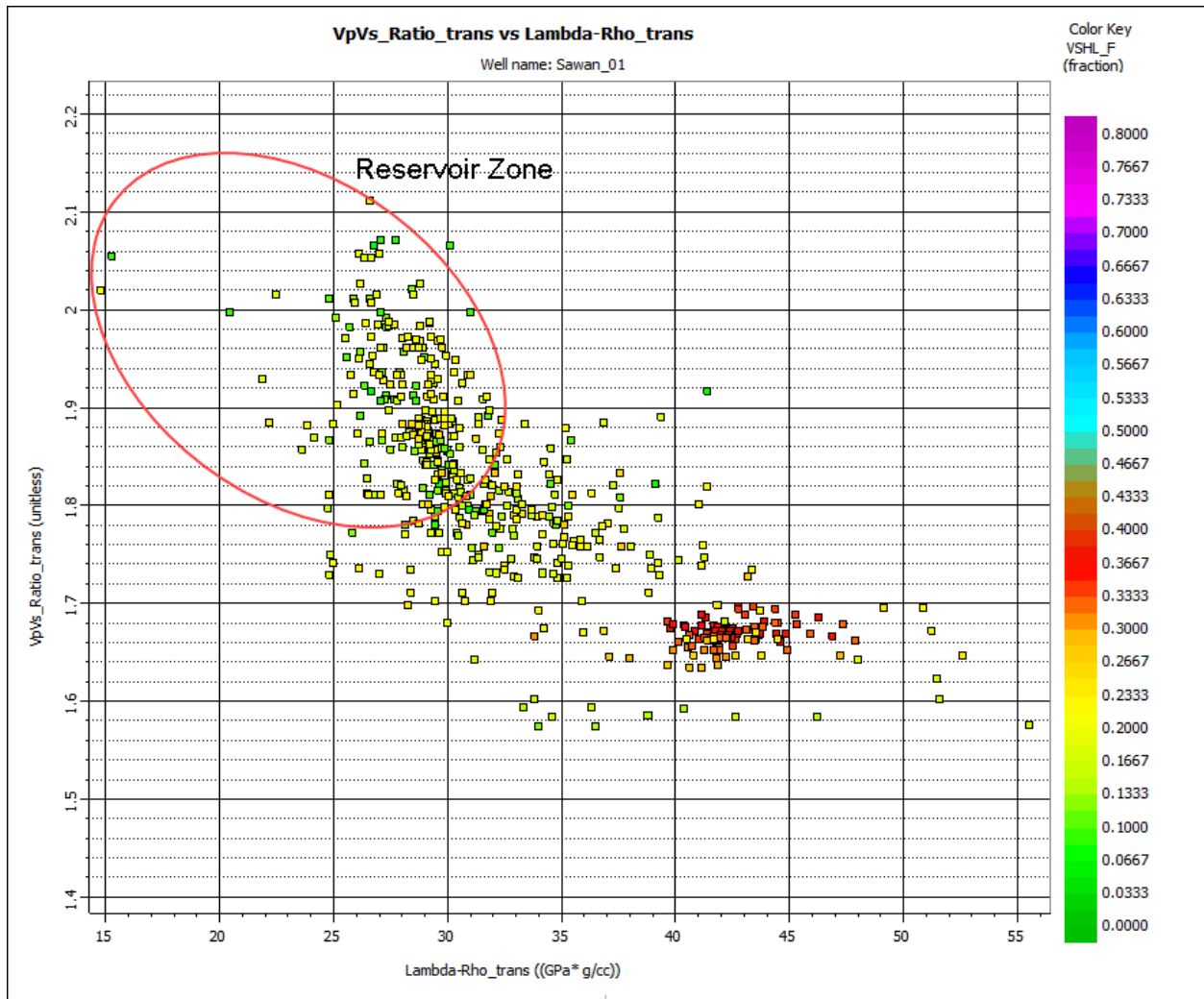


Figure 6.3: VpVs Ratio cross plotted with Lambda-Rho colored coded with shale volume indicating the zone of interest.

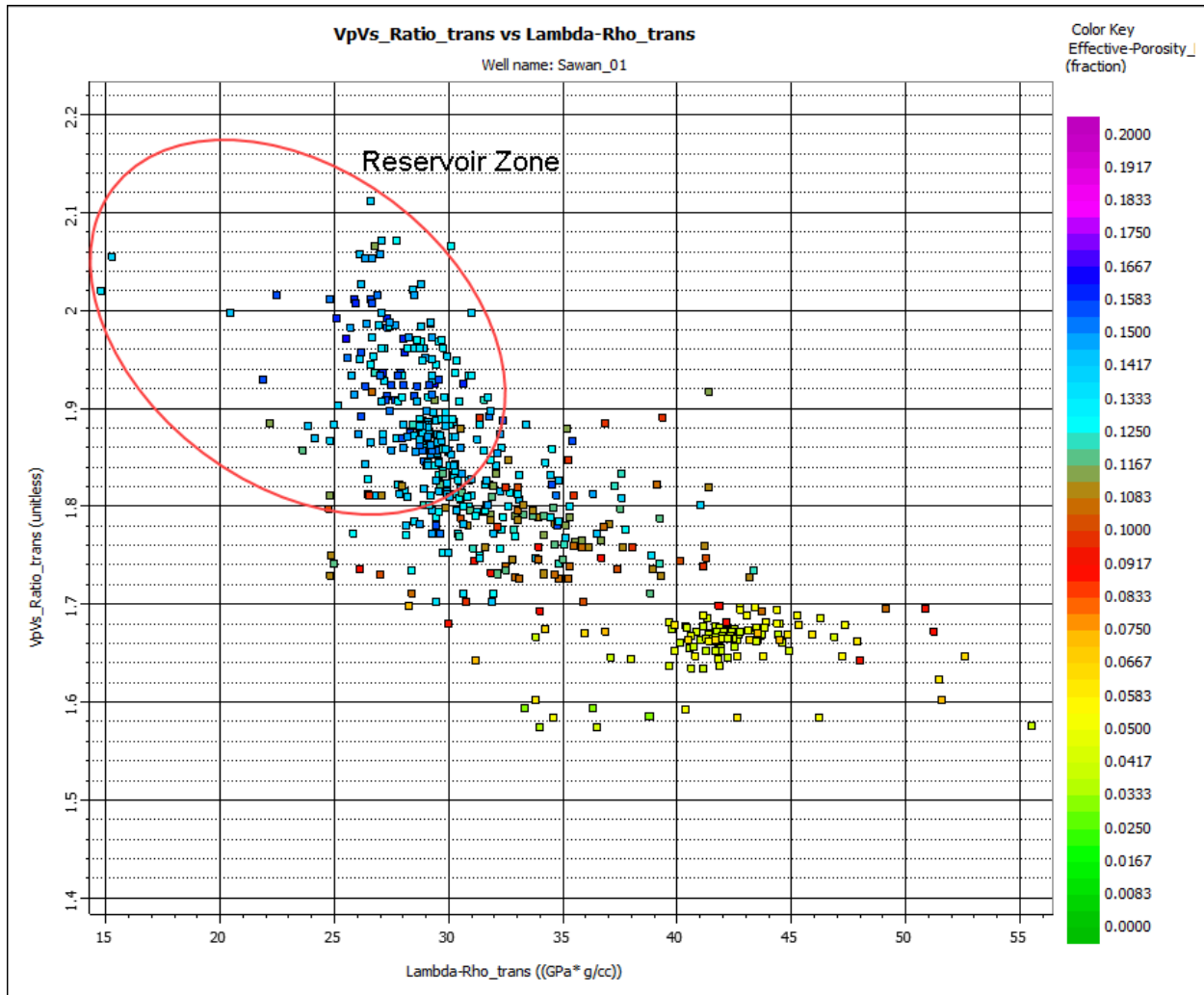


Figure 6.4: VPVs Ratio crossplotted against Lambda-Rho color coded with effective porosity indicating the zone of interest.

The VPVS ratio has also been crossplotted against P-Impedance log to confirm the zone of interest with shale volume taken on z-axis (Figure 6.5). The low impedance values, relatively high VPVS ratio and low shale volume indicates the gas zone as has been highlighted in the Figure 6.5. The same plot color coded with effective porosity indicates that the zone of interest has high effective porosity (Figure 6.6).

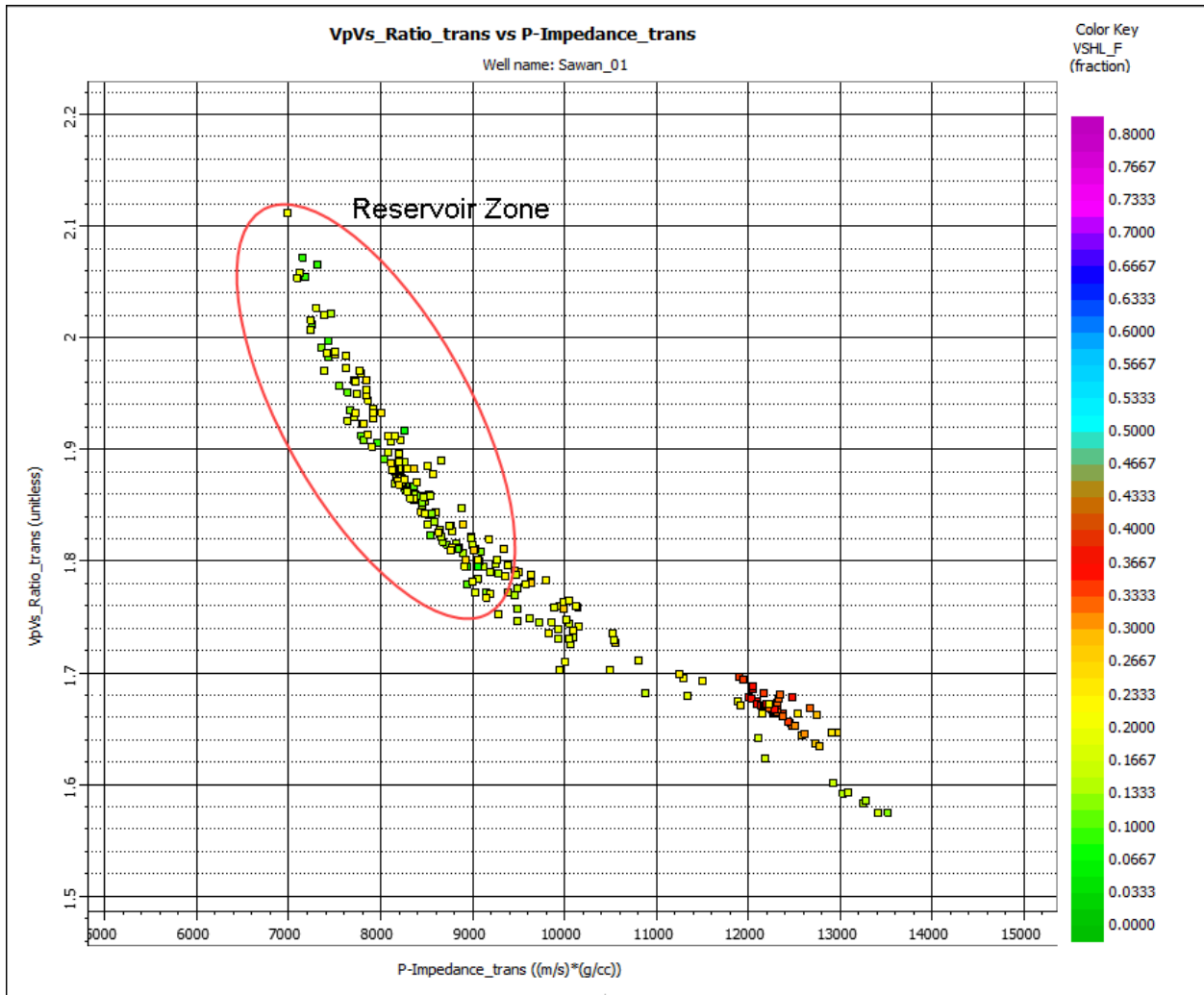


Figure 6.5: VpVs Ratio crossplotted with P-Impedance with effective porosity on z-axis indicating zone of interest.

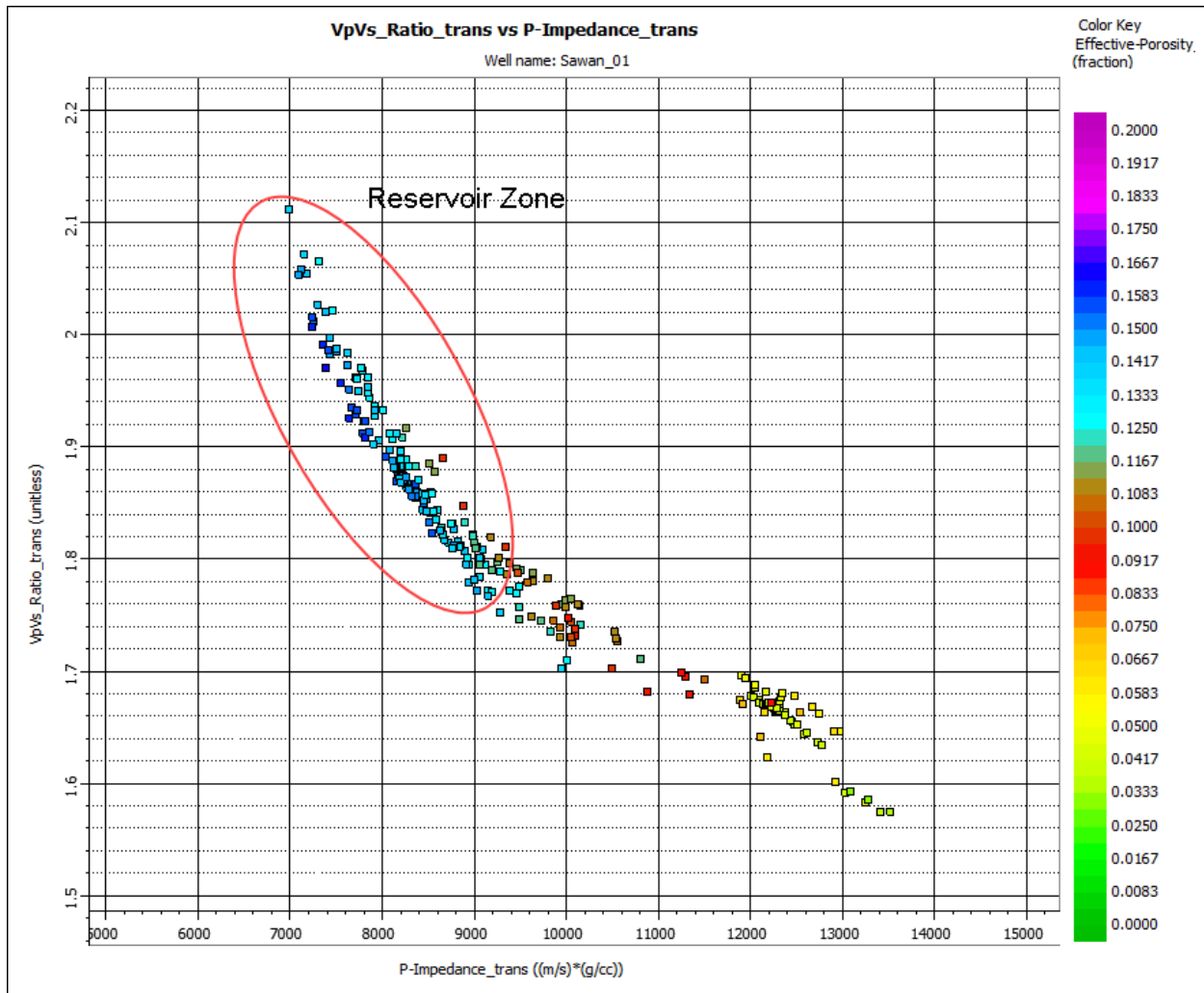


Figure 6.6: VpVs Ratio crossplotted with P-Impedance colored coded with shale volume indicating zone of interest.

The final crossplot has been developed for the Lambda-Rho log with the P-Impedance log color coded with shale volume in Figure 6.7 and effective porosity in Figure 6.8. The relatively low impedance values, relatively low Lambda-Rho values and low shale volume indicates the presence of gas bearing sands (Figure 6.7). This is further confirmed by the high effective porosity values as can be seen for the same zone in Figure 6.8.

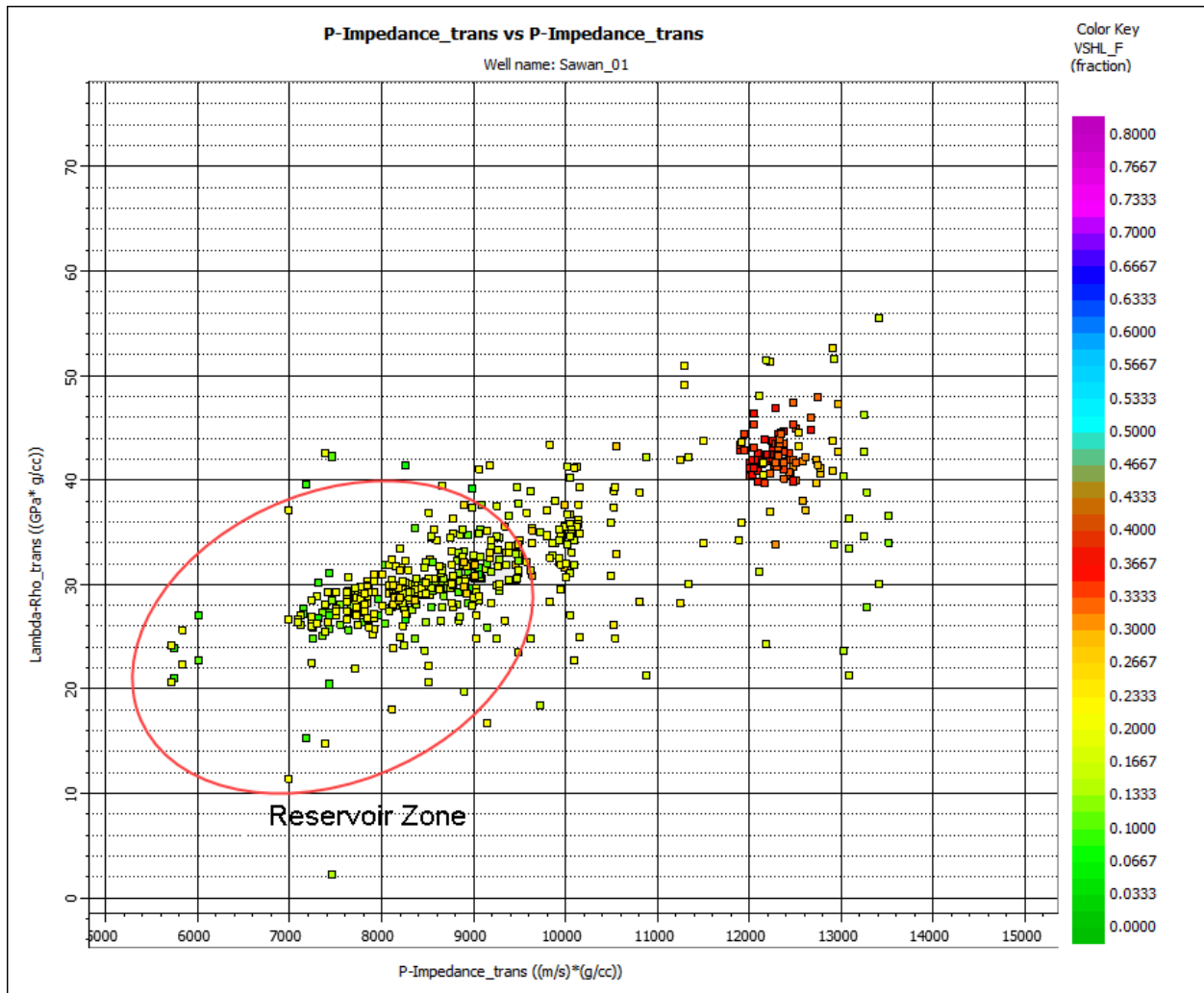


Figure 6.7: Crossplot between Mu-Rho and Lambda-Rho colored coded with shale volume indicating zone of interest.

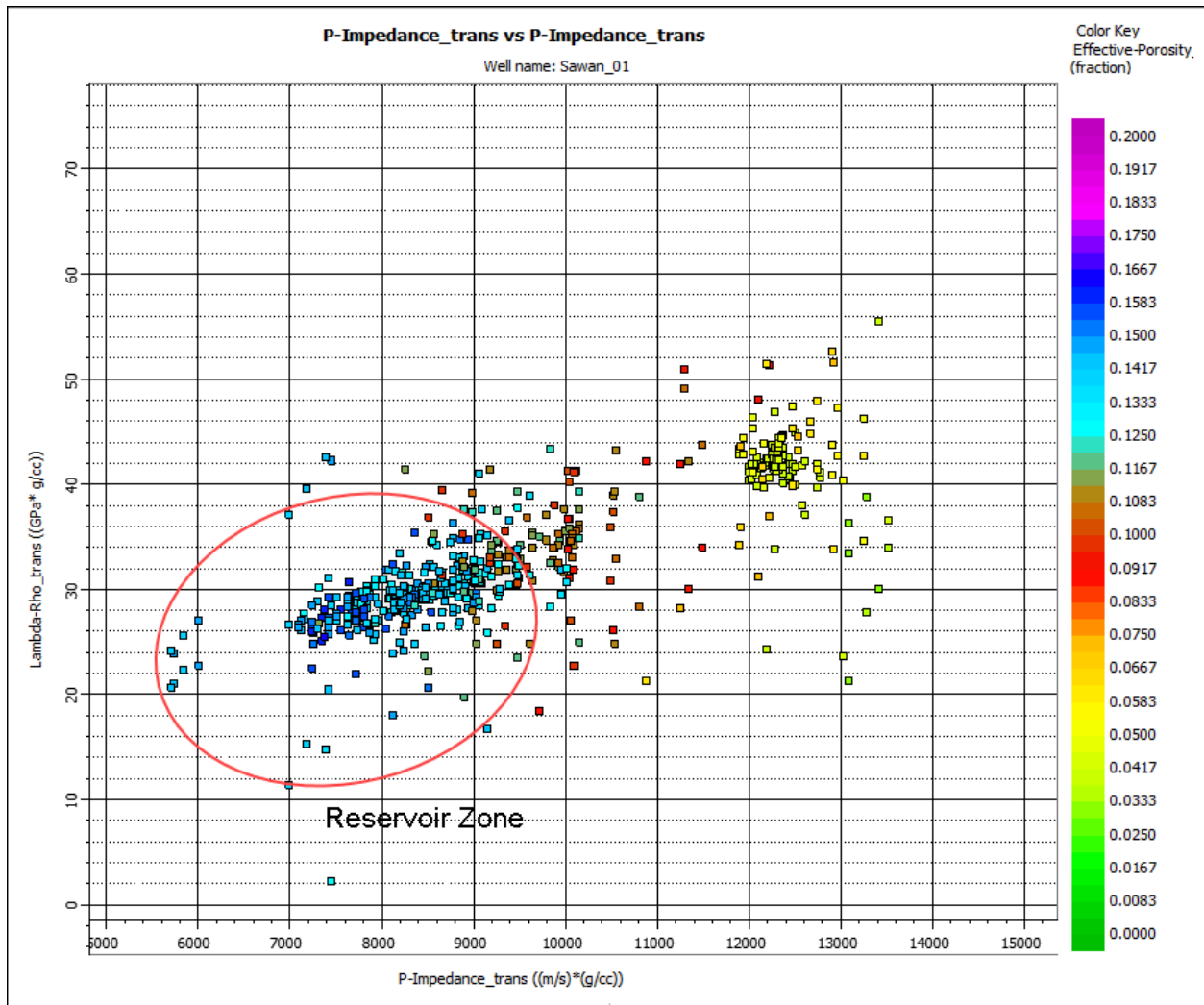


Figure 6.8: Crossplots between Mu-Rho and Lambda-Rho colored coded with shale volume indicating zone of interest.

DISCUSSIONS & CONCLUSIONS

The study area lies in the center of the Sawan block. 3D seismic data is used for studying Sawan block as 3D data gives detailed information of sub surface as compared to 2D data. All three wells Sawan-01, Sawan-07, Sawan-08, lies in the 3D cube. Sawan-01 lies in the southernmost part of the 3D cube. Sawan-07 lies in the center and Sawan-08 in the northern most part. Spectral Decomposition on 3D data helps to identify the zones showing amplitude anomalies. Petrophysical analysis is used to identify reservoir interval and to get the reservoir properties. The C-Sand of Lower Goru formation is acting as potential reservoir in study area therefore the focus of this study is reservoir interval.

The following conclusions can be drawn from this study:

Time and Depth contours shows that C-sands have shallow depth in the north western and central part of the 3D cube and have steeper depths in the north eastern and south eastern part of the data cube.

The appearance of C-Sand on seismic section is not straight but curved. This is due to erosion caused by paleo channels. That's why they are also called channel sand deposits.

Petrophysical analysis includes interpretation of three wells Sawan-01, Sawan-07, Sawan-08. The reservoir quality Sand i.e. C-Sand is encountered in all wells at different depths but variation in depth is very low because the wells are in close proximity to each other. C-Sand is encountered at 3220m to 3310m slab.

The thickest reservoir interval is encountered in Sawan-01 which is 105m thick. Sawan 07 and Sawan-08 contains 90m and 70 m thick reservoir interval. The upper 75m of Sawan-01 appears as good quality reservoir as compared to the bottom 30m.

Facies analysis indicates the reservoir is sand prone and shows high concentration of quality sand. Cross plot indicates the change in facies with decrease in porosity and increase in GR values.

Sawan-07 is most producing well in this area has high Hydrocarbon saturation, effective porosity and low Volume of Shale followed by Sawan-08 and Sawan-01.

Spectral Decomposition is used to identify probable Sand channel existing in the area. Spectrum analysis is used to know the survey spectrum of the study area. The envelope sub bands are generated from 8Hz to 70Hz.

At low Frequencies, thick amplitude anomalies appear which shows the energy trapped in reservoir both in section and map view. The channel geometry does not clearly appear at low frequency 8Hz to 16Hz but scattered on overall map.

From 19Hz to 27Hz the scattered amplitude anomaly decreases and proper channel geometry appears on map view along which all the wells used in study are drilled.

From 27Hz to onwards high frequencies the amplitude anomaly starts disappearing so that small patches of entrapped energy appear in areas around reservoir and the channel geometry on map view also fades the shape of channel.

15Hz to 27Hz is the dominant frequency range best describes the channel geometry and reservoir interval in both section view and map view.

In inversion analysis results are much clear in Modal based inversion technique in which D and C sands are dominant reservoirs

According to Band Limited inversion results are almost same like Modal based inversion Low impedance areas are producing

In Maximum Likelihood Sparse Spike results are not much accurate but still reservoir zones are dominant up to maximum extent

In Rock physics crossplots different attributes are plotted against each other and results are drawn for reservoir zone identification

From P-Impedance and Mu-rho results are identifying the reservoir zone

Similarly, From Lambda-rho and Mu-rho, P-Impedance and P-Impedance and Mu-rho and Lambda rho are also identifying the reservoir zone properly

References

- Afzal, J., Kuffner, T., Rahman, A., and Ibrahim, M., 2009,
- Afzal, J., Kuffner, T., Rahman, A., Ibrahim, M., (2005). Seismic and well-log based sequence
- Ahammed, S., Hai, M. A., Islam, D. M. R., & Sayeem, S. A. (2014), Petro-Physical analysis of reservoir rock of Fenchuganj Gas Field (Well# 03) using wireline log. American Journal of Engineering Research (AJER), 3(8), 37-48.
- Ahmad, N., Fink, P., Sturrock, S., Mahmood, T., & Ibrahim, M. (2004). Sequence stratigraphy as predictive tool in Lower Goru Fairway, Lower and Middle Indus Platform, Pakistan. PAPG, ATC, 85-104.
- Ahmad, N., Fink, P., Sturrock, S., Mahmood, T., & Ibrahim, M. (2004). Sequence Stratigraphy as Predictive Tool in Lower Goru Fairway, Lower and Middle Indus Platform, Pakistan. PAPG, ATC 2004.
- Ahmad. N. and Chaudhry. S, 2002, "Kadanwari Gas Field, Pakistan: a disappointment turns into an attractive development" Published by Geological Society Publishing House, Petroleum
- Alam, M.S.M., Wasimuddin, M., and Ahmad, S.S.M., (2002). Zaur structure, a complex traps in poor seismic data area, BP Pakistan Exploration and Production inc. AAPG Search and
- Ali, A., Alves, T. M., Saad, F. A., Ullah, M., Toqeer, M., & Hussain, M. (2018). Resource potential of gas reservoirs in South Pakistan and adjacent Indian subcontinent revealed by post-stack inversion techniques. Journal of Natural Gas Science and Engineering, 49, 41-55.
- Ali, A., M. Kashif, Hussain, J. Siddique, I. Aslam, and Z. Ahmed (2015), An integrated analysis of petrophysics, cross-plots and Gassmann fluid substitution for characterization of Fimkassar area, Pakistan: A case study, *Arab. J. Sci. Eng.* 40, 1, 181–193
- Alimoradi, A., Moradzadeh, A., Bakhtiari. (2011). Methods of water saturation estimation:
- and Pickford, S. (2001). Rock Physics for the Rest of Us -An Informal Discussion. Cseg
- Applying rock physics tools to reduce interpretation risk. Cambridge university press. Bacon,
- Asquith, G. B. and Gibson, C. R. (1982). Basic well log analysis for geologists. American
- Asquith, George B., Daniel Krygowski, and Charles R. Gibson. "Basic well log analysis. Vol. Association of Petroleum Geologists, Tulsa, 216.
- American association of petroleum geologists, (2004).
- Avseth, P., Mukerji, T., & Mavko, G. (2005). Quantitative seismic interpretation:

Bacon, 2007 reservoir mapping By M. Bacon, R. Simm, T. Redshaw

Badley, M. E., (1985), "Practical Seismic Interpretation", D. Riedel Publishing Company & Dordrecht, Holland. International Human Resources Development Cooperation.

Bakker, Peter. "Image structure analysis for seismic interpretation." Delft University of

Barnes, A. E. (2001). Seismic attributes in your facies. CSEG recorder, 26(7), 41-47.

Bender, F., & Raza, H. A. (1995). Geology of Pakistan, p.50–120.

Bender, F.K. and Raza, H.A. (1995) Geology of Pakistan. Castagna, J. P., Sun, S., and Seigfried, R. W. (2003). Instantaneous spectral analysis: Detection of low frequency shadows associated with hydrocarbons, The Leading Edge, 22,120-127. Between the Indian and Arabian plates recorded in ophiolites and related sediments.

Bowers, G. L. (1995). Pore pressure estimation from velocity data: Accounting for overpressure mechanisms besides undercompaction. SPE Drilling & Completion, 10(02) 89-95.

Bruce, B., & Bowers, G. (2002). Pore pressure terminology. The Leading Edge, 21(2), 170-173.

Catuncanu, O. (2006). Principles of sequence stratigraphy. Elsevier. Chopra, S., & Marfurt, K. J. (2014). Churning seismic attributes with principal component analysis, Arcis Seismic Solutions, Calgary.

Catuneanu, O., Abreu, V., Bhattacharya, J. P., Blum, M. D., Dalrymple, R. W., Eriksson, central portion of the lower Indus basin of In Proceedings of an international seminar. Islamabad, Pakistan, Ministry of Petroleum and Natural Resources (pp. 106-119).

Chopra, S., & Huffman, A. R. (2006). Velocity determination for pore-pressure prediction. The Leading Edge, 25(12), 1502-1515.

Chopra, S., Castagna, J.P., Portniaguine, O. (2006). Seismic resolution and thin-bed reflectivity inversion, Arcis Seismic Solutions, Calgary.

Coffeen, J.A., 1986, Seismic Exploration Fundamentals, Penn Well Publishing Co. Dewar, J., decomposition in reservoir characterization: The Leading Edge, 18, 353-360. Posamentier, H.

Discovery Article # 90149 © 2012 PAPG/SPE ATC. 2-4 November 2002. Islamabad, Pakistan. p. 1-3.

Donaldson, E. C., & Tiab, D. (2004). Petrophysics: Theory and Practice of measuring reservoir rock and fluid transport properties. Gulf Professional Publishing.

Dutta, N. C. (2002). Geopressure prediction using seismic data: Current status and the road ahead. *Geophysics*, 67(6), 2012-2041.

Eaton, B. A. (1969). Fracture gradient prediction and its application in oilfield operations.

Eaton, B. A. (1972). The effect of overburden stress on geopressure prediction from well logs. *Journal of Petroleum Technology*, 24(08), 929-934.

Effects on Density and Neutron Porosity Logs Acquired in Highly Deviated Well. In SPWLA

Emery, D., & Myers, K. (Eds.). (2009). *Sequence stratigraphy*. John Wiley & Sons. Goodwyne, Olar, kamal (2012). Pressure prediction and underbalanced drilling in the deepwater Niger delta, Durham theses, Durham University.

geoscience, Vol. 8. No 4, Nov 2002, Pp 307-316.

Gnos, E., Immenhauser, A., & Peters, T. J. (1997). Late Cretaceous/early Tertiary convergence

Handwerker, D. A., et al. "Synthetic seismograms linking ODP sites to seismic profiles, continental rise and shelf of Prydz Bay, Antarctica. *Proc. Ocean Drill. Prog. Sci. Res.* Vol. 188. 2004. Hart, B. S., 2008, Channel detection in 3D seismic data using sweetness: *AAPG Bulletin*, 92, no. 6, 733-742.

Harrold, T. W., Swarbrick, R. E., & Goult, N. R. (1999). Pore pressure estimation from

Hassan, M., Shamim, M. A., Hashmi, H. N., Ashiq, S. Z., Ahmed, I., Pasha, G. A., Naeem, U. A., Ghumman, A. R., and Han, D. (2014).

Hermanrud, C., Wensaas, L., Teige, G. M. G., Bolas, H. N., Hansen, S., & Vik, E. (1998).

Hilterman, F. J. (2001). Seismic amplitude interpretation.

historical perspective. *J. Pet. Gas Eng.* Volume 2, Issue 3, Pages 45-53.

Holbrook, P., Robertson, H. A., & Hauck, M. L. (1991). Method for determining pore pressure and horizontal effective stress from overburden and effective vertical stresses.

Hottmann, C. E., & Johnson, R. K. (1965). Estimation of formation pressures from log-derived shale properties. *Journal of Petroleum Technology*, 17(06), 717-722.

Houston, TX: Baker Hughes INTEQ, 254.

Hussain, M., Getz, S. L., & Oliver, R. (1991). Hydrocarbon accumulation parameters in the Hydrocarbon Environments.

Ibrahim, M., (2007). Seismic inversion Data, A tool for reservoir characterization/Modelling

- Javid, S. (2013). Petrography and petrophysical well log interpretation for evaluation of Journal of petroleum technology, 21(10), 1-353.
- Kadri I.B., (1995), "Petroleum Geology of Pakistan", PPL, Karachi, Pakistan.
- Kadri IB, (1995). Petroleum geology of Pakistan. Graphic Publishers, Karachi, Pakistan, Karachi, Pakistan, p.70–100.
- Kazmi, A.H., & Jan, M.Q., (1997). "Geology & Tectonics of Pakistan", Graphic Publishers, Karachi, Pakistan.
- Kemal, A., 1992, Geology and New Trends for Hydrocarbon Exploration in Pakistan, P202-205.
- Kingston, D. R., Dishroon, C. P., & Williams, P. A. (1983). Global basin classification system. AAPG bulletin. Mahoney, J. J. (1988). Deccan traps. In Continental flood basalts (pp. 151-194). Springer, Dordrecht.
- Law, B. E., & Spencer, C. W. (1998). Memoir 70, Chapter 1: Abnormal Pressure in M., Simm, R., & Redshaw, T. (2007). 3-D seismic interpretation. Cambridge University Press.
- Mapping in Badin Area, Sindh, Pakistan. Sindh University Research Journal SURI (Science Memoir 70, Chapter 4: Shale Porosities from Well Logs on Haltenbanken (Offshore Mid-
- Mendoza, A., Torres-Verdin, C., & Preeg, W. (2006, January). Environmental and Petrophysical mudrock porosities in Tertiary basins, Southeast Asia. AAPG bulletin, 83(7), 1057-1067.
- Munir, A., Asim, S., Bablani, S. A., & Asif, A. A. (2014). Seismic Data Interpretation and Fault
- Munir, K., Iqbal, M. A., Farid, A., & Shabih, S. M. (2011). Mapping the productive sands of Lower Goru Formation by using seismic stratigraphy and rock physical studies in Sawan area, southern Pakistan: a case study. Journal of Petroleum Exploration and Production Technology, 1(1), 33-42.
- Munir, K., Iqbal, M. A., Farid, A., & Shabih, S. M. (2011). Mapping the productive sands of Lower Goru Formation by using seismic stratigraphy and rock physical studies in Sawan area, southern Pakistan: a case study. Journal of Petroleum Exploration and Production Technology, 1(1), 33-42.
- Munir, K., Iqbal, M.A., Farid, A. *et al.* 2014. Mapping the productive sands of Lower Goru Formation by using seismic stratigraphy and rock physical studies in Sawan area, southern Pakistan

Naseer, M. T., & Asim, S. (2017b). Continuous wavelet transforms of spectral decomposition analyses for fluvial reservoir characterization of Miano Gas Field, Indus Platform, Pakistan. *Arabian Journal of Geosciences*, 10(9), 210.

Naseer, M. T., & Asim, S. (2017d). Detection of Cretaceous incised-valley shale for resource play, Miano gas field, SW Pakistan: Spectral decomposition using continuous wavelet transform. *Journal of Asian Earth Sciences*.

Neal, J., & Abreu, V. (2009). Sequence stratigraphy hierarchy and the accommodation succession method. *Geology*, 37(9), 779-782.

Norway) Show No Influence of Overpressuring.

Osborne, M. J., & Swarbrick, R. E. (1997). Mechanisms for generating overpressure in sedimentary basins: a reevaluation. *AAPG bulletin*, 81(6), 1023-1041.

P. G. & Giles, K. A. (2009). Towards the standardization of sequence stratigraphy. *EarthScience Reviews*, 92(1), 1-33.

p.90–150.

Kazmi, A.H., and Jan, M.Q., (1997). *Geology and Tectonics of Pakistan*, Graphic publishers,

Partyka, G. A., J. M. Gridley, and J. Lopez, 1999, *Interpretational applications of spectral*

Payton, C. E. (Ed.). (1977). *Seismic stratigraphy: applications to hydrocarbon exploration* (Vol. 26, pp. 1-516). American Association of Petroleum Geologists.

Qayyum, F., de Groot, P., & Hemstra, N. (2012). Using 3D Wheeler diagrams in seismic interpretation—the HorizonCube method. *First break*, 30(3), 103-109.

Raza HA, Ali SM, Ahmed R (1990) *Petroleum geology of Kirthar Sub-basin and part of the Kutch Basin, Pakistan*. *Pak J Hydrocarb R* 2(1):29–73.

Rider, M. (1996), *The geological Interpretation of Well Logs*. 2nd Edition, Rider-French Consulting Ltd., Sucherland.

sandstone reservoir quality in the Skalle well (Barents Sea).

Sawan Gas Field - A case study, PAPG, ATC. INTEQ, B. H. (1999). *Petroleum Geology*.

Sayers, C. M., Johnson, G. M., & Denyer, G. (2002). Predrill pore-pressure prediction using seismic data. *Geophysics*, 67(4), 1286-1292.

Series), 46(2).

Stark, T. J. (2005, January). Generation of 3D seismic "Wheeler Diagram" from a high resolution Age Volume. In 2005 SEG Annual Meeting. Society of Exploration Geophysicists.

Stratigraphy of the early cretaceous, lower Goru "c" sand of the Sawan gas field, middle Indus Technology (2002)

Tectonophysics, 271(1-2), 1-19. Hamada, G. M. (1996). An Integrated Approach to Determine Shale Volume and Hydrocarbon Potential in Shaly Sand. In SCA paper 9548, presented at SCA Intl. Symposium (pp. 12-14).

W., & Allen, G. P. (1999). Siliciclastic sequence stratigraphy: concepts and applications (Vol. 7). Tulsa: SEPM (Society for Sedimentary Geology).

Zaigham N.A., Mallick K.A., 2000, Bela ophiolite zone of southern Pakistan: Tectonic setting and associated mineral deposits: GSA Bull. 112, 3, 478-489.